ASSESSING PARTICULATE MATTER AND BLACK CARBON EMISSIONS FROM HOMES USING TRADITIONAL AND ALTERNATIVE COOKSTOVES IN RURAL NEPAL

by

Sutyajeet I. Soneja

A dissertation submitted to Johns Hopkins University in conformity with the requirements for the degree of Doctor of Philosophy

Baltimore, Maryland

July 2014

ABSTRACT

Billions of people throughout the developing world use traditional cookstoves fueled with biomass (such as wood, dried animal manure, and crop residue). Inefficient combustion of biomass results in the formation of large amounts of particulate matter (PM) air pollution. Light reflecting black carbon is a significant component of this PM. Black carbon is considered a short-term climate agent with an average atmospheric residence time on the order of days to weeks, compared to some greenhouse gases that can have an atmospheric residence time of years to centuries. In addition to having an effect on regional hydrological cycles, black carbon deposition on glaciers, sea, or land ice causes a decrease in surface albedo, thus resulting in an acceleration of the melting process. The Himalayas, an area containing the largest snow and ice mass outside the North and South Poles, are vulnerable to black carbon deposition from highly prevalent biomass cooking in surrounding countries. Deposition of black carbon from air pollution has the potential to impact the availability of glaciers in this region, which act as a water source for close to a billion people throughout South and East Asia. As a result, due to the larger population, biomass for cooking in South Central Asia has the potential to impact climate change on a local and global scale.

It is believed that a large majority of black carbon production in South Asia is a result of cooking with biomass fuels. However, biomass cooking is not the only source of black carbon. Mobile (diesel vehicles) and stationary (brick kilns) sources can also be significant emitters. This study estimates black carbon emissions associated with traditional and alternative cookstoves at the household level. This study can be further separated into three main components.

The first component is a methods paper focusing on improved quality control for a commonly used particulate matter sampling method. Great uncertainty exists around indoor biomass burning exposure-disease relationships due to lack of detailed exposure data in large health outcome studies. Passive nephelometers can be used to estimate high particulate matter (PM) concentrations during cooking in low resource environments. Nephelometric concentration readings can be biased due to particle growth in high humid environments and differences in compositional and size dependent aerosol light scattering characteristics. Chapter 2 explores relative humidity (RH) and gravimetric equivalency adjustment approaches for the pDR-1000, which is used to assess indoor PM concentrations for a cookstove intervention trial in Nepal. Furthermore, new integrated RH and gravimetric conversion methods are presented because they have one response variable (gravimetric $PM_{2.5}$ concentration), do not contain an RH threshold, and are more straightforward than previously proposed approaches.

The second component focuses on characterizing the amount of particulate matter and black carbon that exit the house during the use of traditional, open-design cookstoves in village homes. Cookstove emissions create indoor exposures and contribute to ambient air pollution through passive exchanges between indoor and outdoor air (indirect venting) and direct venting (i.e., chimney) to the outdoors. A fraction of PM produced during cooking will settle and deposit on indoor surfaces as well as in cracks within the walls of the house, while the rest will escape to the outdoor environment (known as exfiltration). Currently, there is a poor understanding of how much cooking-related PM exfiltrates to the outdoor environment. Chapter 3 presents air exchange rates and PM exfiltration estimates from homes in rural Nepal that utilize traditional, open-design cookstoves. Estimates of variability are provided for exfiltration as a function of housing and fuel characteristics in a real-world setting. Furthermore, this chapter assesses the black carbon to $PM_{2.5}$ ratio produced by biomass cooking in order to estimate black carbon exfiltration from homes. In combination with an assessment of indoor PM concentrations, PM and black carbon exfiltration fractions can be used to estimate house emissions to ambient air in order to better assess regional air quality and climate change impacts.

The third component (Chapter 4) extends upon this work by presenting exfiltration estimates of PM that exit to the outdoors via the combined route of indirect (natural) and direct (chimney) ventilation for alternative cookstoves being studied in a large, cookstove intervention trial in rural Nepal. Characterizing these exfiltration pathways allows for homes to be treated as a source, hence aggregating variability related to stove emissions.

Future work will utilize estimated black carbon emissions in combination with estimates of cookstove use and cooking pattern estimates to serve as inputs for spatial regression modeling that will allow for the prediction of ground level black carbon concentrations across much of Northern India and Southern Nepal (the Indo-Gangetic Plain). Since a large fraction of the world's biomass cookstove users are in South Central Asia, this project provides significant insight of cookstove emission to atmospheric contribution.

Thesis Advisor:

Dr. Patrick N. Breysse, Professor, Department of Environmental Health Sciences, Bloomberg School of Public Health, Johns Hopkins University, Baltimore, MD

Thesis Committee:

Dr. James M. Tielsch, Professor and Chair, Department of Global Health, School of Public Health and Health Services, George Washington University, Washington, DC

Dr. Frank C. Curriero, Associate Professor, Department of Epidemiology, Bloomberg School of Public Health, Johns Hopkins University, Baltimore, MD

Dr. Benjamin Zaitchik, Assistant Professor, Department of Earth and Planetary Sciences, School of Arts and Sciences, Johns Hopkins University, Baltimore, MD

Dedication

This dissertation is dedicated to the late Dr. Alison Geyh.

For taking time out of her day to respond to an E-mail from someone she had never met, heard of, nor had any vested interest in.

For investing her time and energy into me when coming back to pursue my doctorate was only an idea.

For changing the course of my life.

To the future, whatever it may hold

To making a difference for the better good

To success in all endeavors, no matter how bold

To the improbable becoming reality.

May the future favor those that are bold, smart, kind hearted, and Me.

Acknowledgements

Throughout the course of pursuing my doctorate, I have been fortunate, blessed, and downright lucky to have been supported by so many wonderful people.

First and foremost, my gratitude goes towards my research advisor, Dr. Pat Breysse. Pat's support, guidance, and collegiality have been unwavering. I suppose this comes with great experience and mentoring many students, but he knew when to guide me, when to let me vent, and when to let me figure things out on my own. His persistent confidence inspired me to keep going. I have truly enjoyed working with him and moreover, am thankful for his friendship and relentless kindness towards me.

Another research advisor that I consider a co-mentor and have a deep gratitude towards is Dr. Jim Tielsch. I don't recall the first time I met Jim, but the first thing I recall him saying to me is something I will never forget. In a small room, surrounded by colleagues in Sarlahi, Nepal after work hours the words "Welcome to the REAL subcontinent" is a phrase I will never forget. Disagreeing and not really understanding what that meant at the time, that phrase begin a journey that has had an impact on my life that is parallel to none. Jim's guidance, unfaltering support, friendship, and patience with me are all things I am thankful for. Between Jim and Pat, I could not have asked for a better tag team to help guide and influence my development.

To my thesis readers and the rest of my exam committee members whose contributions greatly improved this work and challenged me to do better: Frank Curriero, Ben Zaitchik, Peter Lees, Ana Rule, D'ann Williams, Will Checkley, Bill Spannhake, and Joanne Katz. I am particularly grateful to Frank Curriero for his guidance, encouragement, and commitment to not just myself but all of his students. Ben Zaitchik for serving on my thesis research committee from the beginning and helping me to keep in mind the big picture and the direction to take my work. Ana Rule and D'ann Williams for their added support preparing me for my field sampling campaign and supporting me throughout the process during my time in Nepal. Will Checkley and Joanne Katz were also influential in guiding me during my time in Nepal.

I would also like to recognize the country of Nepal and all of the people I met while living there. First and foremost, the NNIPS researchers, supervisors, and staff. Dr. Subarna Khatry for his support, ingenuity, jokes, and for not holding me to the requirement that all PhD students passing through NNIPS land drink the frog's pee. It was a great pleasure getting to know, working with, and understanding the great accomplishments he has achieved despite having to work in such a challenging environment. Steve LeClerq for his guidance, stories, interesting lifestyle, and friendship. His openness towards everyone was refreshing and his approach to life inspiring. The NNIPS Kathmandu office staff, especially Dambar, Shakun, Ram, and Kayestha for their friendship and support. Also to Kedar for not only his friendship, but also incredible dance moves. The NNIPS field site supervisors: Uma Shankar Sah (for his laughter and constant losses in arm wrestling matchups), Shishir V. Shrestha (for his calm, cool guidance), Shiv Raj Bhattarai (for the greeting every day of "for my friend has come again from the land of the USA"), Punya Prasad Dahal (for his unprecedented dance moves, jokes, and take on life), Laxman Raymajhi (for his kindness), Keshab Dhakal (for his curiosity), Dhruba Kadkha (for his thoroughness), and Gobind Prasad Mainali (for his failed attempts at trying to play a joke on me). Their support, kindness, and friendship enriched my experience while in Nepal beyond measure. To Shakya and his wife (also known as his home minister) for inviting me into their home, watching over me, showing me much love and warmth, and for the endless supply of fresh avocados when they were needed most. Additional staff that I worked closely with: Ms. Samjhana Magar for her never-ending smile and wealth of knowledge she imparted upon me about the culture, daily life, and friendship; Mr. Bharat Bahadur, a man of few words but relentless in his work ethic and precision; and to Mr. Pramod Sah who I worked the closest with. Pramod's relentless work ethic, integrity, resourcefulness, precision, and wholeheartedness are qualities I came to know and admire. I am most thankful for our daily conversations about life, friendship, and the opportunity to get to know his family.

I am thankful for the support provided by the women of Sarlahi that were my roommates for over a year, especially to Neha Naithani, Alison Connor, Aimee Summers, and Laveta Stewart. Also to Lisa Kraine and Michelle Mergler. Relating to the experience of living in Nepal is something only a few can understand and I am glad and fortunate our paths crossed. They taught me, among many things, that women are always right and I am truly grateful for their friendship and advice.

Recognition goes to my other friends in Nepal who indirectly supported me, especially: Pujan and Michelle as well as their Hotel Courtyard library where much work was done, many interesting stories were told, and a place where I have many fond memories of; Kate for being a good friend; To Anoj and Amit for being my two compadres in Sarlahi; And also to Jogi, Dulari, and the rest of their family, especially Asmi and Rohan, for inviting me into their home and being great friends.

Much appreciation goes to JHU staff and admin support doing all of the behind the scenes work, with a special thanks to Jana Mihalic, Tim Greene, Fred Van Dyk, and Chrissy Torrey.

Additional thanks to Lance Wallace and Andrew Persily of the National Institutes of Standards and Technology, Steve Chillrud and Beizhan Yan of Columbia's Lamont Doherty Earth Institute, Dr. Mike Boyette of NCSU for setting an example, and remaining JHU faculty that influenced me during my time in Baltimore and abroad in Nepal such as Luke Mullany.

To my friends that I have met and have supported me along the way, especially: Rachel Zamoiski and Joan Casey for being normal, Jesse Berman for his love of ESPN, Jonathan Coulter and Frances Belmonte for being sounding boards, Henrik Salje for letting me take out my frustrations of life in our weekly racquetball matchups, Talia Chalew and Pam Dopart for listening to my non-school related complaints, Chen Chen for her support in my work, and Andrew Azman for being Andrew.

To my friends of old that have always been there for me and whom I could rely on no matter what, particularly: Wes Hudson for his constant encouragement and willingness to travel anywhere with me, Dave Francisco for his stories with nameless people, Ahmad Atari for his love of football, Richard Wong for his always appropriate jokes, and especially Noor Atari who reinforced in me at a young age to be stubborn when necessary and highlighting the fact that nice guys finish first.

Finally, my love and gratitude go to the most important people in the world to me: My Mom and Dad. To my Mom for always being concerned about my well-being, constant laughter, and endless supply of wisdoms courtesy of Dr. Oz. To my Dad for his quiet, yet unyielding support in all my endeavors and pursuits. My siblings deserve great recognition as well. Rishi for his infectious laugh, Ravi for his perfection in everything he pursues, Shiv for his jokes and persistence, and Krishna for her great smile irrespective of any life situation. Regardless

of what I am doing or where I may be in life, their unfaltering love, support, and care is something I am deeply grateful for.

Funding Sources

This work was performed with grant support from the National Institute of Environmental Health Sciences (ES015558; ES003819; P50ES015903; P01ES018176), Environmental Protection Agency (R832139), the Thrasher Research Fund (02830-4), and a seed grant from the Environment, Energy, Health, and Sustainability Institute (E^2SHI) at Johns Hopkins. Additional support was provided in the form of tuition, health insurance, and stipend courtesy of a National Institute of Environmental Health Sciences T32 Training Grant.

Table of Contents

List of Tables

Chapter 2

Chapter 3

Chapter 4

Chapter 5

List of Figures

Chapter 1

Chapter 2

Chapter 3

Chapter 4

Chapter 5

Chapter 6

1 Introduction

The research presented in this dissertation focuses on the topics of air pollution and climate change in what is one of the most heavily inhabited and climate sensitive regions in the world. Specifically, an examination is conducted into the importance of cooking with solid fuels in a rural population and how emissions from traditional and alternative methods contribute to climate change. The work conducted for this dissertation is intended to contribute to the overall body of knowledge regarding exposure assessment and climate change emissions as a result of cooking within a low-income country. The following sections review why the climate change agent black carbon is important, how it relates to cooking with biomass fuels, and gaps in our knowledge.

Black Carbon: Overview and Importance

Black carbon is a component of particulate matter (PM) produced during incomplete combustion[1]. Sources include power plants, industrial facilities, cars and trucks, forest and wild fires, as well as residential biomass fuels (i.e., wood, dried animal manure, or crop residue) used for cooking and heating[1]. During incomplete combustion not all carbon is converted to CO_2. Depending on source and combustion characteristics, various amounts of carbon monoxide (CO), volatile organic compounds (VOCs), semi-volatile organic compounds (sVOCs), organic carbon (OC) and black carbon (BC) are formed[2]. The term “black” refers to the fact that these particles absorb visible light. This absorption can be exploited for measurement purposes (i.e., measure the light reflectance from a filter-collected air sample). More importantly, the light absorbance can lead to changes in global energy balance and eventually to warming[2]. Black carbon is considered a short-lived climate-forcing agent, with an average residence time in the atmosphere of a few days to weeks compared to CO_2 or other greenhouse gases that can range from years to centuries[3,4].

Black carbon can alter the environment in two ways. First, suspended particles in the sky absorb sunlight, thereby causing the atmosphere to warm[1]. Black carbon is the leading anthropogenic absorber of incident solar radiation in the atmosphere, being approximately 1 million times stronger than CO_2 per unit of mass[3]. Conversely, this also causes less sunlight to reach the Earth's surface (referred to as dimming). There is reasonable consensus within the scientific community that the atmospheric solar heating is much larger than the effect of surface dimming, thus leading to a net warming of the surface and atmosphere[5]. Depending on the range of conditions (e.g., makeup of the particulate or topographical features of the land), black carbon particles can get hot enough to vaporize water and prevent clouds from forming resulting in additional heating of the Earth's surface. Conversely, black carbon particles could seed clouds causing them not to coalesce into denser forms resulting in more clouds but less rain fall[6–8].

Black carbon also alters the environment by directly heating surfaces due to deposition, resulting in changes in surface albedo (i.e., decreasing surface reflectivity) and contributing to the accelerated melting of Arctic sea and land ice, glaciers, and seasonal snow covers[3]. Within the Himalayas, black carbon may be responsible for as much as 50% of the total glacial retreat that has been seen thus far[9]. The combined global warming impact of one kilogram of black carbon via multiple warming pathways is estimated to be on average 500 to 680 times larger than one kilogram of CO_2 over a 100-year time frame and 1,500 to 2,200 times larger over a 20-year time frame[3]. Because of this, recent studies have estimated that black carbon is the second or third largest overall contributor to global warming, surpassed only by CO_2 and possibly methane[3]. Since black carbon has a much shorter residence time relative to greenhouse gases, mitigating these emissions is an attractive target for producing significant results quickly in the effort against climate change[3,10].

Cooking with Biomass Fuels: Relevance and Impact

Approximately half the world's population utilizes biomass fuels for cooking or heating, most of which are in developing nations[11–13]. Examples of biomass fuels include wood, dried animal manure, crop residue, and charcoal. The extensive worldwide use of cookstoves reliant upon biomass fuels is cause for grave concern due to the extremely high particulate matter concentrations and other pollutants produced within the home[14–16]. A significant portion of this particulate matter is comprised of black carbon[4,7]. Elevated indoor exposures to particulate matter as a result of biomass burning are common for women and children. These subpopulations spend a significant amount of time indoors cooking or near the fire, thus placing them at a high risk for developing associated health effects[17]. In general, health effects attributed to particulate matter exposure are linked to particle concentration, size, and composition with much of black carbon believed to be in the ultrafine ($<0.1\mu m$) to fine ($<2.5\mu m$) range[18]. A substantial body of literature has linked biomass fuel use to several chronic diseases including ischemic heart disease, chronic obstructive pulmonary disease (COPD), and lung cancer. Exposure to high indoor concentration has also been shown to result in acute lower respiratory infections (ALRI) in children[11,13,19]. Based on 2012 data, the World Health Organization estimated that 4.3 million premature deaths occur worldwide annually as a result of exposure to indoor air pollution created by biomass cooking[20–22]. Indoor air pollution associated with biomass burning is a significant contributor to morbidity and mortality and changes in cookstove technology have been proposed to reduce indoor emissions and improve the health outlook. Organizations such as the Global Alliance for Clean Cookstoves of the United Nations Foundation, working in partnership with other agencies, governments, and the private sector, have invested significant resources to replace traditional, open-design cookstoves with new, cleaner stove technology[23]. Improved stoves attempt to reduce fuel consumption, increase thermal efficiency, and/or redirect particulate matter to the exterior environment via the use of a chimney. However, new stoves that utilize a chimney require further study in order to better understand their potential to further degrade ambient air quality due to the redirection of pollution outdoors. The potential increase in particulate matter emitted outdoors could also further exacerbate the impact upon climate change by increasing the amount of black carbon released per cooking event to the atmosphere.

Cookstoves and Climate Change: Focusing on the Indo-Gangetic Plain

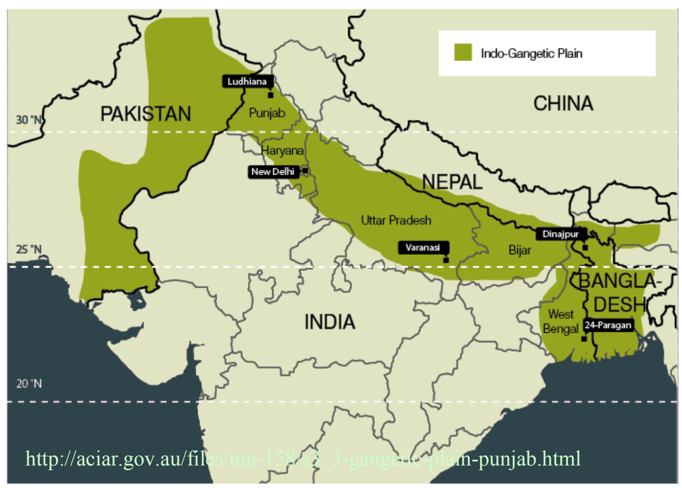

Figure 1: Shaded area indicating location of the Indo-Gangetic Plain (IGP) region

The production of black carbon from the burning of biomass fuels is a major contributor to climate change[1]. Of the total black carbon emissions present globally, ~20% of annual emissions are believed to be a result of biomass burning during cookstove use[24]. In South Asia, biomass cooking alone is believed to contribute about two-thirds of black carbon emissions[9]. An area identified as a regional hotspot for production of black carbon emissions from biomass fuel use is the Indo-Gangetic Plain (IGP)[3]. In this region, black carbon entering the atmosphere and its subsequent deposition on glaciers and snow pack is thought to be a significant contributor to the changing climate[25]. The IGP is one of the most densely populated regions in the world, with its inhabitants reliant upon the surrounding mountains and a predictable hydrological cycle for its water supply[3,4,26].

People across South and East Asia rely on the annual glacial and snow pack melt from the Himalayan-Hindu Kush region as a source of fresh water[3,26]. However, these glaciers along with annual snow pack are experiencing an accelerated retreat and are threatening the water supply for this region[26]. While greenhouse gases play a role in contributing to this retreat, the pace of the retreat along with a 0.3°C warming per decade over the past 30 years indicate that other factors are contributing to this changing climate[26]. In addition to the diminishing presence of glaciers and snow pack, changes to the cyclical seasonal weather patterns in South Asia are becoming more evident. Noting an increase in intense precipitation events and how annual monsoons are deviating from their typical timetables highlights changes to these patterns[4,27]. This instability is threatening the livelihoods of nearly 1 billion people, especially farmers who rely on this fertile land to feed a considerable segment of the global population[7,8].

Areas of Uncertainty and Research Opportunities

Climate change and epidemiological models concerned with particulate matter and black carbon fate and transport in the IGP rely on emission air pollution source inventory data within this region. Emission inventories are generated via several methods, including estimates based upon emission factors developed in laboratories, demographic data including population and fuel estimates, remote sensing applications, and source apportionment models reliant upon measurements from ice core samples[24–26,28]. However, due to the lack of in situ data, emission estimate profiles for particulate matter and black carbon are subject to large uncertainty, subsequently resulting in climate change and epidemiological prediction models having considerable variability[25]. Significant inconsistency exists for published black carbon emissions, with regional scale emissions having considerable, 2-5 fold, uncertainty[4,25,29]. Accurate emission data is needed to allow agencies and organizations to properly estimate the impact of black carbon production created by traditional and improved cookstoves, thus allowing resources to be allocated in a manner that would be cost efficient, protective of human health, and be effective for efforts geared towards mitigating climate change. Furthermore, understanding the contribution cookstoves play in the creation of these emissions, specifically from data collected in situ, is critical towards decreasing variability currently seen in emission profiles.

Study Overview and Objectives

This dissertation provides a comprehensive assessment of the household-level black carbon emissions from traditional, open-design cookstoves as well as alternative stoves in an area within the Indo-Gangetic Plain. Understanding the contribution that traditional and alternative cookstoves play in the production of black carbon is critical to validating existing climate models and making effective decisions with regards to improved cookstove design replacement programs. This dissertation addresses several specific research area needs. The research goals are presented under the following chapter outline.

Chapter 2 presents improved quality control methods for particulate matter monitoring equipment used to assess indoor air pollution associated with the use of biomass fuels. The methods presented combine an adjustment for relative humidity and gravimetric equivalency conversion in extremely high indoor concentration environments using a nephelometric device for measurement.

Chapter 3 presents the first directly measured exfiltration estimates of particulate matter that exit to the outdoors via passive exchange in village homes that utilize traditional, open-design cookstoves. Estimates of variability are provided for exfiltration as a function of housing and fuel characteristics in homes located in rural Nepal. Furthermore, this chapter assesses the black carbon to PM ratio produced by cooking with biomass in traditional stoves. By characterizing these emission characteristics, homes can be treated as a source and particulate matter and black carbon emission rates could be determined based upon the indoor concentration.

Chapter 4 extends upon the work from Chapter 3 to present first-ever measured exfiltration estimates of particulate matter in a village-like home in rural Nepal for improved cookstoves that utilize a chimney to increase ventilation. This chapter provides important information needed to assess the contribution of improved cookstoves on outdoor air quality.

Chapter 5 presents a spatial characterization of ambient $PM_{2.5}$ and black carbon during cooking and non-cooking periods across several villages in rural southern Nepal. This chapter also outlines an approach to developing a spatial prediction model in order to estimate concentrations of these agents at unsampled locations. Ultimately, this research effort is designed to provide a better understanding of the association between indoor and outdoor $PM_{2.5}$ and black carbon at small-scale spatial variability.

Chapter 6 discusses future impact this research will have on developing remote sensing applications in the IGP region. If remote sensing applications can be used to generate accurate emission inventories across the IGP, proper health and economic impact assessments can be conducted. Subsequently, these efforts can be used as communication tools to educate and inform policy makers in order to highlight areas requiring attention and measures needed to mitigate associated climate change issues. Chapter 7 presents a summary of the conclusions, along with public health significance. Appendix A contains the abstract to a paper that I have co-authored on a related topic during my PhD training.

2 Humidity and Gravimetric Equivalency Adjustments for Nephelometer-Based Particulate Matter Measurements of Emissions from Solid Biomass Fuel Use in Cookstoves

Introduction

Assessment of exposure-disease relationships related to use of solid biomass fuels (wood, dried animal manure, and crop residue) for cooking and other household energy needs in the developing world has become a top priority[1]. With approximately 3 billion people using solid biomass fuels, large scale interventions using new, more efficient cooking technologies are being conducted to reduce adverse health effects associated with solid biomass fuel use[1,2]. The success of these efforts will hinge in part on the degree to which new stove technology reduces pollutants and the corresponding reduction in disease. Uncertainties in the exposure-disease relationships make designing interventions difficult since the exposure reduction targets are not known. Currently, great uncertainty exists around the exposure-disease relationships due to lack of detailed exposure data in large health outcome studies. Recent reviews have highlighted the need to conduct more detailed exposure assessments in health studies of household air pollution (HAP) and cookstoves[2,3].

Particulate matter (PM) is a principal emission from biomass combustion and significant contributor to morbidity and mortality. PM measurement technology available for cookstove exposure assessments were designed for use in developed countries where PM concentrations are typically 2 to 3 orders of magnitude lower[2]. Filter-based integrated gravimetric samplers are difficult to use in biomass burning cookstove settings because the high PM concentrations require low flow rates and short sample times to minimize sampler overload. Furthermore, limitations in battery life, specifically for the air pump component of the sampler, make collecting samples for a day or more problematic in low resource settings where access to electricity can be limited. Passive nephelometric devices for measuring PM have several advantages over filter-based integrated sampling methods. They can be used for longer periods on a single charge and do not require a filter, so overloading is less of a problem.

Nephelometers, however, have a number of important limitations. Since light scattering is an indirect measure of PM concentration, the devices need to be calibrated against a gravimetric standard. Nephelometers come pre-calibrated using standard fine dust test aerosol (Arizona road dust)[4]. Since the particle size distribution and composition of cookstove PM is different from Arizona road dust, the instrument response needs to be adjusted to account for differences in PM characteristics. In addition, since many aerosols are hygroscopic and will increase in size at high humidity, nephelometer response needs to be adjusted for humidity effects[5–8].

The purpose of this paper is to describe humidity and gravimetric adjustment approaches for the DataRAM pDR-1000 (Thermo Scientific, Franklin, MA) used to assess indoor PM concentrations in a large cookstove intervention trial in Nepal (registered at Clinicaltrials.gov, NCT00786877). This nephelometer measures airborne PM passively, providing a direct, continuous readout with data storage for subsequent analyses[4]. The pDR uses light (wavelength of 880nm) with a scattering coefficient range (1.5×10^{-6} to 0.6 m^{-1}) to illuminate particulate and estimate light scattered[4,5]. Calibration by the manufacturer is performed using a gravimetric standard, International Organization for Standardization Fine test dust[4]. Given the working principle of the nephelometer and results from previous studies, concentration readings are subject to possible bias as a result of differences in aerosol characteristics and sampling conditions[5–7]. Specifically, adjustments for relative humidity during measurement and conversion to gravimetric equivalents need to be performed.

Background

Adjusting Recorded Particulate Matter Data for Relative Humidity

Changes in particle size distribution with increasing humidity can result in an overestimation of PM concentration[8]. To account for the influence of relative humidity (RH) in nephelometric measurements, a correction factor is typically applied. This correction factor can be calculated as the ratio of the humidity influenced PM nephelometric concentration to the humidity independent PM concentration. Dividing the nephelometric measurements by this correction factor will adjust for the PM-humidity bias. Since PM composition and size may impact how humidity is accounted for, it is preferable to estimate the correction factor in laboratory settings where particulate size and composition can be carefully varied and characterized[9,10]. However, when laboratory studies are not feasible, or aerosol characteristics are unknown or highly variable, the correction factor can be estimated using statistical models and field sampling data. Published approaches to assessing humidity bias adjustment have used either measurement from paired filter-based monitors (corrected for humidity by equilibration of filters in humidity controlled weigh rooms prior to weighing) or from nephelometers with a heater attached to the inlet[7,11]. Richards *et al.* utilized heaters attached to the inlet of nephelometers to eliminate the influence on PM measurements from high RH levels[6], while Wu *et al.* questioned the ability of the heater attached to the inlet to remove the influence from high RH[8]. Since filter-based monitors incorporate a humidity equilibration step in the weighing process, paired gravimetric and nephelometer samples are more commonly used to estimate humidity correction factors.

Utilizing data from different sources to account for RH, previous studies demonstrated two main humidity adjustment equations to estimate the correction factor. An empirical adjustment equation derived from experimental data of Laulainen *et al.*[12] fits well with data from several studies[11,13]:

$$\text{Correction Factor} = \frac{\text{Nephelometric PM}}{\text{Gravimetric PM}} = a + \frac{b \times RH^2}{1-RH} \qquad (1)$$

where a is equal to 1 and b is equal to 0.25, as reported by Chakrabarti *et al.*[11]. No discussion was given regarding the determination of these parameters.

Another adjustment derived from simple linear regression by Richards *et al.*[6], was proven to fit well in data presented by Wu *et al.*[7]:

$$\text{Ln}(\text{Correction Factor}) = \text{Ln}\left(\frac{\text{Nephelometric PM}}{\text{HAN PM}}\right) = a + b \times \text{Ln}(1 - RH) \qquad (2)$$

where a and b are empirically determined parameters by linear regression, and the denominator is humidity adjusted nephelometric PM concentration (HAN PM) measured by a nephelometer with a heated inlet.

These equations apply for RH values above 60%, which is believed to be the threshold at which nephelometers begin to significantly overestimate particle concentrations as a result of RH increase[7,10,11].

Converting Recorded Particulate Matter Data to Gravimetric Equivalents

To estimate equivalent mass concentrations, passive nephelometer readings are usually adjusted to account for differences in the manufacturer calibration aerosol and the real-world aerosol being sampled using co-located gravimetric samples. Regression models are typically used to relate gravimetric PM measurements and humidity adjusted nephelometric PM[7,11,14–16]:

$$\text{Gravimetric PM} = a + b \times \text{HAN PM} \qquad (3)$$

where a and b are empirically determined parameters by linear regression, and HAN PM is humidity adjusted nephelometric PM. The humidity adjusted nephelometric measurement is generally an overestimate of the gravimetric equivalent PM concentration by a factor ranging from slightly greater than one to three[7,16–19]. None of the previously published gravimetric correction factors have been determined for the large range of concentrations seen in indoor biomass cookstove environments where long-term time-weighted average concentrations can span more than three orders of magnitude[7,14,16–19].

Methods

Study Overview

The study site in rural, southern Nepal was established by the Department of International Health at Johns Hopkins Bloomberg School of Public Health. Under the broad effort known as the Nepal Nutrition Intervention Project - Sarlahi (NNIPS)[20], several studies are underway, one of which includes a cookstove intervention trial designed to assess indoor PM exposure to adverse health effects. Located in Sarlahi District, Nepal, the entire NNIPS site consists of 32 areas referred to as Village Development Committees (VDCs), four of which are currently participating in the cookstove trial. Sarlahi is a rural area located in the Terai region of southern Nepal (on the border with Bihar State in India) and is representative of southern Nepal and most of northern India with elevation approximately 200 meters above sea level[20]. For our study, we utilized data from the parent cookstove trial as well as a substudy within this trial (known as the Simulated Cooking Test). Both studies utilized the pDR-1000 and HOBO U10 Temperature and Humidity Data Logger (Onset Computer Corporation, Pocasset, MA), recording data in 10-second intervals.

Parent Cookstove Trial

Data from air quality studies measuring indoor PM associated with traditional cookstove emissions were collected at this study site. Cooking with traditional stoves, comprised of clay mud, bricks, rice husk, and cow dung, are common in this area of Nepal[21]. The cookstove trial includes 2,854 homes, each with at least two 24-hour indoor PM concentration measurements using the pDR-1000. Data from this study included co-located pDR-1000 and humidity measurements.

Simulated Cooking Test

Co-located pDR-1000, gravimetric PM, and humidity samples were collected during simulated cooking events in a mock house and in homes participating in the parent cookstove trial.

Mock house sampling was conducted in a house built to represent a typical house in this region, determined from data collected during the parent cookstove trial. The mock house consisted of a 1-room floor plan with 1-window and door, with the ability to close and open these features. Housing material consisted of bamboo with mud, logs, and tree branches, while roof material consisted of half tile and half thatch/grass. House dimensions were: length 3.85 meters, width 4.65 meters, ground to the lowest point of the roof 1.8 meters, ground to the apex of the roof 2.7 meters, window 0.6 meters by 0.6 meters (located on the back wall of the house), and door frame 1.28 meters width by 1.64 meters height (located on the front wall). Both the window and door had a hinged wood-framed metal panel attached to it that allowed for opening/closing according to the prescribed test conditions. In addition, a traditional mud-based cookstove with two openings was built inside according to typical practices for stove construction, located on the floor of the back wall. Co-located PM and humidity samples were collected during cooking activities with different fuel types using a standard cooking protocol.

To assess pDR-1000 performance, a modified version of the Water Boiling Test (WBT) 3.0 was used[22]. A standard cooking session was simulated by bringing 2 pots of water (5 Liters in each) to a rolling boil from ambient temperature (approximately 30 minutes). The fire was then extinguished. Passive PM sampling was initiated 30 minutes prior to the cook test and continued for an additional two hours post-fire, while gravimetric sampling took place only during the active flame period. For this analysis, Passive PM data were examined only during the active flame period. In addition, pDR-1000s were zeroed before every test using procedures recommended by the manufacturer. A limited number of co-located pDR samples were collected in the mock house to assess precision, which resulted in an average precision of 11%. This value is in good agreement with a previously published study finding precision to be from 3% to 13%[5].

Gravimetric PM was collected with a $PM_{2.5}$ inlet (BGI, Waltham MA) on Teflon filters (37mm 2.0μm pore PTFE Membrane Filter w/ PMP ring Pel Life Sciences, Ann Arbor MI) using a personal sampling pump (5400 BGI Inc., Waltham MA) at a flow rate of 4L/min. Flow rates were calibrated before and after sampling using a Drycal Flowmeter (DC Light BIOS Intl., Butler NJ). Filters were pre and post-weighed in a temperature and humidity controlled weighing room using a XP2U Microbalance (Mettler Toledo, Columbus OH) located at the Johns Hopkins Bloomberg School of Public Health.

Pre-weighed Teflon filters were loaded into Polypropylene filter cassettes (SKC Inc., Eighty Four PA), along with filter pads (Pall Life Sciences, Ann Arbor MI) and 37mm drain discs (model no. 230800 Air Diagnostics and Engineering, Harrison ME) at the Harioun clinic in a field-developed clean box to minimize contamination during assembly while in

Nepal. The sampling equipment in the mock house was located 1 meter from the stove and 1.8 meters above the floor. After sampling, the filter cassettes were placed in plastic bags until returned to the United States for post-weighing. For quality control purposes, duplicate gravimetric samples were collected for 10% of the test runs, resulting in an average duplicate precision of 12% and relative SD of 9%. Limit of detection was calculated to be 5μg and all filter weights were blank corrected (2μg).

Upon completion of testing in the mock house, the same test protocol was performed in 50 occupied homes that were randomly selected from the 2,854 households involved in the parent cookstove trial from two of the four cookstove VDC's. Due to equipment failure during sampling, 10 homes were excluded from analysis. Homes chosen reflected typical housing based on preliminary data from the NNIPS cookstove intervention trial study (i.e., have 1 window/door, similar in size and composition to the mock house). Eligible homes met the criteria of only using cookstoves for personal food production, agreeing to not have any other sources of combustion ongoing in the house during testing, and were confirmed to ensure that no occupants used tobacco. Testing was conducted midday in order to minimize interference to participants' daily routines as well as smoke infiltration from surrounding homes' cooking activities. Fuel type was allowed to vary based on cooking preferences of the home. The type of fuel was observed for subsequent analysis of results by fuel type.

Statistical Analysis

Data from different fuel types, including wood, crop waste, and wood with anything else (i.e., dung, crop waste, or a mixture), window/door status (all closed vs. anything open), home type (mock vs. occupied), and kitchen size were incorporated into the analysis to evaluate different adjustment equations. The influence of these variables on humidity and gravimetric adjustment was evaluated by adding these variables into regression models, and then assessed for inclusion in the final model based upon significance of their p-values and other standard regression model evaluation procedures[23].

Root mean square errors (RMSEs) of predicted values in each equation were calculated in order to assess fit and accuracy of prediction of the equations to our data. RMSE was estimated by incorporating all data points into the equation when parameters were not estimated from our data. For equations where parameters were estimated from our data, the RMSEs were calculated by conducting leave-one-out cross validation. In detail, one data point was removed out of 65 total points as a test point, whereupon parameters for the equation were trained (i.e., re-estimated) with the remaining 64 data points and used to predict a value for the test point. This process was repeated 65 times for each data point; at each iteration the squared residual error (difference between the predicted and "true" test point) was calculated and then averaged. The square root of these mean squared errors (RMSE) provides a measure of prediction accuracy on the original scale of the data.

Cross validation was also conducted to assess overall fit and prediction accuracy for the two-step quality control methods. After initially removing one data point randomly, the humidity adjustment equation was trained with the remaining data points. Parameters of the gravimetric conversion equation were then ascertained with the same data points adjusted for RH. Applying the test value sequentially on both equations, we were able to calculate the cross validated RMSE.

All statistical analyses were performed in the R Statistical Computing Environment (Version 3.0.2; 2013-09-25, Vienna, Austria). Packages used for data analysis and graphics creation were chron[24] and ggplot2[25].

Results and Discussion

Humidity adjustment

Three separate humidity adjustment equations derived from Equations (1) or (2) (referred to as (1a), (1b), and (2a) in Table 1) were examined. Equation (1a) was derived from Equation (1), with the parameters given in Chakrabarti's 2004 publication[11]. For Equation (1b), we fitted Equation (1) with our data collected in the mock house and occupied homes, where the correction factor was calculated as the ratio of average pDR-1000 PM concentration and the corresponding gravimetric $PM_{2.5}$ concentration. Similarly, we fitted Equation (2) with our data to derive Equation (2a). Table 1 presents the regression parameters for the three equations. The range of nephelometric PM concentration data was observed to be from ~600 $\mu g/m^3$ to ~66,000 $\mu g/m^3$.

As shown in Figure 1, all humidity adjustment equations agree well with each other and provide a reasonable description of the correction factor versus humidity results. According to the RMSE estimated by cross validation presented in Table 1, all equations performed equally with a suggestion that Equation (2a) provided a slightly better fit. Adjustment with and without a 60% humidity threshold did not make a large difference in fit, with Equations (1b) and (2a) performing slightly better without a threshold and Equation (1a) performing better with a threshold. Although Equation (1b) and Equation (2a) were based on different approaches, both demonstrated similar fitted lines and RMSE after incorporating experimental data, suggesting that as long as experimental data were incorporated, applying any of the two humidity adjustment equations will not dramatically affect the results.

Below 40% RH, most data points have correction factors less than 1.0, with all correction factors less than 1.0 for RH less than 30%, indicating underestimation of PM concentration by nephelometers at very low humidity. Similar trends were identified in Chakrabarti *et al.*

where this underestimation was noted to start at 20% RH[11]. This observed trend could be due to PM size reduction during low RH levels. In addition, filter weights were determined after filter equilibration at 35% RH supporting the observation of pDR-1000 underestimation relative to gravimetric at low humidity. It should be noted that a substantial increase from a correction factor above 1.0 was not observed until 70% RH in our data, 75% RH in Chakrabarti's 2004 data, and 50% and 65% RH in Day's 2001 data[11,13]. These results, combined with our observation of a negative bias at low humidity, suggest that the choice of 60% RH threshold for humidity is not well supported.

Table 1. Summary of regression parameters and RMSE for the three humidity adjustment equations.

Equation	Parameter a (95% CI)	Parameter b (95% CI)	RMSE† with Threshold	RMSE† without Threshold
Equation (1a)*	1#	0.25#	0.506	0.514
Equation (1b)**	0.72 (0.65, 0.79)	0.38 (0.33, 0.44)	0.521	0.495
Equation (2a)***	-0.72 (-0.82, -0.62)	-0.82 (-0.93, -0.71)	0.515	0.490

#Based on original Chakrabarti equation, no confidence intervals were provided[11]
*Equation (1a) = Chakrabarti's original humidity adjustment equation
**Equation (1b) = Chakrabarti's humidity adjustment equation fitted with simulated cooking test data
***Equation (2a) = Richards's humidity adjustment equation fitted with simulated cooking test data
†RMSE is unitless

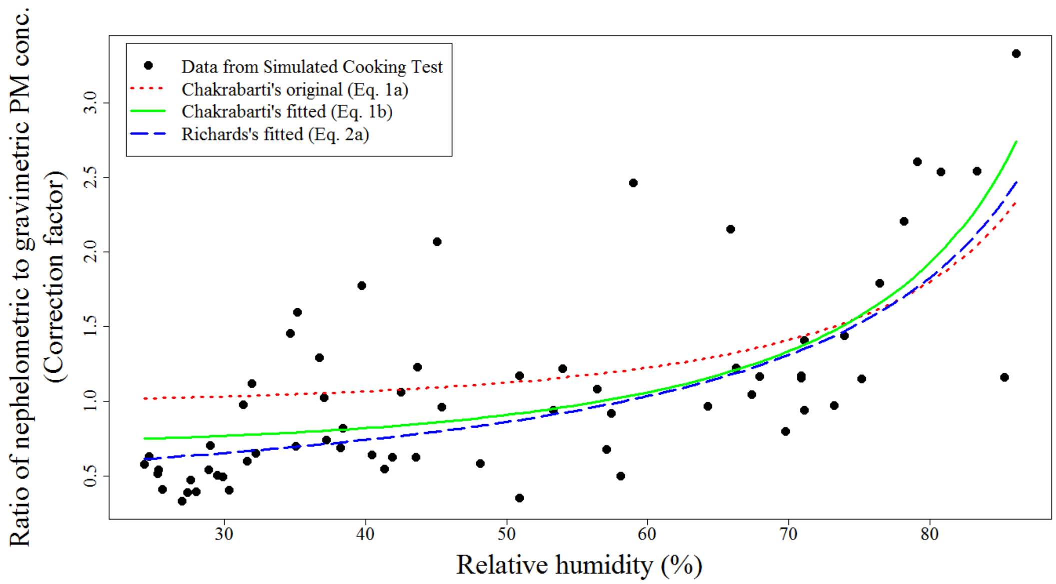

Figure 1: Humidity adjustment Equations (1a), (1b), and (2a) displayed with data collected during cooking for both the mock house and occupied homes.

To illustrate the influence of the three humidity adjustment Equations (1a, 1b, and 2a) using real-world samples, we compared 24-hour PM concentration data adjusted for RH collected using pDR-1000's in 10 homes within the parent cookstove trial. As shown in Figure 2, the means of humidity adjusted nephelometric PM concentrations are similar using the three adjustment equations across all household average RH values, while Equation (1b) and Equation (2a) without a threshold lead to higher means of adjusted values in the lower RH range. These results illustrate that humidity adjustment without threshold provides better compensation for the negative bias at low humidity, which is consistent with the RMSE values reported in Table 1.

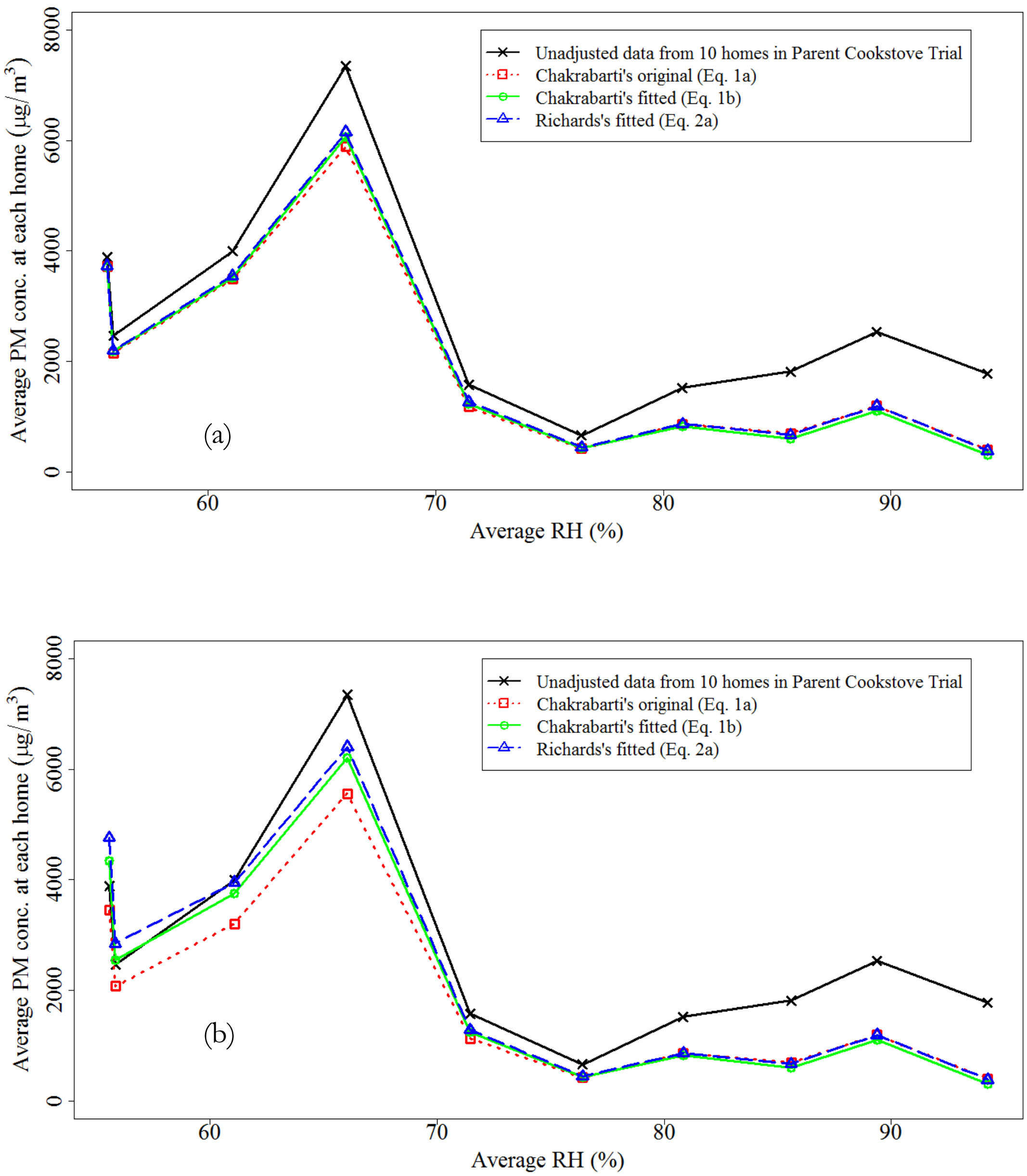

Figure 2: Average PM concentrations of 10 homes adjusted with three humidity adjustment equations (a) with a RH threshold and (b) without a RH threshold.

An additional comparison of the three humidity adjustment equations was conducted by applying the humidity adjustment equations to 24-hour pDR data from all 2,854 homes. There was no statistically significant difference in the mean PM concentrations after humidity adjustment for the equations (Equations (1a), (1b), and (2a)) that incorporated a 60% RH threshold (ANOVA p=0.7). Mean PM concentrations were statistically different when the same equations incorporating no RH threshold were used (Kruskal-Wallis $p<0.0001$). However, when only considering equations trained with our data (Equations (1b) and (2a)), we identified no significant difference with or without a RH threshold. These results are consistent with the relationship demonstrated in Figure 1.

Gravimetric Conversion

Once the humidity adjustments were made, we compared the adjusted pDR-1000 average results to the co-located gravimetric $PM_{2.5}$ concentrations using four equations (Equation (3) previously discussed, along with Equations (4-6) discussed below). From the linear regression equation (Equation (3)), estimated gravimetric PM concentration is equal to humidity adjusted nephelometric PM times the slope coefficient, while forcing the equation through the origin. Our Simulated Cooking Test data had average concentrations that spanned more than three orders of magnitude. In addition, our data in Figure 3 indicated a non-linear relationship between humidity adjusted nephelometric PM and gravimetric PM. Therefore, we evaluated the linear relationship between the natural log of both gravimetric PM and humidity adjusted nephelometric PM (Equation (4)):

$$\text{Ln(Gravimetric PM)} = a + b \times \text{Ln(HAN PM)} \qquad (4)$$

where *a* and *b* are empirically determined parameters by linear regression of log transformed experimental data. We also evaluated a slightly altered version of Equation (4). Recognizing that the gravimetric to nephelometric PM relationship had a turning point, we included a spline term that yielded the following equation.

$$\text{Ln(Gravimetric PM}_{2.5}) = a + b \times \text{Ln(HAN PM)} + c \times (\text{Ln(HAN PM)} - d) \qquad (5)$$

where d represents the spline point and c is equal to zero when the natural log of nephelometric PM is smaller than d. A range of possible spline points was determined by observing the relationship between gravimetric and humidity adjusted PM concentrations. This range spanned 7.5 to 12 for natural log of nephelometric PM concentration. Utilizing increments of tenths, values within this range were fitted into the equation. Resulting cross-validated RMSEs were compared to choose the best spline point (d). Another equation we evaluated to assess the nonlinear gravimetric to nephelometric relationship was in quadratic form

$$(\text{Gravimetric } PM_{2.5}) = a + b\times\text{Ln}(\text{Nephelometric PM}) + c\times(\text{Ln}(\text{Nephelometric PM}))^2 \quad (6)$$

where parameters were empirically determined by regression.

Table 2 and Figure 3 summarize the regression parameters and RMSE values for four gravimetric conversion equations (Equations (3), (4), (5), and (6) respectively) with data adjusted using three humidity adjustment approaches (Equations (1a), (1b) and (2a) with and without a 60% RH threshold). Based upon the RMSE values, the new linear gravimetric conversion equation with log transformed variables fits better to RH adjusted data (both with and without a threshold) compared to the traditional linear approach. Moreover, the new linear gravimetric conversion equation utilizing a quadratic variable (Equation (6)) fits the best to RH adjusted data (both with and without a threshold) compared to all equations, but only slightly better than the equation utilizing a spline variable (Equation (5)). The curves in Figure 3(a) and 3(b) are consistent with the RMSE values estimated via cross validation. The range of gravimetric PM concentration in our study was observed to be from ~600 $\mu g/m^3$ to ~26,000 $\mu g/m^3$, while the upper limit for most other published studies[16] did not exceed 600 $\mu g/m^3$. This broader range of PM concentration relative to other studies is one possible explanation for this observed improved performance when utilizing either a log transformed, spline, or quadratic approach during gravimetric conversion. The RMSE values in Table 2 are relatively similar by approach, suggesting that utilizing the three RH adjustment equations, with or without a 60% RH threshold, provide similar gravimetric equivalent estimates with a preference towards a spline or quadratic approach.

Table 2. Summary of gravimetric equivalency conversion for the three humidity adjusted results (with and without a 60% RH threshold) utilizing a linear, linear with log transformed variables, linear with log transformed and spline variable, and linear with log transformed and quadratic variable equations.

Equation Type	Coefficient and RMSE Values	With threshold			Without threshold		
		Eq. 1a	Eq. 1b	Eq. 2a	Eq. 1a	Eq. 1b	Eq. 2a
Linear eqn. (Equation 3)	a	0	0	0	0	0	0
	b	0.848	0.845	0.831	0.892	0.757	0.696
	RMSE†	3927	4002	4005	3956	3982	3955
Linear eqn. w/ log transformed variables (Equation 4)	a	2.726	2.750	2.753	2.723	2.510	2.395
	b	0.711	0.707	0.706	0.715	0.724	0.730
	RMSE†	2889	2977	2969	2932	3001	2990
Linear eqn. w/ log transformed and spline variables (Equation 5)	a	0.859*	0.872*	0.822*	0.565*	0.921*	0.868*
	b	0.949	0.948	0.953	0.995	0.921	0.917
	c	-4.051	-0.411	-0.416	-0.430	-0.471	-0.502
	d	8.4	8.4	8.4	8.2	8.9	9.1
	RMSE†	2703	2768	2773	2742	2650	2620
Linear eqn. w/ log transformed and quadratic variables (Equation 6)	a	-4.867*	-4.945	-4.951	-4.994*	-6.049	-6.607
	b	2.502	2.527	2.522	2.544	2.722	2.809
	c	-0.105	-0.106	-0.106	-0.107	-0.115	-0.119
	RMSE†	2682	2750	2759	2715	2652	2619

*Not significantly different from 0 (p>0.05).
†RMSE is μg/m^3

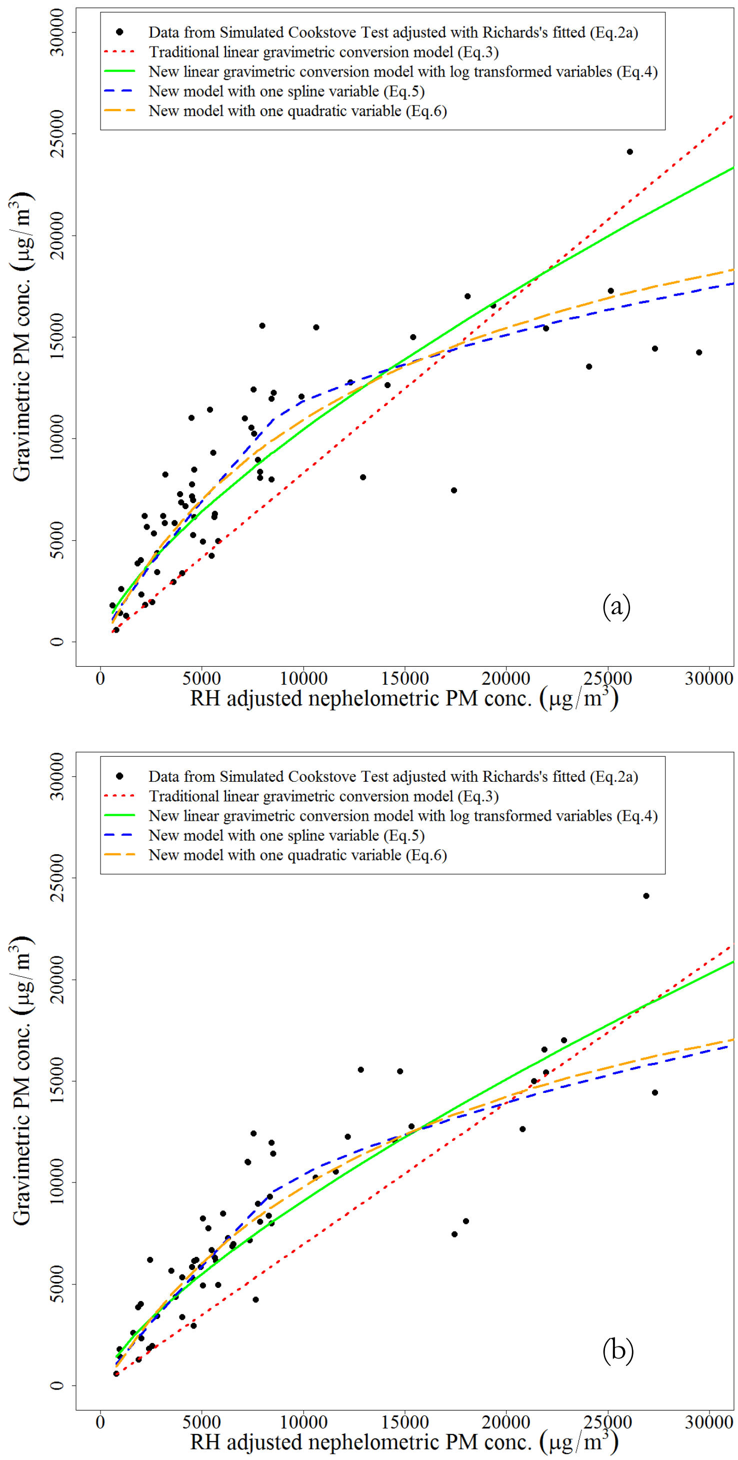

Figure 3: Linear, linear with log transformed variables, linear with spline variable, and linear with quadratic variable equations for gravimetric conversion based on nephelometric PM concentrations adjusted with RH adjustment Equation (2a). (a) RH adjustment with 60% threshold; (b) RH adjustment without 60% threshold

Combined Quality Control Method versus the Two-Step Method

To simplify the two-step process, we propose combining the humidity and gravimetric equivalency adjustments into one equation. Based on the humidity adjustment work by Richards *et al.* and the linear gravimetric conversion equation with log transformed variables (Equations (2) and (4), respectively), a combined humidity and gravimetric equivalency adjustment equation was derived. This derivation yielded:

$$\text{Ln(Gravimetric PM}_{2.5}) = 3.102 + 0.701\times\text{Ln}(1-\text{RH}) + 0.717\times(\text{Ln(Nephelometric PM)} \quad (7)$$

where parameters were determined based on data from the simulated cooking test.

Unlike the traditional two-step quality control method, which has RH adjustment and gravimetric conversion done separately, the 60% RH threshold is not used for this new combined quality control method (Equation (7)). Given the issues associated with the arbitrariness of 60% RH threshold and the possible negative bias at low humidities discussed earlier, excluding it when conducting adjustments improves the accuracy of the adjusted data.

Another combined humidity and gravimetric equivalency adjustment equation was derived from Equations (2) and (5), respectively. This derivation yielded inclusion of a spline term, thus resolving into:

$$\text{Ln(Gravimetric PM}_{2.5}) = 1.577 + 0.691\times\text{Ln}(1-\text{RH}) + 0.913\times(\text{Ln(Nephelometric PM)} + d\times(\text{Ln(Nephelometric PM)} - f) \quad (8)$$

where f is 8.1. This was determined by examining the relationship between the gravimetric and unadjusted nephelometric PM, and comparing cross-validated RMSEs of equations with different spline points as described above. This relationship was further evaluated via the use of RMSE to finalize f. It should be noted that when the log nephelometric PM concentration is >f, the parameter d=-0.254; otherwise, the parameter d=0, thus resulting in the spline term being excluded.

An additional combined approach was developed from Equations (2) and (6), respectively. This approach resulted in a quadratic term, which yielded:

$$Ln(Gravimetric\ PM_{2.5}) = -0.176 + 0.692\times Ln(1-RH) + 1.471\times(Ln(Nephelometric\ PM) - 0.043\times(Ln(Nephelometric\ PM))^2 \quad (9)$$

Parameters from Equations (8) and (9) were determined from the simulated cooking test.

To evaluate the combined approaches (Equations (7), (8), and (9)) we compared their performance to the eighteen combinations of RH adjustment and gravimetric conversion for the traditional two-step quality control method (linear gravimetric equivalency equations eliminated) (Table 3). As shown in Table 3, regardless of which RH adjustment equation used, there is minimal impact on the prediction accuracy of the two-step approach. The two-step quality control combinations with and without the 60% RH threshold have similar accuracy in prediction when both quality control methods are applied, thus further supporting the rational of not including a threshold.

According to Table 3, the combined equation approach utilizing a spline (Equation (8)) provides the best RMSE amongst the three combined approaches. The combined quality control methods have RMSE values that are higher than the lowest reported RMSE values for the two-step approaches. However, it is important to consider potential explanations that could result in these varying RMSE values. The approach of the two step quality control methods utilize the same reference value twice, which could lead to overfitting, thus a lower RMSE value.

An important point to note is that at lower PM concentration and RH ranges, the quality control methods suggest that nephelometric data may underestimate gravimetric concentration. This could be the result of our broad range in PM concentration values collected during biomass fuel combustion, which has not been well studied utilizing the pDR-1000. It should also be noted that making adjustments below nephelometric PM concentration of 600 μg/m^3 could lead to uncertainty due to the absence of data below this value.

Table 3. Summary of different overall pDR-1000 adjustment approaches comparing the RMSE values.

Quality Control Method Type	Approach Number	RMSE (μg/m^3)
Combined Approach (1)	1	3066
Combined Approach--spline (2)	2	3007
Combined Approach—quadratic (3)	3	3243
Equations (1a), (1b), & (2a) (without threshold)+Equation (4)	4, 5, 6	2922, 2959, 2962
Equations (1a), (1b), & (2a) (without threshold)+ Equation (5)	7, 8, 9	2641, 2600, 2593
Equations (1a), (1b), & (2a) (without threshold)+ Equation (6)	10, 11, 12	2696, 2628, 2607
Equations (1a), (1b), & (2a) (with threshold)+Equation (4)	13, 14, 15	2925, 2948, 2948
Equations (1a), (1b), & (2a) (with threshold)+Equation (5)	16, 17, 18	2652, 2687, 2689
Equations (1a), (1b), & (2a) (with threshold)+Equation (6)	19, 20, 21	2716, 2736, 2744

Further analysis explored the impact of fuel type (wood, crop residue, mix of wood and other), home type (occupied vs. mock), kitchen size, and window/door status on Equation (7). These variables were not statistically significant and therefore were not included.

Even though the two-step combinations provide for a better fit according to the RMSE values, the new combined quality control method holds several advantages for future applications. First, the combined quality control method involves only one reference value, excluding the possibility of over-fitting with having to use multiple reference values. In addition, it is quicker and easier to perform an adjustment using an integrated approach (as done in Equation (7)) than to have to perform multiple steps as is done in the two-step approach. Furthermore, integration of a spline or quadratic term requires additional examination of data in order to properly assess whether their use is warranted. For our data, the equation with the spline term (Equation (8)) provides for the best RMSE across all one-step equations. Given this along with the advantages of using a one-step method, Equation (8) is believed to be the best approach with all that has been presented.

Conclusions

In this paper we have explored a range of humidity and gravimetric equivalency adjustment approaches. Three approaches (Equations (1a), (1b), and (2a)) to humidity adjustment all performed equivalently (similar RMSE values). Previous research suggests that humidity overestimation bias is observed when humidity exceeds 50% to 75%[11,13]. Our results suggest that an overestimation bias is close to the 75% RH value. In addition, an underestimation bias exists at very low RH (<30%). As a result, we have proposed humidity adjustment equations that encompass the entire RH range. Furthermore, the humidity adjustment using the equation by Chakrabarti *et al.* (Equation (1a)), which was derived by sampling ambient PM in Southern California, performed similarly to humidity adjustments calculated using cookstove PM samples collected in Nepal. This suggests that humidity adjustments do not vary widely based on the characteristics of the PM being sampled.

Given the wide range of concentration in our study, the new linear gravimetric conversion equations with log transformed variables performed better than the traditional linear regression gravimetric conversion equation. Furthermore, gravimetric conversion equations incorporating a spline or quadratic term provided for the best fit amongst equations with log-transformed variables. The two-step quality control combinations utilizing the new linear gravimetric conversion equation with log transformed variables also have better accuracy in prediction than those utilizing the traditional linear gravimetric conversion equation (data not shown). Our PM concentration range, collected during biomass burning, was much broader than other published studies, which could explain why the new linear gravimetric conversion equations with log transformed variables and either a spline or quadratic term demonstrated a better fit. Moreover, given the higher concentration range observed in our study, the adjustments proposed should be applied for nephelometric PM concentration ranging from ~600 $\mu g/m^3$ to ~66,000 $\mu g/m^3$.

In general, utilization of the traditional two-step method is less preferred than the integrated RH and gravimetric conversion methods presented in this paper (Equations (7), (8), and (9)) for a variety of reasons. Principally, the integrated method is preferred because it only involves one response variable (gravimetric $PM_{2.5}$ concentration), avoids overfitting, does not contain a RH threshold, and is relatively quick and straightforward. For our data, we recommend using the combined method that includes a spline term (Equation (8)) for quality control, based on the RMSE value. In order to achieve the best adjustment, we recommend readers to assess their own data to choose which combined quality control method to utilize, using the approaches outlined in this paper. Providing an approach to determine humidity corrected gravimetric equivalent $PM_{2.5}$ concentrations will allow systematic comparison exposure response relationships in health studies using the pDR-1000.

3 Determining Particulate Matter and Black Carbon Exfiltration Estimates for Traditional Cookstove Use in Rural Nepalese Village Households

Introduction

The Himalayan glaciers, also known as the third pole of the world, provide fresh water via glacial melt to more than a billion people across South and East Asia[1]. These glaciers have begun melting at an alarming rate over the past decade, increasing the potential for these glaciers to undergo significant retreat by midcentury thus threatening the fresh water supply for this region[1]. Furthermore, alterations in the overall hydrological cycle in South Asia is becoming more apparent[2]. Monsoons are deviating from typical seasonal patterns, thus having a wide range of impact upon a number of groups within this region including farmers who are responsible for feeding a significant portion of the world's population[3,4]. While it is believed that glacial retreat is driven by an increase in global warming due to greenhouse gases, the rapidity of the retreat along with a 0.3°C warming per decade over the past 30 years indicate that other factors may be at play[1]. Primarily, black carbon emitted into the atmosphere and subsequent deposition on glaciers and snow pack is thought to be a major contributor to the change in climate and accelerated glacial retreat in this region[5].

Black carbon (BC), a component of particulate matter (PM), is produced by the incomplete combustion of fossil fuels, the burning of biomass from forest fires, and through households as well as factories that use wood, dried animal manure, or crop residue for cooking or other energy needs[6]. Worldwide, more than three-quarters of the black carbon produced is thought to come from developing countries, generated from cookstoves, open burning, and older diesel engines[4]. It is estimated that around 2.7 billion people worldwide cook using biomass fuel, most of which are poor and in developing countries[7]. Annual emissions of BC from biomass burning in cookstoves have been estimated at 20% of the total global BC emissions[8]. Biomass cooking alone is believed to contribute about two-thirds of BC emissions within South Asia[9].

Within the Himalayas, BC may be responsible for as much as 50% of the total glacial retreat seen thus far[9]. Recent studies have estimated that BC is the second or third largest overall contributor to global warming, surpassed only by CO_2 and possibly methane[10]. It is important to note however, that BC has an average residence time in the atmosphere of a few days to weeks relative to greenhouse gases which range from years to centuries[10]. Due to the short residence time in the atmosphere, mitigating BC emissions can produce almost immediate effects in terms of reduced radiative forcing and subsequently large co-benefits for public health[10,11]. Regional scale BC emission estimates, however, have a significant, 2-5 fold, uncertainty[5]. The Indo-Gangetic Plain region (IGP) has been identified as a regional hotspot for BC emissions[10]. The IGP is one of the most densely populated regions and large uncertainties exist for published BC emissions[12,13].

Background

Cookstove emissions create indoor exposures and contribute to ambient air pollution through passive exchanges between indoor and outdoor air (indirect venting) and direct, active venting (i.e., chimney) to the outdoors. Salje *et al.* recently identified exfiltration of biomass pollution as a significant contributor to indoor PM pollution in non-biomass using homes in Dhaka, Bangladesh[14]. Open-design cookstoves, where combustion byproducts are expelled directly into the indoor environment, result in high concentrations of PM and other pollutants inside the home[15–19]. BC and PM emission factors for different stove designs have been determined in laboratory settings[20–22]. These emission factors can vary by 5-6 fold depending on fuel type[20]. In addition, the BC component of PM under 2.5 micrometers in diameter ($PM_{2.5}$) has been shown to vary from 5-52% using laboratory-based test burns[20]. Laboratory-based studies are of limited utility for estimating household BC and PM emissions because they lack the ability to incorporate factors present in real-world scenarios. Characterization of cookstove emissions emanating from a house requires an assessment of the fraction of PM remaining indoors and exfiltrating from the house. A fraction of PM will settle and deposit on indoor surfaces as well as in cracks within the walls of the house, while the rest will exfiltrate to the outdoor environment. Studies translating laboratory-based cookstove emissions to ambient emissions from a house often use hypothetical air exchange and particle deposition rates resulting in a fractional exfiltration estimate. For example, an 80% exfiltration estimate of PM emitted by biomass combustion, a non-published value based upon hypothetical particle deposition rates, has been cited[20] without any field validation. Furthermore, measurement of air exchange rates in village housing is extremely limited[23–25] compounding our poor understanding of how much PM may be exfiltrating to the outdoor environment. Estimates of the amount of PM and BC that exfiltrate from homes are needed to reduce uncertainty in emission inventories. Furthermore, exfiltration estimates can be used to evaluate the impact of cookstove interventions (i.e., use of a chimney), designed to improve indoor air quality, on outdoor air quality.

This paper presents air exchange rates and PM exfiltration estimates from homes in rural Nepal that utilize traditional, open-design cookstoves. Estimates of variability are provided for exfiltration as a function of housing and fuel characteristics in a real-world setting. Furthermore, this paper assesses the BC to $PM_{2.5}$ ratio produced by biomass cooking in order to estimate BC exfiltration from homes. In combination with an assessment of indoor PM concentrations, PM and BC exfiltration fractions can be used to estimate house emissions to ambient air in order to better assess regional air quality and climate change impacts.

Methods

Study Overview

Located in rural southern Nepal, the study site was established by the Johns Hopkins Bloomberg School of Public Health Department of International Health. Under the broad effort known as the Nepal Nutrition Intervention Project - Sarlahi (NNIPS), a parent cookstove intervention trial is underway. This community-based, cluster randomized, step-wedge trial is characterizing indoor PM exposure in ~3,000 homes from traditional and alternative cookstoves, assessing primary health outcomes that include acute lower respiratory illness in children 1-36 months of age (ALRI), as well as birth weight and preterm birth among newborn infants[26]. Located in Sarlahi District, Nepal, the NNIPS site consists of 32 areas referred to as Village Development Committees (VDC's), 4 of which are currently participating in the cookstove intervention trial. Sarlahi is a rural area located in the Terai region of southern Nepal (on the border with Bihar State in India) and is representative of southern Nepal and most of northern India with elevation approximately 200 meters above sea level[26]. The exfiltration assessment was nested within the large cookstove intervention trial. Cooking with traditional stoves, comprised of clay, mud, bricks, rice husk, and cow dung, are common in this area of Nepal[27]. The typical cooking style in the area involves the burning of biomass fuels (wood, dried animal manure, and crop residue) in traditional, open-design mud cookstoves without direct ventilation to the exterior[26].

Mock and Occupied Home Sampling

In order to assess exfiltration estimates of PM, a mock house was built at the research site in Sarlahi District, Nepal. Based on parent intervention trial study data, the house was representative of a typical household kitchen in this area with respect to size, material, and number of openings. Homes in this region typically consist of mud, wood, brick or cement

Figure 1: Mock house built in study area

walls with thatch roofs[26]. The mock house consisted of a 1-room floor plan with 1-window and door, with the ability to close and open these features. Housing material consisted of bamboo with mud, logs, and tree branches, while roof material consisted of half tile and half thatch/grass. House dimensions were: length 3.85m, width 4.65m, ground to the lowest point of the roof 1.8m, ground to the apex of the roof 2.7m, window 0.6m by 0.6m (located on the back wall of the house), and door frame 1.28m width by 1.64m height (located on the front wall). Both the window and door had a hinged, wood-framed metal panel that allowed for opening/closing. In addition, a traditional mud-based cookstove with two openings was built inside according to typical practices for stove construction, located on the floor of the back wall.

Air quality data collected in the mock house included PM concentration collected passively with a DataRAM pDR-1000AN (Thermo Scientific, Franklin, MA), carbon monoxide concentration with an EasyLog USB CO Monitor (Lascar Electronics, Eerie, PA), and relative humidity using the HOBO Data Logger (Onset Corp., Bourne, MA). All of these devices were co-located, collected in the center of the house before, during, and after simulated cooking events (discussed later), and recorded data in 10-second intervals. The pDR-1000 was zeroed in the field prior to each deployment using procedures recommended by the manufacturer.

In addition, gravimetric $PM_{2.5}$ was collected with a $PM_{2.5}$ inlet (BGI, Waltham, MA) on Teflon filters (37mm 2.0μm pore PTFE Membrane Filter w/ PMP ring Pel Life Sciences, Ann Arbor, MI). A personal sampling pump (5400 BGI Inc., Waltham, MA) was utilized at a flow rate of 4 L/min. Flow rates were recorded before and after sampling using a Drycal Flowmeter (DC Light BIOS Intl., Butler, NJ). Filters were pre and post-weighed in a temperature and humidity controlled weighing room using a XP2U Microbalance (Mettler Toledo, Columbus, OH) located at the Johns Hopkins Bloomberg School of Public Health. Pre-weighed Teflon filters were loaded into polypropylene filter cassettes (SKC Inc., Eighty Four, PA), along with filter pads (Pall Life Sciences, Ann Arbor, MI) and 37mm drain discs (Model #230800 Air Diagnostics and Engineering, Harrison, ME) at the Harioun clinic in a field-developed clean box to minimize contamination during assembly while in Nepal. After sampling, the filter cassettes were sealed in plastic bags until returned to the United States, where they were disassembled and post-weighed. For quality control and assurance purposes, 10% duplicate samples were collected and all filter weights were blank corrected.

Fuels utilized during simulated cooking events in the mock house were derived from survey data from the parent cookstove trial. This data indicated that the most common types of fuel were wood by itself and a mixture of wood/dung/crop waste[28]. Fuel sources were obtained from the same area, same person, and subsequently sun dried to standardize moisture content. The same person performed all of the simulated cooking events in the mock house. Each fuel combination was tested three times. In addition, two boundary conditions were tested, where both the window and door were either completely open or closed during mock house testing.

The same test protocol was performed in 50 occupied homes randomly selected from the 2,854 households involved in the parent cookstove trial from two of the four cookstove VDC's. Homes chosen reflected typical housing based on data from the NNIPS cookstove intervention trial study (i.e., have 1 window/door, similar in kitchen size and composition to the mock house). Eligible homes met the criteria of only using cookstoves for personal food production, agreeing to not have any other sources of combustion (including tobacco) ongoing in the house during testing. Testing was performed midday to minimize interference to participants' daily routines as well as smoke infiltration from surrounding homes' cooking activities. Fuel type utilized and window/door status were observed in order to allow cooking preferences of the home to remain intact. The individual in the home that did the most cooking performed the simulated cook session and was supervised by local staff for protocol compliance. Kitchen volume and number of windows/doors were also recorded. Furthermore, setup was performed at the local VDC field office to protect the equipment.

Exfiltration Fraction Method Development

The air exchange rate (AER) and subsequent exfiltration fraction (EF), or the amount of PM that exits a home via natural ventilation, were determined via the concentration decay method[29]. This method involves measuring pollutant decay over time once the source of the contaminant is terminated or removed in order to determine passive air exchange rates between indoor to outdoor[29,30]. Hypothetical decay curves for a non-reactive gas and PM

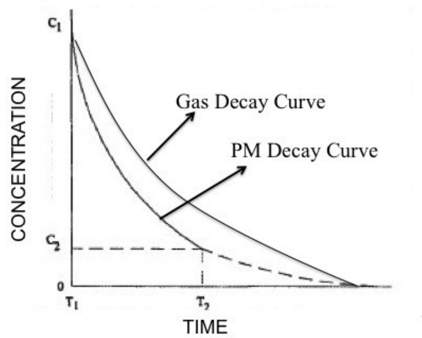

Figure 2: Hypothetical decay curves for PM and a non-reactive gas.

illustrating the concentration decay method are displayed in Figure 2. Assuming that the house is a simple one-room structure (i.e., no tight internal partitions), it can be treated as a single zone and a mass balance continuity equation can be used to estimate the exchange of air between indoors and outdoors. For non-reactive gases (i.e., no other mechanism of removal) this model assumes that the air exchange carries the pollutant from inside to out, or visa versa if one is interested in infiltration. The air exchange rate (AER) is calculated assuming perfect mixing conditions[29] using

$$\frac{Q}{V} = k * \frac{Ln\left(\frac{C_2}{C_1}\right)}{(t_2 - t_1)} \qquad (1)$$

where Q is the ventilation rate in m^3/minutes, V is the room volume (m^3), C_2 and C_1 are concentrations at various points in time, t_2 and t_1 are the corresponding time points (minutes), and k is a factor used to account for imperfect mixing conditions. The AER, $\frac{Q}{V}$, is determined by regression of $Ln(\frac{C_2}{C_1})$ of the non-reactive gas against Δ time. Equation (2) illustrates the simple linear regression model used to obtain this value.

$$Ln(C) = \beta_0 + \beta_1 \times t + \varepsilon, \text{ where } \varepsilon \sim N(0,\sigma^2) \qquad (2)$$

Where C is the concentration of the tracer gas, t represents time (minutes), and β_1 represents the AER. Ventilation studies typically utilize a tracer gas not commonly found in the environment, such as sulfur hexafluoride (SF_6), to measure AER's[31]. Given logistical limitations regarding acquisition and transportation of SF_6 to the study site, carbon monoxide (CO), deemed a viable substitute[32], was utilized as the tracer gas. CO was suitable because the concentrations produced inside the home during cooking were more than two orders of magnitude higher than background.

Figure 3 summarizes passive exfiltration pathways for PM from a house. For homes with traditional, open-design stoves, PM exfiltrates through open windows and doors as well as through cracks in the roof and walls (PM_E in Figure 3). Exfiltration for PM is complicated by the fact that the decay over time will be governed by the losses due to settling, surface deposition, as well as exfiltration. Calculating the AER based on the PM decay curve will therefore overestimate the real passive air exchange. To address this problem, two decay curves were measured as indicated in Figure 2. The slope of the PM decay curve was calculated in the same manner as the CO decay curve, utilizing Equations (1) and (2). The fraction of PM decay associated with exfiltration was calculated by comparing the simultaneous AER's of CO and PM. Since CO is a non-reactive gas, its AER will not be affected by surface deposition. As shown in Figure 2, the decay rate for PM will be faster than that for a gas. The ratio of the AERs, Equation (3), provides an estimate of the fraction of PM that exfiltrates to the ambient air:

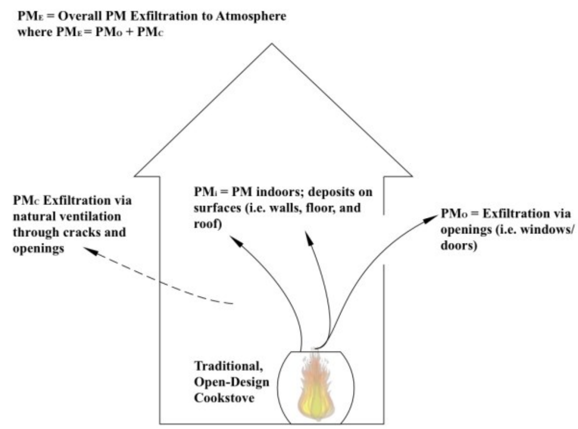

Figure 3: Pathways for particulate matter (PM) exfiltration from a house

$$EF_{PM} = \frac{S_{CO}}{S_{PM}} \tag{3}$$

where S_{CO} and S_{PM} are the slopes of the respective decay curves, or the AERs, when plotted according to Equation (2).

Exfiltration Fraction Test Protocol

A simulated cooking session was performed to create a fire within the stove resulting in elevated concentrations of PM and CO within the home. Prior to ignition, air-sampling equipment was deployed in the mock house at a height of 1m in front from the edge of the stove and 1.8m off the floor to maintain consistency between readings. Placement of sampling equipment in occupied homes relative to the mock house was slightly altered due to logistical limitations.

By generating PM and CO concentrations that were orders of magnitude higher than outdoors, PM and CO infiltration from outdoor air into the home (assumed to be low relative to the indoor generated contaminants) when using Equation (2) could be ignored. To determine PM and CO decay curves, a modified version of the Water Boiling Test (WBT) 3.0 was used[33]. A cooking session was simulated by bringing 2 pots of water (5 Liters in each) to a rolling boil from ambient temperature. The fire was then extinguished and remnant fuel removed from the house to halt further emissions. Passive PM, CO, and RH sampling were initiated 30 minutes prior to the cooking session and continued for an additional two hours post-fire extinguishment. Gravimetric sampling for $PM_{2.5}$ took place only during the active flame period. Passive PM and CO concentration decays were examined only after the flame was extinguished. Equations (2) and (3) were applied to the decay curves to determine the AERs for CO and PM and associated exfiltration fraction. All tests were performed during the Spring of 2012, considered the dry season as the outdoor temperature is moderate to high and precipitation is minimal.

Determining the BC fraction of $PM_{2.5}$

$PM_{2.5}$ filter samples were collected during the active flame period of the simulated cooking session in both the mock house and occupied homes in order to assess BC content of the PM using an optical method described by Yan et al[34]. It is assumed that BC is mostly contained on smaller particles (i.e., PM< 2.5 μm)[35], therefore measuring PM over a broader size distribution is not necessary.

Mixing Factor Assessment

Air exchange rate studies that utilize tracer gas decay techniques typically assume that the air in the space being tested is well-mixed[29]. If the air is not uniformly mixed, a mixing factor, k, can be used to obtain more accurate AER estimates[36–39]. The mixing factor is equivalent to 1 when the air is perfectly mixed and is <1 when incomplete mixing is present. In order to assess the degree of mixing in the test house, we compared the decay measured as described above to a decay curve measured with artificial mixing.

Tests conducted in the mock house during February of 2014 sought to assess decay curves between these two conditions. From the same sampling point, CO decay was measured (using the same modified water boil test) post-fire extinguishment as described above. For tests with mixing, two pedestal fans (Super Deluxe iii Crompton Greaves Corporation, Mumbai, India) were placed 0.5m from the wall in the northeast and southwest corners. Both fans rotated in 90° intervals and were placed such that their combined oscillation fields covered the entire room. To mix the air, both fans were turned on at their lowest setting upon one of the pot's reaching boiling point. When the second pot reached boiling point, the fire was extinguished and remnant fuel removed. The fans continued to run for an additional minute post fuel removal. CO concentration decay data was extracted from this point forward and analyzed accordingly to determine the AER. Fuel type was restricted to wood only and window/door status was set to either all open or all closed (with n=10 for each). Mixing factor, designated as k, is defined as

$$k = \frac{\text{MA}}{\text{NAM}} \qquad (4)$$

where MA is the average air exchange rate (h^{-1}) for the (ideal) artificially, well-mixed tests and NAM is the average air exchange rate (h^{-1}) for the non-artificially mixed tests that assumes perfect mixing conditions. If the ratio of the two exchange rates is equal to 1 then the space can be considered well-mixed[39].

Data Analysis

Exploratory analyses generating summary statistics for CO AERs, PM and CO ventilation rates, exfiltration fraction by fuel type and window/door status, and BC to $PM_{2.5}$ ratio were created. A linear mixed effects model approach with a random intercept and slope was utilized to examine household factors that are predictive of PM exfiltration. This regression model took the form

$$\text{EF}_{ijk} = \beta_0 + \beta_1 \times F_i + \beta_2 \times WD_j + b_{0k} + b_{2k} + \varepsilon_{ijk} \qquad (5)$$

where b_{0k}, b_{2k}, and errors ε_{ijk} are independent, Normal $(0,\sigma^2)$.

The fixed effects were fuel type (F) and status of window/door during cooking (WD). The random effect was house type (mock house designated as all one category and occupied homes, conversely, individually categorized), with the window/door status also being conditioned by house type to attain the random slope model.

For the mixing factor analysis, a Mann-Whitney-Wilcoxon test was applied to see if the ratio of the two AER means were different from 1 (perfect mixing). These values were assessed in order to determine whether or not perfect mixing could be assumed and if a mixing factor must be applied to AER measurements.

All statistical analyses were performed in the R Statistical Computing Environment (Version 3.0.2; 2013-09-25). Packages used for data analysis and graphics creation were chron[40], car[41], agricolae[42], lattice[43], plyr[44], ggplot2[45], mratios[46], and lme4[47].

Results and Discussion

An example of decay curves for PM and CO post-fire extinguishment determined in an occupied house is presented in Figure 4. Both curves mimic the hypothetical curves presented in Figure 2 and a similar relationship is seen for all tests performed. The more rapid decay of PM indicates that surface losses are significant.

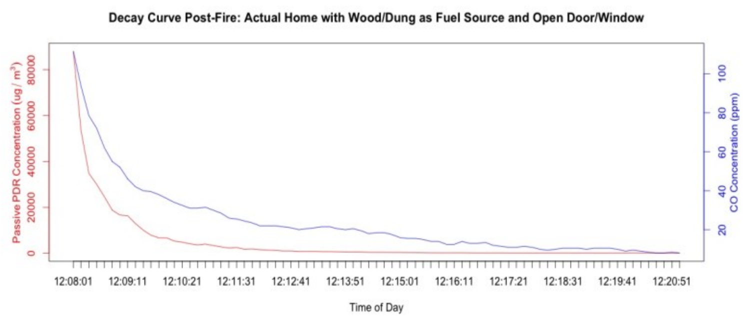

Figure 4: Example of PM (red) and CO (blue) decay curves post-fire extinguishment in an occupied house

Mixing Factor Analysis

Results for the mixing factor analysis are reported in Table 1. The mean (95%CI) AER for non-artificially mixed tests was 9.9 h^{-1} (4.7, 15.1), with artificially mixed tests yielding 7.5 h^{-1} (4.5, 10.5). These means are not statistically different (p-value = 0.63) suggesting that the well-mixed model assumption (k = 1) is not unreasonable, thus allowing the assumption of perfect mixing. The homes in this region are small and typical occupant movement creates air movement within the house that contributes to the overall mixing. To our knowledge this is the first study to evaluate the well-mixed assumption in a village-like home within a developing country.

Table 1. Results of Mixing Factor Analysis

Mixing Status	N	Average Air Exchange Rate Per Hour (95% CI)	MA/NAM Ratio (95% CI)
Mixed Artificially (MA)	10	7.5 (4.5, 10.5)	0.76 (0.34, 1.46)*
Not Artificially Mixed (NAM)	10	9.9 (4.7, 15.1)	

*p value >> 0.05

Air Exchange, Ventilation Rate, and Exfiltration Fraction Evaluation

Summary statistics of AERs, ventilation rates, and exfiltration fraction, with AER and

Table 2. Summary Statistics for Exfiltration Fraction, Air Exchange, and Ventilation Rates

	Data Type	N	Mean (95% CI)	Range	10th %	25th %	Median	75th %	90th %
PM Exfiltration Fraction (%)	All Data	50	26.4 (22.4, 30.5)	5.8-57.6	10.3	14.8	22.1	37.4	45.4
	Mock House	20	23 (15.9, 30.1)	6.3-57.6	8.9	13.6	19	28.2	45.3
	Occupied Homes	30	28.7 (23.7, 33.6)	5.8-53.6	10.7	16.6	30.9	38.7	45.4
Air Exchange Rate ($hour^{-1}$) calculated from CO decay curve	All Data	50	11.9 (9.7, 14.1)	2.3-41.8	4.2	6.8	10.6	15.5	20.5
	Mock House	20	9.6 (5.4, 13.8)	2.3-41.8	3.8	4.7	6.8	9.7	17.9
	Occupied Homes	30	13.4 (11, 15.6)	4.2-35.2	7.5	9.1	11.7	15.8	21.7
Ventilation Rate (m^3/min) calculated from CO decay	All Data	50	6 (4, 7.9)	0.6-31.5	1	2.3	4	5.6	13.8
	Mock House	20	6.4 (3.6, 9.3)	1.6-28.1	2.5	3.2	4.6	6.5	12
	Occupied Homes	30	5.7 (2.9, 8.4)	0.6-31.5	0.9	1.7	3.2	5.1	15.3
Ventilation Rate (m^3/min) calculated from PM decay	All Data	50	22.5 (17.9, 27.1)	2-72.9	6	12.3	17.3	28.7	46.5
	Mock House	20	27.6 (22.3, 32.9)	15.2-63.2	17.2	19.3	25.7	29.6	40.8
	Occupied Homes	30	19.1 (12.3, 26)	2-72.9	3.6	8.6	13.8	17.1	49.8

ventilation rates calculated from the decay curves, are provided in Table 2.

Air exchange rates based on the CO decay curves are reported in Table 2, with a mean (95%CI) for all tests equivalent to 11.9 h^{-1} (9.7, 14.1). Examining CO AER by window/door status yielded an average of 5.9 h^{-1} (4.4, 7.3) for the closed category (n=10) and 13.4 h^{-1} (10.9, 16) for having an opening present (n=40). This trend follows expectations for window/door status, with an opening present allowing for increased airflow and hence a higher average AER. Limited field studies examining AER in village housing have been conducted. Measured AER for Indian village homes have been recorded between 7 to 30 per hour[23]. A more recent study in village homes located in Peru reported a range of AER's between 0.5 h^{-1} to 20 h^{-1} depending upon partition presence[24]. This range of values presented for AERs in village homes is in agreement with results found in rural Nepal village housing, which is similar in housing style to much of the Indo-Gangetic Plain region. In addition to demonstrating similarities across village housing, these findings contribute to the expansion of field-based residential AER data. Accurate estimation of AERs is critical to understanding cookstove contributions to ambient air pollution as well as the broader climate change impacts that may be associated with traditional vs. alternative stoves. Ventilation rates, which are a function of the home volume and air exchange rate, are also presented for all tests in Table 2. The ventilation rates calculated from CO decay for the mock house under varying conditions averaged 6.4 m^3/min and ranged from 1.6 to 28.1 m^3/min. Occupied homes' CO ventilation rates similarly averaged 5.7 m^3/min and ranged from 0.6 to 31.5 m^3/min. As expected, mock house ventilation rates were similar to the occupied homes.

The average (95%CI) PM exfiltration fraction for all tests (n=50) was 26.4% (22.4, 30.5), with values ranging from 5.8% to 57.6%. Mock and occupied home EF averages (95%CI) were 23% (15.9, 30.1) and 28.7% (23.7, 33.6), respectively. EFs for the mock and occupied houses were not statistically different, thus conforming to the expectation that the designed mock house kitchen is representative of a typical kitchen in this area. EF distributions broken down by window/door status and fuel type are presented in Figures 5 and 6, respectively. In Figure 5, the average (95%CI) EF for closed window/door status was 18.2% (13.1, 23.2), while having an opening present resulted in an increase to 28.5% (23.8, 33.2). Furthermore, the range of EF data is less variable when the window/door are both closed relative to having an opening present. Comparing open vs. closed conditions yielded statistically different results (discussed below), with the trend being consistent regarding increased exfiltration when doors and/or windows are open. When partitions are closed, airflow through the kitchen is reduced, resulting in less exfiltration and a range of values with a relatively smaller spread in contrast to having openings.

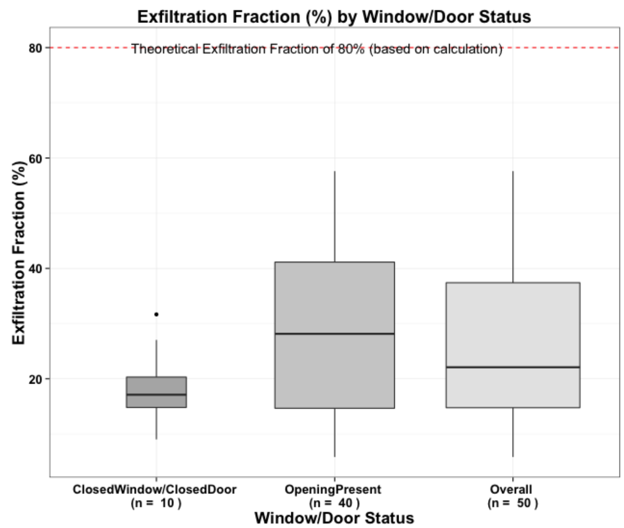

Figure 5: Exfiltration fraction presented by window/door status

Figure 6 gives EF data for all tests broken down by fuel type. A wide range of fuel types were tested in the occupied homes because these were the fuel types used by the families during the testing period. They included wood, mixture of wood/dung/crop residue, mixture of dung/wood, mixture of crop residue/wood, and crop residue. Only wood and mixture of wood/dung/crop residue were evaluated in the mock house because these were the two fuel types most prevalent in the parent cookstove trial. Fuel categories consisting of a mixture still had wood as the primary fuel source. EF for fuel types of wood and crop residue by themselves had similar averages (95%CI) of 30.2% (25.6, 34.8) and 28.1% (13.9, 42.4), respectively.

Crop residue is a mixture of materials with the potential to produce a wide range of particle sizes when burned, hence the potential for particle size distribution to be broader relative to wood. Subsequently, one would expect that the EF variability for crop residue should be larger than that seen for wood, which is shown in Figure 6.

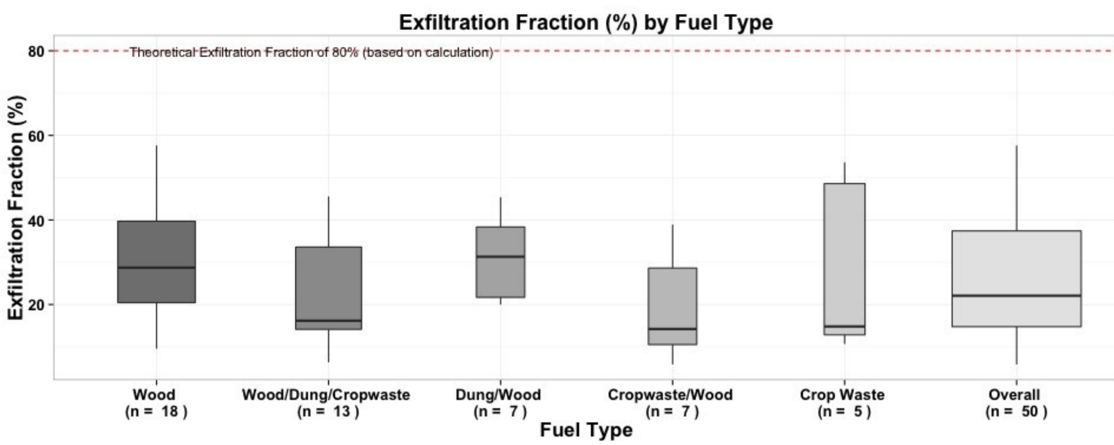

Figure 6: Exfiltration fraction presented by fuel type

Both Figures 5 and 6 have a value of 80% exfiltration labeled on them, which is a modeled value with no field validation that has been previously cited but not independently published[20]. The 80% exfiltration is significantly greater than the averages of the EF data, along with the upper limits of the ranges, presented in the overall EF data (Table 2) and in Figures 5 and 6.

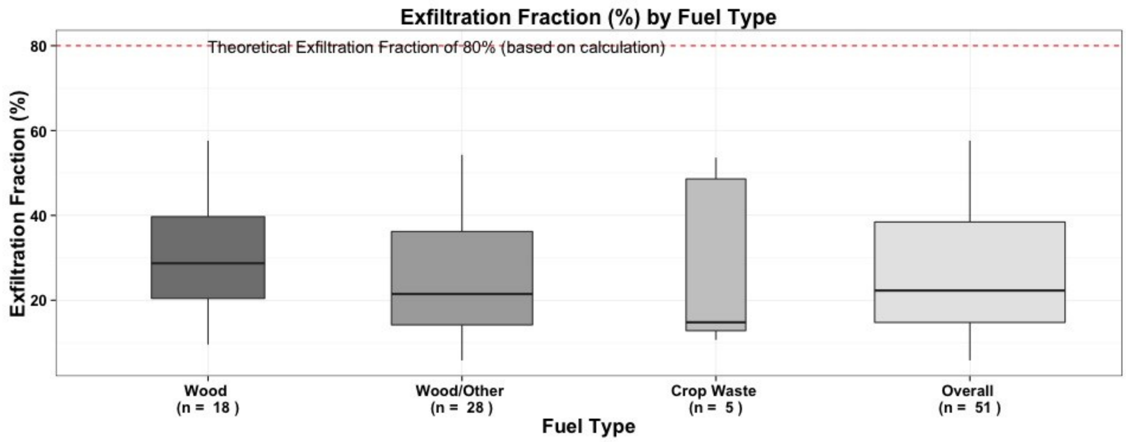

Figure 7: Exfiltration fraction presented by pooled fuel status

Utilizing a linear mixed effects model, factors that may impact EFs were evaluated. Pooling of categories for fuel type was necessary due to the small sample sizes of certain fuel categories. With wood being the dominant fuel source for the categories of dung/wood, wood/dung/crop residue, and crop residue/wood, these three sources were combined into one category and called wood/other. EF by pooled fuel type distributions is displayed in Figure 7. The regression model examined window/door status (everything closed vs. opening present) and fuel type (wood only and wood/other), with crop residue excluded due to the small sample size. Regression results are presented in Table 3 with reference levels for the covariates being wood for fuel type and everything closed for window/door status. Window/door status proved to be a significant covariate (p=0.022), while pooled fuel type status was marginally significant (p=0.0621). Regression results indicate that having an opening present resulted in an 11.37% increase in exfiltration, while switching fuel type from wood to wood/other resulted in a 7.64% decrease in exfiltration. The relevance of these covariates follows expectations that exfiltration of PM can be attributable to presence of openings in a house along with particle size distribution which can vary based upon fuel type.

Table 3: Results of mixed effect model evaluating Exfiltration Fraction

Covariates	Beta Estimate	Standard Error
Fuel type - Wood/Other	-7.64	3.83
Window/Door status - Opening Present	11.37	4.51

Ratio of BC to $PM_{2.5}$ Analysis

Of the $PM_{2.5}$ filters collected during valid exfiltration fraction tests (n=50), due to very high PM concentrations during cooking 37 were too saturated to estimate using the optical analysis method for BC. The excluded filters exceeded the optical method's upper threshold detection limit which resulted in questionable prediction of BC values[34,51]. Fuel category for the 13 samples with acceptable loadings for BC analysis were broken down into wood (n=2), wood/other (n=9), and crop residue (n=2).

Table 4: Summary statistics for black carbon to $PM_{2.5}$ ratio

	N	Mean (95% CI)	Median	Range
$PM_{2.5}$ Concentration (ug/m^3)	13	4352.9 (3097.4, 5608.4)	4025.1	1430.9- 8382.3
Black Carbon Concentration (ug/m^3)	13	1516.1 (1027.6, 2004.7)	1219.7	630.8-3182.4
Black Carbon to $PM_{2.5}$ Ratio (%)	13	36.8 (28.5, 45.1)	34.9	17.6-68

Concentration summary statistics of BC and $PM_{2.5}$, along with ratio estimates are provided in Table 4. Conducted only over the active cooking period of the simulated cooking test, the mean (95%CI) ratio was 36.8% (28.5, 45.1), ranging from 17.6% to 68%. The relationship

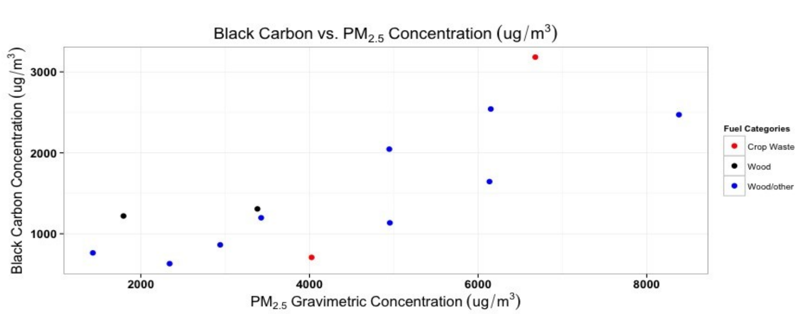

Figure 8: Black Carbon vs. $PM_{2.5}$ concentration ($\mu g/m^3$) illustrated by fuel type

between $PM_{2.5}$ and BC concentration is displayed in Figure 8. It is noteworthy that a nonlinear trend appears to exist as $PM_{2.5}$ concentration increases, keeping in mind the small sample size.

Multiple studies have reported BC to PM ratios. For example, Rau (2007) reported elemental carbon values from wood smoke particles ranging from 3 to 38%[50], while other studies of wood smoke have reported ratios that range from 8 to 53%[52]. Another study reported this ratio for a 24 hour integrated $PM_{2.5}$ measurement to be from 6.3 to 7.6%[53]. Our estimates agree well with published data, further validating estimates determined in laboratory and field settings.

Limitations

While a comprehensive effort was put forth, certain limitations exist. While we tried to keep combustion characteristics constant in the mock house, burn rate, air-fuel ratio, flame turbulence, and combustion temperature were not measured. These factors can influence particle size distribution. Another limitation present was that particle size distribution was not measured. Regarding determination of exfiltration, although particle size for combustion tends towards being extremely small, it is unknown the fraction of PM that may become lodged in cracks while exiting the house (where larger particles are more likely to become lodged). Future work should also seek to address the incorporation of activity patterns in real-world homes to assess if multiple family members within a home create changes in air exchange rates. Seasonality may also play a role in terms of certain fuel types being more prevalent and is an area that requires further exploration as sampling took place during one season (Spring). Mixing factor analysis was limited by a small sample size and an assessment conducted in a mock house. Although our findings indicated a mixing factor not statistically different from 1, a larger sample size will provide more confidence in this result. Furthermore, additional tests assessing mixing are needed in occupied homes to assess variability across housing type. With regards to evaluation of BC, several limitations existed. Due to extremely high PM concentrations witnessed, oversaturation for the BC analysis occurred. In addition, all data collected for BC analysis was conducted utilizing a simulated cooking event (water boil test) and further assessment over the course of actual cooking events is needed to assess the generalizability of the mock house testing. Finally, our testing was limited to one area and one stove type, thus results may not extrapolate to other areas and stoves. Data are needed on different housing stock, different stoves (traditional and improved), and analysis is also needed to assess the impact chimneys may have on exfiltration.

Conclusions

This paper presents in situ PM exfiltration estimates from village homes in rural Nepal that utilize traditional, open-design cookstoves. The use of traditional, open-design cookstoves in village homes resulted in a 26% average PM exfiltration fraction (range from 6% to 58%) due to natural ventilation. This value represents a significant departure from the theoretical estimate of 80% previously cited. A linear mixed effects model determined that window/door status was a significant predictor for exfiltration with an 11% increase in exfiltration when an opening was present, while fuel type was marginally significant. An average air exchange rate of 12 h^{-1} was found to be in the range published in previous studies conducted in village homes. In addition, the mixing factor analysis yielded a value of 0.76, which was not statistically different from 1, allowing for the assumption of perfect mixing. To our knowledge, the approach utilized to determine PM exfiltration in this low resource, field-based setting has never been done before. Furthermore, this study agrees with other published BC to $PM_{2.5}$ ratio measurements with a value of 37%.

4 Characterizing Particulate Matter Exfiltration Estimates for Intervention Cookstoves in a Village-Like Household in Rural Nepal

Introduction

Approximately 10% of all human energy use is expended by half the world's population using biomass (i.e., wood, dried animal manure, and crop residue) for daily cooking and energy needs, most of which are in developing countries[1–3]. The use of inefficient, open-design cookstoves that expel combustion byproducts directly into the indoor environment result in extremely high pollutant concentrations within the home[4–6]. Indoor air quality is of major concern in biomass burning homes as particulate matter concentration can range from ambient background concentrations to as high as 15 mg/m^3 during cooking periods[4,7,8]. In addition, severe forest and environmental degradation is occurring due to harvesting of fuels (such as wood) and their resultant combustion byproducts[10]. The need to intervene in order to improve indoor air quality and health effects is clear[3,7,9–14]. As a result, organizations such as the Global Alliance for Clean Cookstoves of the United Nations Foundation[15] have undertaken a massive effort to implement alternative stoves to reduce the health burden. In parallel, many studies have been conducted or are underway focusing on characterizing the pollutant reduction and health improvement associated with alternative stoves[16]. Many of the alternative cookstoves attempt to increase thermal efficiency, reduce fuel consumption, and/or include a chimney to redirect pollution outdoors. However, the potential for these interventions to degrade outdoor air quality is receiving little attention[45]. The redirection of pollutants outdoors via a chimney will increase health burden associated with outdoor air pollution and could exacerbate climate change.

Climate change caused by the burning of biomass fuels is a major concern due to the production of black carbon (BC)[17]. A component of particulate matter (PM), BC is a short-lived climate-forcing agent and when emitted into the atmosphere can alter the overall hydrological cycle of a region or deposit on snow or ice and accelerate the melting process[18,19]. A region of particular concern for BC production from biomass fuel burning is the Indo-Gangetic Plain region[19]. Climate models have attempted to estimate the impacts of BC pollution[20–24]. PM and BC emission estimates (climate change model inputs) are subject to large uncertainty, subsequently leading to climate change and epidemiological prediction models having wide variability[25]. Developing a more comprehensive understanding of the contribution cookstoves play to these emissions, specifically from data collected in situ, is critical to contributing towards the development of more comprehensive emission profiles for this region.

PM emission factors for different stove designs have been estimated in laboratory settings[26–28] and to a lesser degree in field conditions[28,29]. These emission factors can vary by 5-6 fold depending on fuel type[26]. For studies examining the impact of outdoor air quality, either on health or climate change, the source of concern is the house and stove together. Stove-based emission factors do not provide for a direct estimate of the amount of pollution leaving, or exfiltrating, from the house. The house, to a greater or lesser degree, provides a barrier to pollutants leaving or entering. A fraction of PM produced during cooking events will settle and deposit on surfaces indoors, including cracks within the walls of the house. Remaining PM can escape to the exterior environment either via direct (chimney) or indirect (natural ventilation) routes. Developing estimates for PM fraction exiting to the exterior from village households during cooking will contribute towards the reduction of uncertainty in emission profiles.

Little is known about air exchanges and pollution exfiltration from homes in low and middle-income countries (LIMC) utilizing traditional stoves. Furthermore, even less is known about how cookstove interventions (i.e., use of a chimney), designed to improve the indoor environment, may exacerbate the degradation of outdoor air quality. With regards to how much pollutant exfiltration may be occurring due to direct venting of cookstoves, a study by Grieshop *et al.* utilized PM concentration data from previous studies collected indoors and outdoors, along with a mass-balance approach, to estimate the fraction of a stove's emission retained in a household[10]. With no bounds of uncertainty, they estimated that a fractional value of 0.3 (30%) of emissions are retained in the house, allowing us to infer that 70% of emissions from vented stoves exit the house via a chimney[10]. Additional studies have reported mixed results regarding the differences of stove efficiencies and PM emission factors for vented biomass stoves versus traditional stoves in field settings within developing countries[2,29,30]. Further study is needed to estimate the fraction of PM that remains indoors versus what is vented to the exterior for homes utilizing cookstoves with a chimney.

The focus of this paper is to present exfiltration estimates of PM that exit to the outdoors via the combined indirect (natural) and direct (chimney) ventilation routes for alternative cookstoves being studied in a large, cookstove intervention trial in rural Nepal. Exfiltration estimates were determined in a real-world setting, with this work building upon PM and BC exfiltration estimates for traditional, open-design cookstoves[31]. Characterizing these estimates allows for homes to be treated as a source. Using exfiltration factors, PM emission rates could be determined based on measurements of indoor concentration, providing a more comprehensive assessment of the potential for alternative cookstoves with chimneys to impact outdoor air quality.

Methods

Study Overview

The Department of International Health within the Johns Hopkins Bloomberg School of Public Health has a study site located in rural, southern Nepal. Situated within the Nepal Nutrition Intervention Project - Sarlahi (NNIPS), a parent cookstove intervention trial is underway. This community-based, cluster randomized, step-wedge trial is characterizing indoor PM exposure in ~3,000 homes from traditional and alternative cookstoves, assessing primary health outcomes that include acute lower respiratory illness in children 1-36 months of age (ALRI), as well as birth weight and preterm birth among newborn infants[8]. The NNIPS site, located in Sarlahi District, consists of 32 areas referred to as Village Development Committees (VDC's), 4 of which are involved in the cookstove trial. Located in the Terai region of Nepal (on the border with Bihar State, India), Sarlahi is representative of southern Nepal and most of northern India with elevation approximately 200 meters above sea level[8]. The typical cooking style in the area involves the burning of biomass fuels (i.e., wood, dried animal manure, and crop residue) in traditional, open-design mud cookstoves without direct ventilation to the exterior[8]. Common in this area of Nepal, traditional stoves are made from clay, mud, bricks, rice husk, and dried cow dung[32]. The alternative stoves included in the parent study utilize the same fuel sources and methodological approach to cooking relative to traditional stoves.

Alternative Stove Overview

A traditional, open-design cookstove and four types of alternative stoves were utilized for this study (shown in Figure 1), all of which are part of the parent cookstove trial. The first alternative stove was a commercially constructed cookstove called the Envirofit

G3300/G3355 (Envirofit International, Fort Collins CO) and is referred to as Envirofit Stove Original Model or ESOM. This stove has a double pot attachment (the G3355 model) and a detachable chimney (produced by the NNIPS project), which allows for combustion byproducts to be directed to the exterior. This stove was designed in close cooperation with Oakridge National Research Laboratory, Colorado State University's Engines and Energy Conversion Laboratory, and the Shell Foundation (www.envirofit.org). Manufactured in China, it is comprised of alloy metal and the combustion chamber is made of ceramic[33]. As the parent cookstove trial was progressing, Envirofit slightly altered the design of the stove. The opening directly above the fire was centered and increased from 13.5cm to 19cm in order to "significantly improve the heat transfer to both the 1st and 2nd pots"[34]. Subsequently, the 2nd stove type studied was the manufacturer altered G3300/G3355 (referred to as Manufacturer Altered Envirofit Stove or MAES). All remaining Envirofit G3300/G3355 stoves in stock at the field site were locally custom cut, making them the 3rd stove type tested, to match this design change (referred to as NNIPS Altered Envirofit Stove or NAES). The fourth type of alternative stove studied was a site specific, locally constructed, improved ventilated stove (referred to as Improved Mud Brick Stove or IMBS). This stove is made out of the same material as the traditional cookstove, has an access port for cleaning purposes, and includes a chimney that redirects PM to the exterior.

Figure 1: Stove types used for comparison. Top left: Traditional, open-design mud brick stove. Top right: Improved mud brick stove with chimney. Bottom left and right: Envirofit G3300/G3355 model stove (original model/manufacturer altered/NNIPS altered)

Mock Home Sampling

In order to estimate PM exfiltration in a real-world setting, a mock house was built in Sarlahi District, Nepal (shown in Figure 2). This house was representative of a household kitchen in this area. Homes in this region are typically comprised of wood, mud, brick or cement walls with thatch roofs[8]. The mock house included a 1-room floor plan with a closeable window and door. Housing material was made of bamboo with mud, logs, and tree branches, while roof material was split between tile and thatch/grass. House dimensions were length 3.85m, width 4.65m, ground to lowest roof point 1.8m, ground to roof apex 2.7m, window length and width 0.6m (on the back wall), and doorframe 1.28m width by 1.64m height (located on the front wall). The window and door had a hinged, wood-framed metal panel that permitted for opening and closing these features. All stoves were placed on the back wall of the mock house for their respective tests.

Figure 2: Mock house built in study area

For this study, measurements consisted of real-time PM measured using a passive nephelometer (DataRAM pDR-1000AN, Thermo Scientific, Franklin, MA), real-time carbon monoxide (CO) concentration (EasyLog USB CO Monitor, Lascar Electronics, Eerie, PA), and relative humidity (RH) using the HOBO Data Logger (Onset Corp., Bourne, MA). All of these devices were co-located, collected before, during, and after simulated cooking events (discussed below), and recorded in 10-second intervals. The pDR-1000 was zero calibrated using procedures recommended by the manufacturer in the field prior to each deployment. For quality control and assurance purposes, 10% duplicate samples were collected.

Two fuel types, wood and a mixture of wood/dried animal manure/crop residue, were utilized during simulated cooking events. Fuel sources were obtained from the same area, by the same person, and sun dried to standardize moisture content. The same individual conducted all of the simulated cooking events. Two boundary conditions were also included, where both the window and door were either completely open or closed during testing in the mock house.

Alternative Stove Exfiltration Fraction Test: Method and Protocol Development

For homes with traditional, open-design stoves, PM exfiltrates passively (referred to as an indirect pathway) through open windows/doors as well as through cracks in walls and roofs (PM_O and PM_N in Figure 3). For stoves with a chimney, an additional direct pathway of exfiltration exists through ductwork during cooking (PM_C in Figure 3). This pathway is not likely to be a significant exfiltration route during non-cooking periods. The combination of the indirect and direct ventilation pathways during cooking result in an overall exfiltration for PM according to Equation (1) and depicted in Figure 3.

$$PM_E = PM_O + PM_N + PM_C \quad (1)$$

Where PM_E represents overall PM exfiltration, PM_O is exfiltration through open windows/doors (indirect ventilation), PM_N is exfiltration due to porous openings in the walls or roof (indirect ventilation), and PM_C represents exfiltration via a chimney (direct ventilation). Methodology for exfiltration determination for indirect ventilation has been previously described for assessment of traditional, open-design cookstoves[31].

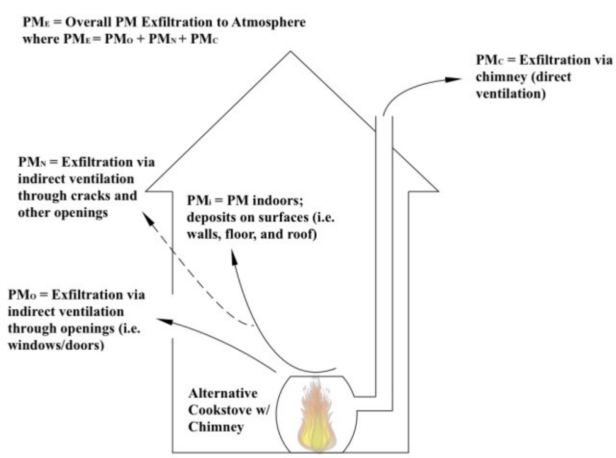

Figure 3: Routes of PM exfiltration for a village home utilizing an alternative stove with chimney

Prior to any testing, air sampling equipment was hung in the center of the house at a distance of 1m in front from the edge of the stove and 1.8m off the floor to maintain consistency between readings. A simulated cooking session consisted of creating a controlled fire within the stove in order to generate elevated concentrations of PM and CO within the mock house that were orders of magnitude above background. The cooking event mimicked local cooking practices and a modified version of the Water Boiling Test (WBT) 3.0 was utilized[35]. A cooking session was simulated by bringing 2 pots of water (5 Liters in each) to a rolling boil from ambient temperature. For all alternative stoves, after one side reached boiling point, pots were switched so that the second pot could reach boiling point. The fire was then extinguished and remnant fuel removed from the house to halt additional emissions from being produced. PM, CO, and RH sampling were initiated 30 minutes prior to the cooking session and continued for an additional two hours post-fire extinguishment. Air exchange rates were calculated for PM and CO concentration decay curves post-fire extinguishment, and exfiltration fraction due to indirect ventilation was determined utilizing a previously established method where the ratio of the slopes of the linearized CO to PM decay curves were calculated[31]. Improved Mud Brick Stove and all Envirofit Stove model tests were performed during the Spring of 2013. Traditional, open-design stove tests were performed in the Spring of 2012[31]. This time of year is considered the dry season as the outdoor temperature is moderate to high and there is minimal rain and humidity is low.

Analysis for PM Reduction and Overall Exfiltration

While it is conceivable that emissions expelled by the chimney can be directly measured, there are many practical difficulties associated with this. Therefore, chimney exhaust losses (direct ventilation) were estimated as the difference in average indoor PM concentration using the alternative cookstoves with and without a chimney. Specifically, the comparison included the Envirofit Stove Original Model without a chimney against all three Envirofit stoves with a chimney (Original Model, Manufacturer Altered, and NNIPS Altered). These three models were assumed to be similar without chimney, therefore, a comparison of each one with and without a chimney was not performed. The Improved Mud Brick Stove with chimney was compared to the traditional, open-design mud brick stove and was assumed to be similar in efficiency.

In order to determine the reduction in indoor PM due to chimney use, a multiple linear regression equation was utilized. The equation assumed the form:

$$\text{Ln(C)} = \beta_0 + \beta_1 \times \text{Stove type} + \beta_2 \times \text{Window/Door status} + \beta_3 \times \text{Fuel} + \varepsilon, \text{ where } \varepsilon \sim N(0,\sigma^2) \quad (2)$$

Where C is the average PM concentration during cooking, β_1 represents the natural log change in concentration due to stove type, β_2 is the natural log change in concentration due to window/door status, and β_3 is the natural log change in concentration due to fuel type. Two comparisons were conducted utilizing this equation. The first comparison was performed using only data involving the Envirofit stoves. This included the Envirofit Stove Original Model without chimney, Envirofit Stove Original Model with chimney, Manufacturer Altered Envirofit Stove with chimney, and NNIPS Altered Envirofit Stove with chimney. The original model without chimney was set as the reference for analysis. The second comparison was performed using only data for the traditional, open-design stove and Improved Mud Brick Stove with chimney, with the traditional stove set as the reference. Performing the comparisons in this manner accounted for the design of the stove types, thus focusing the evaluation on the chimney's impact upon PM reduction. The resulting exponentiation of the stove type Beta coefficient (β_1) from the regression analyses represented the fractional change in PM concentration attributable to use of a chimney. Furthermore, taking 1 minus this fraction yielded the average reduction in PM concentration due to implementation of a chimney, which was converted to a percent.

Utilization of a chimney removes PM via the direct ventilation route. However, the remaining PM indoors, although reduced in concentration due to use of a chimney, will deposit on surfaces as well as exit the house via routes of indirect ventilation. In order to determine the amount of PM that leaves a house via indirect ventilation, additional methods had to be utilized. Exfiltration fraction through routes of indirect ventilation, cracks and window/door (PM_O + PM_N from Equation (1)), was calculated for each test post-fire extinguishment using the ratio of the linearized CO to PM decay curve method briefly mentioned within the *Protocol Development* section and described in further detail by Soneja *et al*[31]. The exfiltration values were then subtracted from 1 in order to represent the fraction of PM remaining indoors. This relationship is displayed in Equation (3).

$$PMf_{in} = 1 - \text{Exfiltration Fraction} \tag{3}$$

Where the exfiltration fraction represents the fraction of PM exiting the house due to indirect ventilation and PMf_{in} is the fraction of PM remaining indoors. In order to determine the average PM concentration during cooking that remained in the home after accounting for routes of indirect ventilation, PMf_{in} was multiplied by the average PM concentration during cooking for all tests that utilized a stove with chimney. This relationship is expressed as:

$$AdjC_{SC} = PMf_{in} \times C \tag{4}$$

where C is the average PM concentration during cooking for stoves with a chimney, PMf_{in} is the fraction of PM remaining indoors, and $AdjC_{SC}$ is the average PM concentration during cooking that remains indoors for stoves having a chimney. Furthermore, $AdjC_{SC}$ represents the average PM concentration indoors after accounting for both direct and indirect ventilation for stoves utilizing a chimney. The traditional stove and Envirofit Stove Original Model without chimney did not have their average indoor PM cooking concentrations adjusted to allow for a comparison of the alternative stoves with chimney against their respective baseline stove. Specifically, the comparison conducted sought to establish the overall exfiltration percentage of PM removed from the house after accounting for direct and indirect routes of ventilation (PM_E in Equation (1) and Figure 3). Using $AdjC_{SC}$ for the stoves with chimney and the unaltered average PM concentration (C) for the traditional and Envirofit Stove Original Model without chimney, multiple linear regression was used in order to assess the total fraction of PM removed from the house via the combined routes of direct and indirect ventilation. The regression equation took the form:

$$\mathrm{Ln}(AdjC_{SC+C}) = \beta_0 + \beta_1 \times \text{Stove type} + \beta_2 \times \text{Window/door status} + \beta_3 \times \text{Fuel type} + \varepsilon, \text{ where } \varepsilon \sim N(0,\sigma^2) \quad (5)$$

where $AdjC_{SC+C}$ represents the average PM concentration during cooking that remains indoors for stoves having a chimney as well as the unaltered average PM concentration during cooking for the traditional stove and Envirofit Stove Original Model without chimney. The remaining covariates (window/door status and fuel type) as well as the interpretation of the Beta coefficients are the same as described from Equation (2). Two comparisons were conducted utilizing Equation (5). The first comparison was performed using only data involving the Envirofit stoves. This included the Envirofit Stove Original Model without chimney, Envirofit Stove Original Model with chimney, Manufacturer Altered Envirofit Stove with chimney, and NNIPS Altered Envirofit Stove with chimney. The original model without chimney was again set as the reference for analysis. The second comparison was performed using only data for the traditional, open-design stove and Improved Mud Brick Stove with chimney, with the traditional stove set as the reference. Performing the comparisons in this manner accounted for the thermal efficiency of the stove types, thus focusing the evaluation on the impact that indirect and direct ventilation have on PM reduction. The resulting exponentiation of the stove type Beta coefficient (β_1) from the regression analyses represented the fraction of change in PM concentration attributable to indirect and direct ventilation. Furthermore, taking 1 minus this fraction yielded the overall exfiltration fraction (PM_E) after accounting for direct and indirect ventilation, which was converted to a percent.

In order to assess if the Improved Mud Brick Stove with chimney overall exfiltration percentage was statistically different from the traditional stove overall exfiltration percentage, traditional stove PM concentration data were adjusted for exfiltration due to indirect ventilation using Equation (4). Another regression analysis was conducted using Equation (5) for all adjusted data for both the Improved Mud Bick Stove with chimney and the traditional stove, subsequently generating a p-value that was reported. Likewise, to assess significance and generate a p-value for the Envirofit stove comparisons, the Envirofit Stove Original model without chimney PM concentration data was adjusted using Equation (4) and a similar regression analysis performed using Equation (5) for all adjusted data for this stove type along with the Envirofit models utilizing a chimney.

All statistical analyses were performed in the R Statistical Computing Environment (Version 3.0.2; 2013-09-25). Packages used for data analysis were chron[36], car[37], agricolae[38], lattice[39], and plyr[40].

Results and Discussion

An assessment of the amount of PM reduction due to inclusion of a chimney (exfiltration due to direct ventilation only) across similar stove types and for the amount of overall exfiltration (due to direct and indirect ventilation) is provided in Table 1. Examining the Improved Mud Brick Stove relative to the Traditional stove, implementing a chimney resulted in an average (95%CI) PM reduction of 18% (-66, 59) with p-value=0.568. The confidence interval is interpreted as the Improved Mud Brick Stove with chimney goes from a 59% decrease in PM concentration to a 66% increase in PM concentration. The confidence

Table 1. Comparison of stoves for PM reduction due to chimney and overall exfiltration

	Stove Type	Sample Size	% PM Reduction due to Chimney		% of Overall Exfiltration†	
			Mean (95% CI)	**P-value**	**Mean (95% CI)**	**P-value**
Mud Brick Stove Comparison	Traditional Mud Brick Stove - No Chimney	20	REF	---	23 (16, 30)*[a]	---
	Improved Mud Brick Stove	10	18 (-66, 59)	0.568	56 (14, 78)	0.115
Envirofit Stove Comparison	Envirofit Stove - No Chimney	12	REF	---	35 (21, 57)*	---
	Envirofit Stove Original Model	12	71 (54, 82)	< 0.001	84 (74, 90)	< 0.001
	Manufacturer Altered Envirofit Stove	10	36 (-5, 61)	0.078	62 (35, 77)	0.063
	NNIPS Altered Envirofit Stove	10	42 (6, 65)	0.029	62 (35, 78)	0.058

*No chimney present, therefore exfiltration only due to indirect (natural) ventilation

†As defined by Equation (1) ($PM_O + PM_N + PM_C$)

a = Values extracted from previous study examining exfiltration fraction for traditional, open-design mud brick stoves in a mock house[(31)]

interval and p-value indicate that there is no statistically significant difference for reducing indoor PM concentration when using the Improved Mud Brick Stove with chimney relative to what is currently used in standard practice (traditional mud stove). It should be emphasized that this assumes thermal efficiency is similar between these stove types. Furthermore, examining the change in overall exfiltration percentage, the combination of indirect and direct ventilation pathways, use of the traditional stove yielded an average (95%CI) overall exfiltration of 23% (16, 30)[31] while the Improved Mud Brick Stove resulted in an increase to 56% (14, 78) of PM exiting the house. Traditional stove exfiltration values were determined in the mock house via a previous study by Soneja *et al.*[31] and are only subject to indirect ventilation routes as the traditional stove does not have a chimney. Evaluating overall exfiltration percentage between the traditional stove and Improved Mud Brick Stove with chimney did not yield a statistically significant difference (p-value of 0.115). Average (SD) concentration measured indoor before accounting for indirect ventilation for the traditional stove was 5702 $\mu g/m^3$ (6526) and 3606 $\mu g/m^3$ (2190) for the Improved Mud Brick Stove with chimney.

Table 1 also provides a comparison for all Envirofit stoves previously described. The Envirofit Stove Original Model with chimney resulted in an average (95%CI) PM reduction of 71% (54, 82) relative to the Envirofit stove without chimney ($p<0.001$). Likewise, relative to the same reference stove, average (95%CI) PM reduction for the Manufacturer and NNIPS Altered Envirofit Stoves were 36% (-5, 61) and 42% (6, 65), respectively. While the former displayed marginal statistical difference from the Envirofit stove without chimney ($p=0.078$), the percentage reduction in PM concentration due to chimney was very similar to the NNIPS Altered Envirofit Stove that was significant ($p=0.029$). Corollary to this, combined overall exfiltration percentage followed a similar trend. The Envirofit stove with no chimney had an overall mean (95%CI) exfiltration of 35% (21, 57), while the chimney inclusive Envirofit Stove Original Model, Manufacturer Altered, and NNIPS Altered yielded values of 84% (74, 90), 62% (35, 78), and 62% (36, 78), respectively. The Envirofit Stove Original Model with chimney had an overall exfiltration percentage that was statistically different than the Envirofit Stove Original model with no chimney ($p< 0.001$), indicating a large amount of PM is redirected to the exterior for Envirofit stoves through the chimney for the original model after accounting for indirect ventilation. Marginal statistical difference was seen for overall exfiltration percentage between the Envirofit Stove Original Model with no chimney and the Manufacturer Altered ($p=0.063$) and NNIPS Altered ($p=0.058$) Envirofit stoves with chimney. In addition, mean (SD) concentrations measured indoor prior to accounting for indirect ventilation were 2543 $\mu g/m^3$ (1611) for the Envirofit Stove Original Model without chimney, 705 $\mu g/m^3$ (414) for the Envirofit Stove Original Model with chimney, 1451 $\mu g/m^3$ (740) for the Manufacturer Altered Envirofit Stove with chimney, and 1360 $\mu g/m^3$ (685) for the NNIPS Altered Envirofit Stove with chimney.

The differences of PM concentration during cooking and overall exfiltration percentage for the altered Envirofit stoves relative to the Envirofit Stove Original Model with chimney are striking. The altered Envirofit stoves higher PM concentrations and lower overall exfiltration percentage suggest that the larger pot openings, while improving the cooking performance, may direct less PM into the chimney. Rather, PM may be escaping from the increased size of the opening, subsequently entering the indoor environment. It should be noted that the Envirofit Stove Original Model with and without chimney cook time was capped at 30 minutes and never reached boiling point. These stoves were tested first and it was thought necessary to conserve fuel, but upon completion of these tests it was noted that doing so was not necessary. This may have been a contributor to measuring lower PM concentration indoors during cooking for the Envirofit Stove Original Model with chimney. Further research is necessary to assess the differences with respect to the altered stoves' efficiency.

The covariates fuel type and window/door status were assessed in the regression models evaluating PM reduction due to chimney and overall exfiltration (Equations (2) and (5)). Neither of these covariates were found to be significant predictors of PM concentration.

Between testing for all stoves, the characteristics of the mock house itself (i.e., volume, surface type) did not change. Therefore, exfiltration fraction due to indirect ventilation regardless of stove type was expected to be similar. Average (SD) exfiltration fraction due to indirect ventilation was 40% (21) for the Envirofit Stove Original Model with chimney, 38% (16) for the Manufacturer Altered Envirofit Stove with chimney, and 33% (14) for the NNIPS Altered Envirofit Stove with chimney. Furthermore, the average (SD) exfiltration fraction due to indirect ventilation for the Improved Mud Brick Stove was 45% (13). A Bartlett's test was conducted to assess exfiltration fraction due to indirect ventilation across all stove types presented. No statistical difference was found ($p=0.624$), aligning with expectations that mock house characteristics remained similar from test to test thereby not impacting indirect ventilation.

Additional analysis was conducted to assess whether there were differences in average PM concentration between the Envirofit Stove Original Model without chimney and traditional stove. Assessing the change in average PM concentration during cooking between these stoves contributes to an additional understanding of the efficiency between them. Regression analysis using Equation (2) for these two stove types found average (95%CI) indoor PM concentration to be 43% (-9, 70) less for the Envirofit Stove Original Model without chimney ($p=0.088$). This reduction in PM concentration for the Envirofit Stove Original Model without chimney, although marginally statistically significant, represents the potential difference in thermal efficiency for this stove model relative to the traditional stove. Fuel type and window/door status covariates were not found to be significant in this analysis.

The increase in overall exfiltration for stoves with chimneys highlights how much more PM is redirected to the atmosphere due to the use of ventilated cookstoves. Overall PM emitted however may also be reduced with the use of more efficient stoves. It is important to recognize, however, that these stoves may burn at higher combustion temperatures, thus shifting the size distribution towards an increase in production of ultrafine emissions which includes black carbon[16,41]. The amount of $PM_{2.5}$ comprised of black carbon measured in traditional stoves using similar fuel sources from a previous study at this location ranged from 17.6% to 68%[31]. However, with the potential for higher combustion temperatures in alternative stoves, this range may shift such that BC comprises a larger proportion of PM emitted. In addition to a higher proportion of BC being created, an increase in production of ultrafine particles is of potential concern because they can be carried farther distances relative to particles of larger size[42,43]. Another important aspect to consider is that even if overall emissions are reduced through the use of alternative stoves such as those presented, the increase in overall exfiltration percentage may negate the benefits provided with reduced indoor emission production as more PM is redirected towards the exterior relative to traditional stoves increasing the ambient air pollution burden. Assessing how the alternative stoves behave with regards to fuel usage and cooking time are also important considerations. For example, in a recent study, Envirofit stoves were found to result in fuel savings for the weight of fuel used per weight of food cooked, however cooking time increased[33]. Other studies have shown inconsistent trends for fuel usage and cook time for alternative stoves[2,44]. Therefore, if the stove needs to be used for longer periods of time, this may negate any fuel savings when used for real cooking events, thus questioning the stove's ability to reduce the climate burden.

Limitations

This study did not examine certain combustion aspects while evaluating the simulated cooking test. Items not measured included burn rate, air-fuel ratio, flame turbulence, and combustion temperature. In addition, changes that might be due to combustion efficiencies were not taken into account for the Improved Mud Brick Stove, Manufacturer Altered Envirofit Stove, and NNIPS Altered Envirofit Stove. Larger sample sizes are needed for all stove types in order to better assess the significance of results that were determined to be of marginal statistical significance. Future work should also seek to address the incorporation of real-world homes and cooking with actual foods.

Conclusion

The use of alternative cookstoves in a village-like home resulted in a higher overall average exfiltration percentage due to direct and indirect ventilation. Relative to the average overall exfiltration percentage for the Envirofit Stove Original Model without chimney (35%), average overall exfiltration percentage was 84% for the Envirofit Stove Original Model with chimney (p-value<0.001), 62% for the Manufacturer Altered Envirofit Stove with chimney (p-value$=0.063$), and 62% for the NNIPS Altered Envirofit Stove with chimney (p-value$=0.058$). For the traditional, open-design cookstove, average overall exfiltration from a previous study in a village-like home was determined to be 23%[31]. Relative to the traditional stove, the locally made Improved Mud Brick Stove with chimney had an average overall exfiltration of 56%, but was not significantly different (p-value$=0.115$).

The large contrast in overall exfiltration between the traditional stove versus alternative stoves highlights the need for an improved understanding of the climate benefits that are believed to come about from implementing such options on a large scale. More research is needed to address the impact of shifting the exposure burden from indoors to outdoors. Consideration needs to be given to investing in interventions such as propane or biogas that will reduce overall pollution rather than shifting the health effects to ambient air pollution and increasing the potential climate impacts by increasing black carbon emissions.

5 Ambient $PM_{2.5}$ and Black Carbon: Characterization and Assessment for Cookstove Intervention Trial Villages

Background and Project Goals

Characterization of ambient $PM_{2.5}$ and black carbon (BC) concentration during periods of cooking and non-cooking at the village level is needed to provide proper regional estimates of PM emissions for future climate change, exposure, and epidemiological applications. Previous chapters have established PM and BC exfiltration estimates for traditional and improved stoves with a chimney at the household level. In addition, the development of an integrated quality control method (Chapter 2) to adjust nephelometric PM values for humidity and gravimetric equivalency sets the stage for comparing $PM_{2.5}$ between the interior and exterior environments. In order to build on these efforts, future work must focus on developing estimates for local-level ambient emissions created by the use of cookstoves. Characterizing local small-scale ambient $PM_{2.5}$ emissions will allow for the development of a $PM_{2.5}$ and BC spatial model to predict cookstove related emissions at unsampled locations in rural areas.

Limited research has been conducted examining ambient small-scale spatial variation of BC in low resource environments at village scale. Furthermore, limited measurements exist examining the indoor to outdoor spatial relationship of BC during cooking events within villages. A recent study conducted in northern India found a diurnal association of ambient BC that coincided with indoor biomass cooking during the morning and evening meal preparation periods (shown in Figure 1)[1]. However, this study utilized a single outdoor air sampler to represent BC across the entire village area, limiting the study's ability to understand small-scale spatial variation. Most studies that assign BC emissions

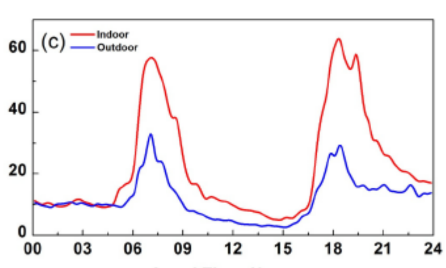

Figure 2: Diurnal pattern of black carbon in a rural Indian village[1]

originating from indoor biomass studies are based upon source apportionment models, controlled lab experiments, satellite imagery analysis, and theoretical calculations[2–4]. Understanding the ambient BC contribution from traditional and alternative cookstoves is needed to validate existing climate models and make effective decisions with regards to improved cookstove design replacement programs.

The work presented in this chapter is nested within a parent cookstove intervention trial, embedded within the larger effort known as the Nepal Nutrition Intervention Project Sarlahi (NNIPS), and revolves around two main objectives. The parent cookstove trial is a community-based, cluster randomized, step-wedge trial, characterizing indoor PM exposure in ~3,000 homes from traditional and alternative cookstoves in order to assess primary health outcomes that include acute lower respiratory illness in children 1-36 months of age (ALRI), as well as birth weight and preterm birth among newborn infants[5]. This trial is being conducted in four adjacent Village Development Committee (VDC) areas (Pipariya, Pidari, Laxmipur, and Kabalasi) within Sarlahi District, Nepal. The first objective of the research presented in this chapter is to characterize outdoor $PM_{2.5}$ and BC concentration during cooking and non-cooking periods across the four VDC's using tools from the field of spatial statistics. To perform this characterization, outdoor air samples were collected across these VDC's in order to measure $PM_{2.5}$ concentration during cooking and non-cooking periods. The second objective is to assess the indoor to outdoor relationship of $PM_{2.5}$ and BC due to cooking with biomass fuels. For the second objective, indoor PM data from the ~3,000 homes participating in the parent cookstove trial will be utilized. Implementing quality control methods developed in Chapter 2 to convert nephelometric PM values to $PM_{2.5}$ equivalents along with exfiltration estimates presented in Chapters 3 and 4, cookstove emissions from homes in the study will be used as point sources and allow for an assessment of household emissions to the outdoor environment. The completion of these objectives will provide preliminary results supporting the creation of a spatially predictive model for ambient $PM_{2.5}$ and BC produced by traditional and improved cookstoves across these 4 cookstove VDCs. Spatial prediction models have not been utilized in this region of the world for village scale applications, thus setting the stage for shifting the existing paradigm on how outdoor BC emissions are evaluated.

Sampling Methodology

Spanning from October 8th, 2012 to February 28th, 2013, outdoor integrated $PM_{2.5}$ samples were collected in each of the 4 cookstove VDC's. Each site was sampled once over the study period during the morning cook session, and again at midday in order to ascertain background levels. Each session involved collecting data for 1.5 hours. An additional 10% of samples were collected during the evening cooking period so that $PM_{2.5}$ concentration could be compared between morning vs. evening cook sessions.

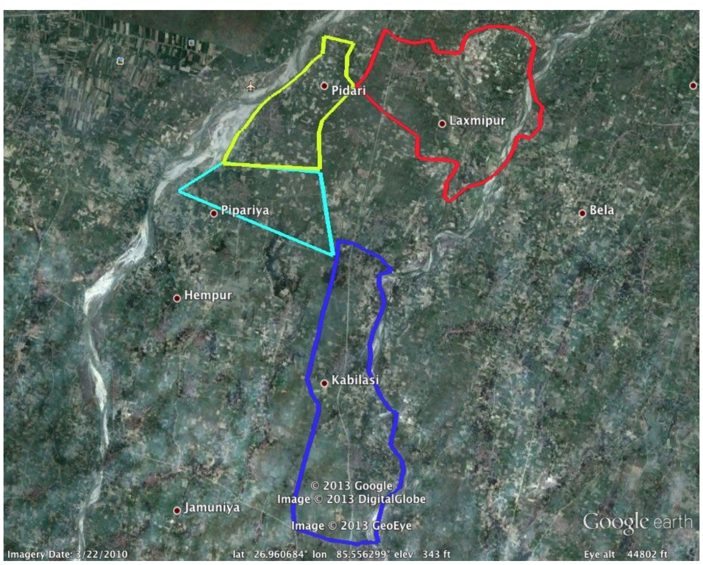

Figure 2: Map of cookstove VDC boundaries

Sampling equipment consisted of a $PM_{2.5}$ inlet (BGI, Waltham, MA) with a Teflon filter (37mm 2.0μm pore PTFE Membrane Filter w/ PMP ring Pel Life Sciences, Ann Arbor, MI) connected to a battery operated sampling pump (5400 BGI Inc., Waltham, MA) running at a flow rate of 4 L/min. Flow rates were recorded before and after sampling at each VDC's field office using a Drycal

Table 1. Sample site information by VDC

VDC	Area (km^2)	Total Number of Sample Sites	Number of Days Sampled	Date Range Sampled
Pipariya	4	40	10	10/8/2012 to 10/19/2012
Pidari	4	40	10	12/17/2012 to 12/28/2012
Laxmipur	9	56	14	1/21/2013 to 2/05/2013
Kabalasi	10	44	12	2/11/2013 to 2/28/2013

Flowmeter (DC Light BIOS Intl., Butler, NJ). Filters were pre and post-weighed in a temperature and humidity controlled weigh room using a XP2U Microbalance (Mettler Toledo, Columbus, OH) located at the Johns Hopkins Bloomberg School of Public Health. Pre-weighed Teflon filters were loaded into polypropylene filter cassettes (SKC Inc., Eighty Four, PA), along with Filter pads (Pall Life Sciences, Ann Arbor, MI) and 37mm drain discs (Model #230800 Air Diagnostics and Engineering, Harrison, ME) at the Harioun clinic in a field-developed clean box to minimize contamination during assembly. Upon completion of sampling, filter cassettes were sealed in plastic bags until returned to the United States where they were disassembled and post weighed. For quality control and assurance purposes, 10% duplicate samples were collected and all filter weights were blank corrected. In order to ascertain BC concentration, Teflon filters underwent an optical analysis technique at Columbia University[6].

VDC borders were mapped (see Figure 2) and populated areas identified in order to design a sampling plan that would locate a higher number of sites in high-density housing areas. This was done for the dual purpose of sampling in areas of potential high BC production as well as logistical limitations. Large sections of VDC's are rice patties or sugarcane fields, therefore inaccessible by vehicle or consistent footpaths. Ease of access was an important factor in order to ensure that the field team could travel between sites in a timely manner during sampling. Samplers were placed at predetermined GPS coordinates that were based upon size of VDC, location of populated areas, presence of roads, and other potential BC sources (i.e., brick kilns). Each cookstove VDC geographic area ranged between 4 to 10 km^2. Area, number of sites, and duration of sampling for each VDC are shown in Table 1.

Due to equipment and personnel limitations, samples were limited to four sites per day. Sampling moved progressively from north to south within each VDC, with each day having new sites until all locations had been covered. A 5th sampler was located at the VDC area centroid for every day of sampling in order to assess and potentially adjust for any temporal relationship that may exist due to samples being collected across multiple days. Samplers were placed on bamboo fashioned tripods to standardize height measurements (~1.8m) across locations and were started and stopped at the same time. Other items noted were distance to major roads and point sources (i.e., brick kilns), as well as meteorological patterns. Meteorological data, including wind speed, wind direction, temperature, rainfall, and humidity, was recorded using an MK-III weather station (Rainwise Inc., Trenton, ME), located on the roof of the Harioun clinic. In addition, traffic counts were hand recorded during sampling at each site.

Figure 3: Images of field staff conducting sampling and weather station (bottom right) at Harioun clinic

Challenges to Ambient Sampling in a Low Resource Setting

Conducting outdoor air sampling in a rural setting within a low-income country had many challenges. The field sampling team was structured such that five people (locally hired) were stationed at each of the sites to monitor the equipment during sampling. In addition, one NNIPS staff member went between sites on motorbike in order to ensure protocol compliance, address equipment issues, and conduct random inspections of the local staff (i.e., ensure no one had abandoned their post). Determining locations of sample sites allowing for this paradigm was challenging. Ideally, sampling points would be spread equidistant throughout each of the VDC's in order to maximize spatial coverage. However, this was not possible given that huge swaths of farmland, rivers, and other obstacles prevented accessing many sites in a practical and timely manner. Therefore, sites were concentrated in areas of high population density and near thruways, with less priority given to sampling in farmlands.

Hiring locals from the different VDCs, where unemployment is high, also proved to be challenging. Hiring criteria included having a mobile phone, being able to read and write sampling times as well as traffic counts, have a method of transportation (e.g., bicycle), and be trustworthy. During sampling of the first VDC (Pipariya), the local community raised many questions about the criteria for our hiring practices. Questions were usually in the context of why one of their own family members or friends had not been hired. When sampling commenced in the next VDC (Pidari), two staff members from the previous VDC were retained because of familiarity with the protocol and equipment. This community objected to staff being hired from outside their VDC, however, no action was taken. For sampling in the 3rd VDC (Laxmipur), the same two staff members were again retained with objections from this community also being raised. However, unlike the previous VDC where locals took no action, on the 2nd day of sampling in this VDC, a large crowd gathered outside the NNIPS VDC field office and protested the retention of staff. The crowd took measures to prevent any additional work from being completed as well as insisted they would limit other NNIPS ongoing operations within the community. The crowd demanded that all 5 staff members on the team be dismissed and workers from the local VDC be hired regardless of the fact that the study had already begun. Eventually, a compromise was reached where all 5 workers were released and a lottery system implemented to randomly hire 5 new workers, all from the local VDC. This experience highlighted the need to keep open lines of communication and maintain positive, transparent relationships with the community where sampling is being conducted in order to quickly resolve issues that may arise while conducting research.

Preliminary Results

The completed ambient sampling of the four VDCs with locations of sample sites identified is shown in Figure 3. Locations where samples are concentrated indicate areas of high-density housing. Furthermore, VDC centroids, where $PM_{2.5}$ measurements were taken everyday in the respective VDC, are marked. It should be noted that a small number of sample sites fell just outside the identified borders of a VDC. This was allowed for logistical reasons, primarily to ensure easy access to the site for the field staff. All sites were sampled during the morning and midday to measure cooking and background $PM_{2.5}$ concentration

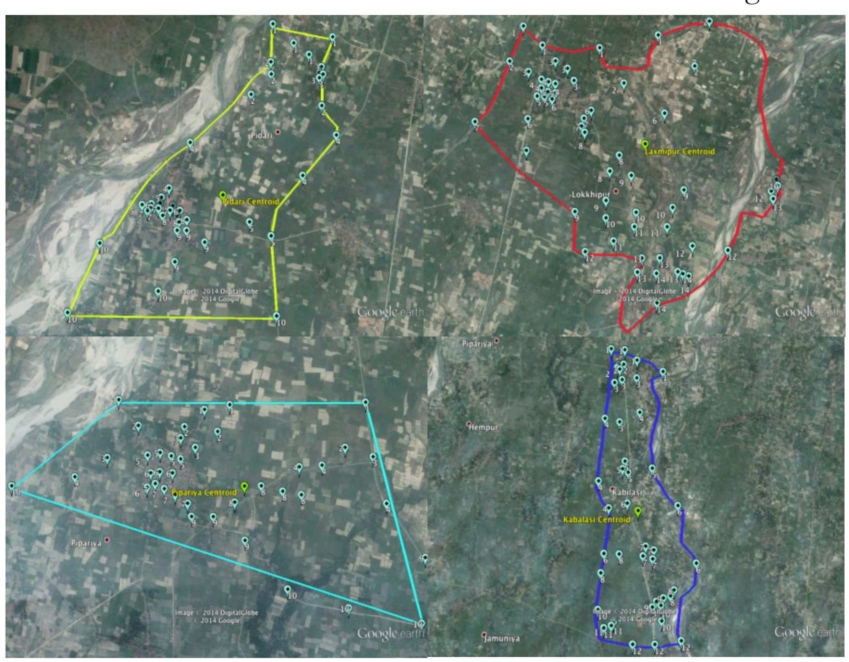

Figure 4: Sample site location map by VDC, with number indicating day sampled. Starting from bottom left, VDC names going clockwise are Pipariya, Pidari, Laxmipur, and Kabalasi.

respectively, with a small subset of sampling performed during the evening cooking session. VDC Laxmipur had the largest number of samples taken due to having a large area (9 km^2) and having 4 brick kilns. Kabalasi had the second most sites sampled (44) because of an equally large area (10 km^2), a major road going through it, and 3 brick kilns.

Table 2. Centroid point measurements - Particulate $Matter_{2.5}$ ($PM_{2.5}$), Black Carbon (BC), and BC/$PM_{2.5}$ Ratio Summary Statistics

VDC	Period	N	$PM_{2.5}$ Concentration (µg/m³) Mean (SD)	$PM_{2.5}$ Concentration (µg/m³) Median (Range)	BC Concentration (µg/m³) Mean (SD)	BC Concentration (µg/m³) Median (Range)	BC/$PM_{2.5}$ Ratio (%) Mean (SD)	BC/$PM_{2.5}$ Ratio (%) Median (Range)
Pipariya	Background	9	125.2 (53.9)	122.5 (44.5-229.3)	6.9 (2.4)	6.8 (4.3-12.3)	6.4 (3)	5.4 (2.3-12.1)
	Morning Cooking	10	125.3 (66.6)	110.5 (44.3-263.6)	7.8 (2.6)	7.3 (5.3-11.9)	7.7 (3.4)	7.8 (2-12.1)
Pidari	Background	10	160.8 (55.2)	147.3 (95.8-252.6)	14.7 (8)	13.1 (6.7-26.7)	8.7 (2.6)	8.5 (5.2-12.5)
	Morning Cooking	9	174.7 (86.3)	164.9 (54.3-330.7)	17.3 (9.4)	14 (5.9-30.6)	9.9 (2.1)	9.8 (7-13.4)
Laxmipur	Background	11	158.2 (48.4)	170.7 (72-206.3)	11.7 (6.8)	11.2 (3.7-25)	7.1 (3)	6.5 (3.4-12.9)
	Morning Cooking	14	150.3 (65.5)	132.4 (59.9-286.4)	17 (8.1)	16.2 (3.5-32.4)	11.3 (3.5)	11.9 (4.4-17.6)
Kabalasi	Background	12	122.4 (43.6)	119.6 (58.3-203.9)	10.9 (3.6)	11.6 (3.6-16)	9.5 (4)	8.9 (3.2-19.2)
	Morning Cooking	12	200.9 (87.2)	156.7 (110.8-397.2)	30.3 (11.4)	25.8 (16.6-49.7)	15.5 (2.5)	15.4 (10.4-20.1)
Pidari	Evening Cooking	2	138.9 (34.4)	138.9 (114.6-163.2)	17.6 (14.1)	17.6 (7.6-27.6)	11.8 (7.3)	11.8 (6.6-16.9)
Laxmipur	Evening Cooking	2	106.6 (86.1)	106.6 (45.7-167.4)	9.8 (4.7)	9.8 (6.5-13.1)	11 (4.5)	11 (7.8-14.2)
Kabalasi	Evening Cooking	1	84.9 (NA)	NA (NA)	7.4 (NA)	NA (NA)	8.8 (NA)	NA (NA)

Centroid measurement summary statistics for $PM_{2.5}$ concentration, black carbon concentration, and the percentage of $PM_{2.5}$ that is comprised of BC, are presented by VDC and period of sampling in Table 2. Locations of centroid samples were in farmland areas, away from high-density housing locales. Across each VDC, a higher $PM_{2.5}$ concentration was expected for cooking periods relative to background levels. However, as seen in Table 2, this is not always the case (e.g., Laxmipur morning cooking vs. background period mean (SD) $PM_{2.5}$ concentration is 150 $\mu g/m^3$ (65) vs. 158 $\mu g/m^3$ (48)). This indicates other factors may be at play, including wind speed/direction or location of centroid relative to housing areas. Evening cooking statistics are also presented, with $PM_{2.5}$ concentration in VDC's Kabalasi and Laxmipur having lower evening concentrations relative to the morning cooking session, keeping in mind the small sample sizes of the evening session. Several filters from the evening samples had to be discarded due to filter cracking or mishandling of equipment. Mean BC concentration and BC/$PM_{2.5}$ ratio were higher for morning cooking periods vs. background for all VDC centroid locations. Having the BC/$PM_{2.5}$ ratio higher across all VDC's for the cooking period indicates that cooking activities may influence the amount of BC present in ambient air. An additional assessment across sampling day of centroid $PM_{2.5}$ measurements for each VDC, separated by sampling period, is presented in Figure 5. The blue line indicates the morning cooking period, red line is background period, and black line is the evening cooking session. As seen in Figure 5, centroid $PM_{2.5}$ concentrations are not consistent day to day. Furthermore, while the background period is expected to be consistently lower than the cooking periods, this is not the case. Other factors, such as wind direction/speed or presence of other sources, could be causing these inconsistencies.

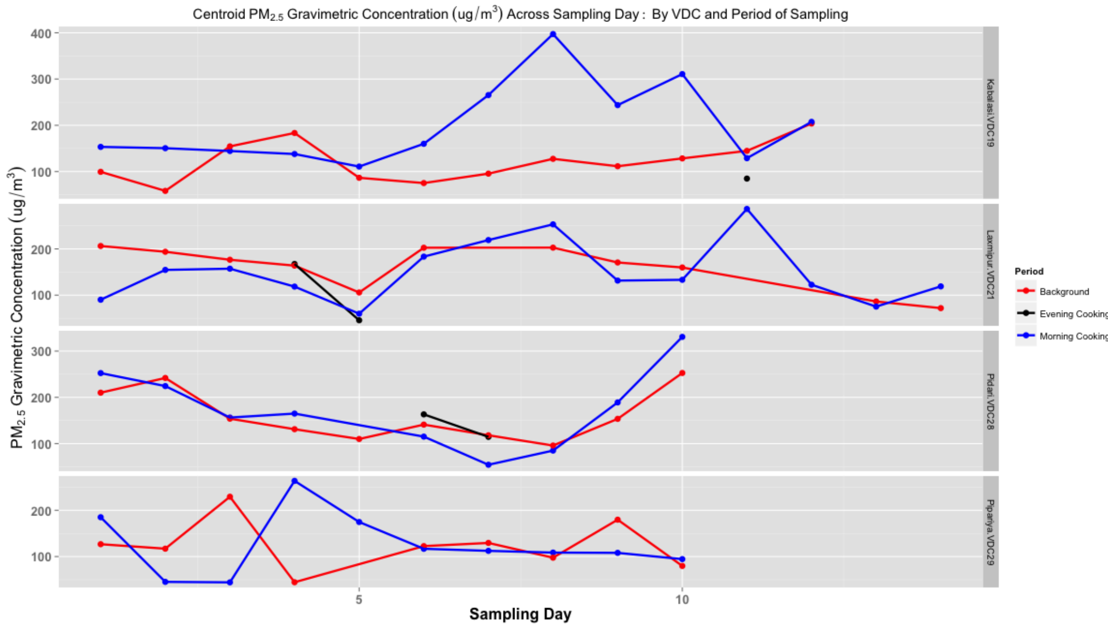

Figure 5: Centroid $PM_{2.5}$ concentration across sampling day, separated by VDC and sampling period.

Summary statistics for all sample sites aggregated (excluding the centroid measurement) across VDC and sampling period are presented in Table 3. With several sites located in or near high-density housing areas, $PM_{2.5}$ and BC concentration, as well as the BC/$PM_{2.5}$ ratio, is expected to be higher during cooking periods relative to background. As presented in Table 3, this is true for all concentration metrics across all VDCs, with the exception of the mean BC/$PM_{2.5}$ ratio for the Laxmipur evening cooking session. The evening cooking session BC/$PM_{2.5}$ average (SD) ratio of 11.7% (3.3) is only slightly lower than the Laxmipur background average (SD) of 13.2% (14.5), keeping in mind the smaller sample size for the evening cooking session.

Table 3. Sampling sites (excluding centroid) - Particulate Matter$_{2.5}$ ($PM_{2.5}$), Black Carbon (BC), and BC/$PM_{2.5}$ Ratio Summary Statistics

VDC	Period	N	$PM_{2.5}$ Concentration (μg/m³) Mean (SD)	$PM_{2.5}$ Concentration (μg/m³) Median (Range)	BC Concentration (μg/m³) Mean (SD)	BC Concentration (μg/m³) Median (Range)	BC/$PM_{2.5}$ Ratio (%) Mean (SD)	BC/$PM_{2.5}$ Ratio (%) Median (Range)
Pipariya	Background	31	114.4 (38.8)	110.8 (30.2-199.7)	8 (3.6)	6.5 (5-18.5)	7.6 (3.7)	7.5 (2.8-21.5)
	Morning Cooking	34	137 (137.5)	100 (29.3-835.4)	15.1 (14.2)	9.3 (5.1-55.1)	13.7 (16.5)	9.6 (3.4-99.8)
Pidari	Background	39	200.2 (73.1)	184.7 (110-438.5)	16.5 (8.9)	14.1 (4-46.6)	8 (2.5)	7.8 (3.6-15.7)
	Morning Cooking	34	238.2 (136.9)	197.8 (111-945.9)	27.1 (15.3)	20.5 (8.9-74.7)	11.3 (3.6)	9.9 (6.4-21.3)
Laxmipur	Background	49	162.1 (94.3)	140 (29.4-504.9)	16.4 (11.5)	13.4 (3.8-62.3)	13.2 (14.5)	9.3 (3-79.3)
	Morning Cooking	51	233.3 (163)	180.1 (47.2-819.8)	34.7 (25)	25.7 (5.5-100.4)	15.7 (6.8)	14.7 (4.8-33.9)
Kabalasi	Background	43	135.1 (47.5)	123.8 (31.6-254.4)	12.7 (4.8)	12.5 (3.7-23.3)	10.1 (4.6)	9.6 (3.3-27.1)
	Morning Cooking	43	230.8 (79.3)	209.6 (29.3-543.7)	37.1 (14.4)	32.3 (21.2-91.1)	17.5 (9.4)	15.4 (8.7-72.4)
Pidari	Evening Cooking	8	403.2 (116.9)	398 (208.5-600.1)	48.3 (16.8)	44.6 (22.3-76.5)	12.2 (3.1)	11.5 (6.8-16.4)
Laxmipur	Evening Cooking	7	755.3 (642.9)	456.6 (174.9-1951)	84.6 (67.6)	79.6 (13.9-216.2)	11.7 (3.3)	11.1 (7.9-17.4)
Kabalasi	Evening Cooking	6	177.3 (86.4)	146 (97.7-304.3)	21.6 (15.5)	22.6 (4.9-46)	11.1 (5.1)	12.9 (4.8-15.5)

Figure 6 presents spread of all $PM_{2.5}$ concentration data across sampling day, separated by VDC. Furthermore, categories of morning cook session (blue), background (red), centroid morning cooking session (grey), and centroid background (black) are presented. Evening cooking session was excluded due to the small sample sizes. In addition, the three highest $PM_{2.5}$ concentration samples were excluded to allow for a clearer graphical display of the daily variation. The removed values all came from the morning cooking session, specifically from VDCs Pipariya (835 μg/m^3), Pidari (946 μg/m^3), and Laxmipur (820 μg/m^3). Generally, cooking periods appear to be higher than background levels, however, this can vary by VDC and sampling day, further indicating the need to account for other

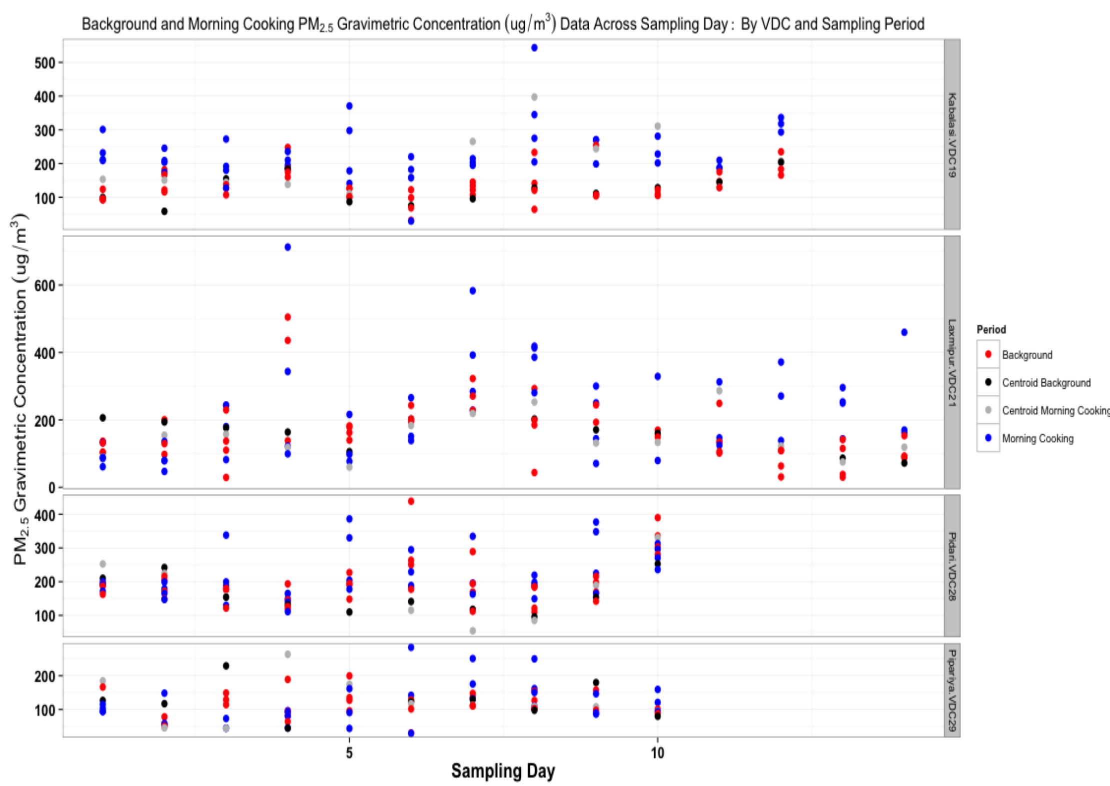

Figure 6: Background and morning cooking $PM_{2.5}$ concentration* across sampling day by VDC and sampling period
***Three highest $PM_{2.5}$ concentration samples were excluded to allow for variation within graphical display to be discernable. Values excluded include morning cook session data from VDC Pipariya (835 μg/m³), Pidari (946 μg/m³), and Laxmipur (820 μg/m³).**

factors when conducting future analysis.

$PM_{2.5}$ concentration, BC concentration, and the ratio of BC to $PM_{2.5}$ can all be evaluated for spatial dependence. As a first-pass, efforts have focused upon examining spatial dependence of $PM_{2.5}$ concentration. In order to assess spatial dependence for $PM_{2.5}$ concentration across all sampled sites, variogram analysis was performed using the classic estimator approach. Variogram analysis, restricted to half the maximum distance, is the standard approach and consistent with common practice to characterize small-scale spatial correlation[7,8]. Figure 7 illustrates the use of a classic variogram estimator for the background and morning cooking periods by individual VDC with no adjustment made to the $PM_{2.5}$ concentration data. Figure 8 presents classic variogram estimators for the cooking and background periods across VDC with natural log adjusted $PM_{2.5}$ concentration data. Log adjusting the $PM_{2.5}$ data was done in order to assess if any difference would exist with data following a more normal distribution. Since the four cookstove VDC's are in close proximity to each other, sample data from each VDC were pooled together to examine spatial dependence across the entire study site. Figure 9 presents classic variogram estimators for unadjusted and log adjusted pooled $PM_{2.5}$ concentration data between the background and cooking periods. Centroid measurements were included in all of these analyses (Figures 7-9) by averaging across the sampling days in each VDC.

Visual inspection of the variograms across unadjusted $PM_{2.5}$ concentration vs. adjusted $PM_{2.5}$ concentration data (Figure 7 and 8) present minimal change. Furthermore, background vs. cooking period variograms in Figures 7 and 8 indicate that in many VDC's the spatial resolution for the samples collected and the number of sample collected may not have been adequate to detect spatial correlation.

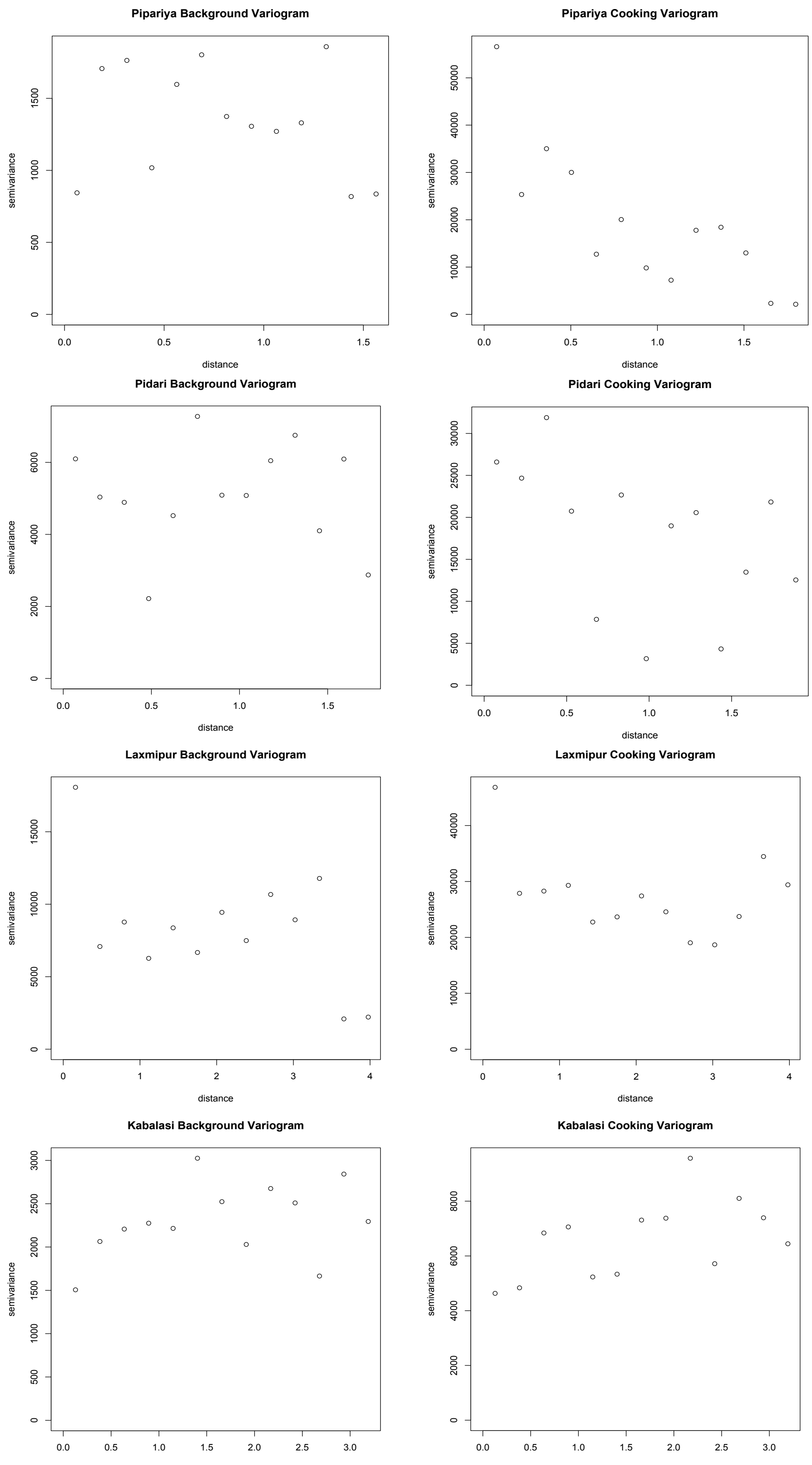

Figure 7: Unadjusted $PM_{2.5}$ concentration classical variogram estimators for background (left column) and cooking (right column) periods by VDC.

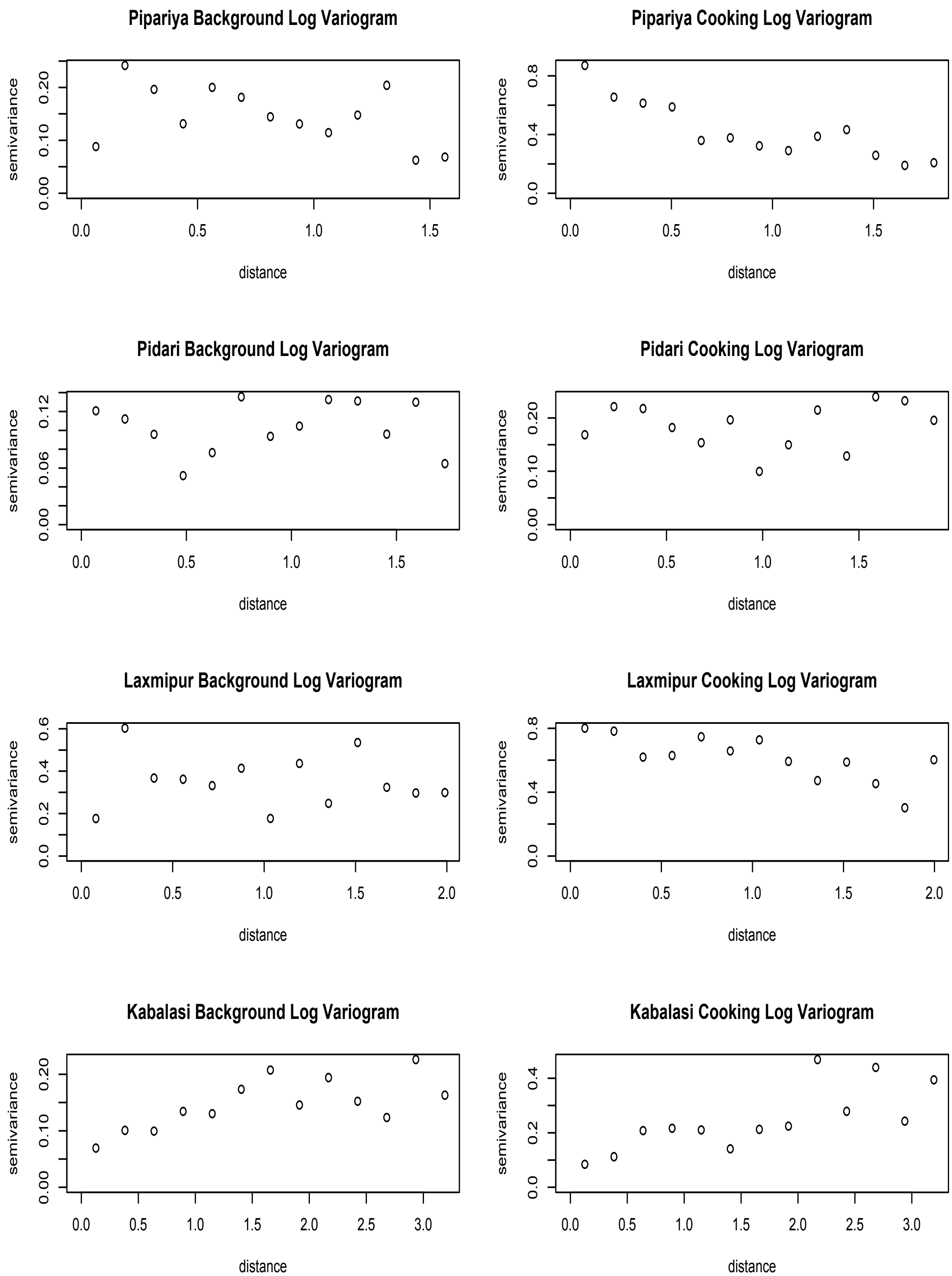

Figure 8: Natural log adjusted $PM_{2.5}$ concentration classical variogram estimators for background (left column) and cooking (right column) periods by VDC.

In addition, examining Figure 9 across cooking or background period, whether unadjusted or log adjusted, a similar conclusion can be reached.

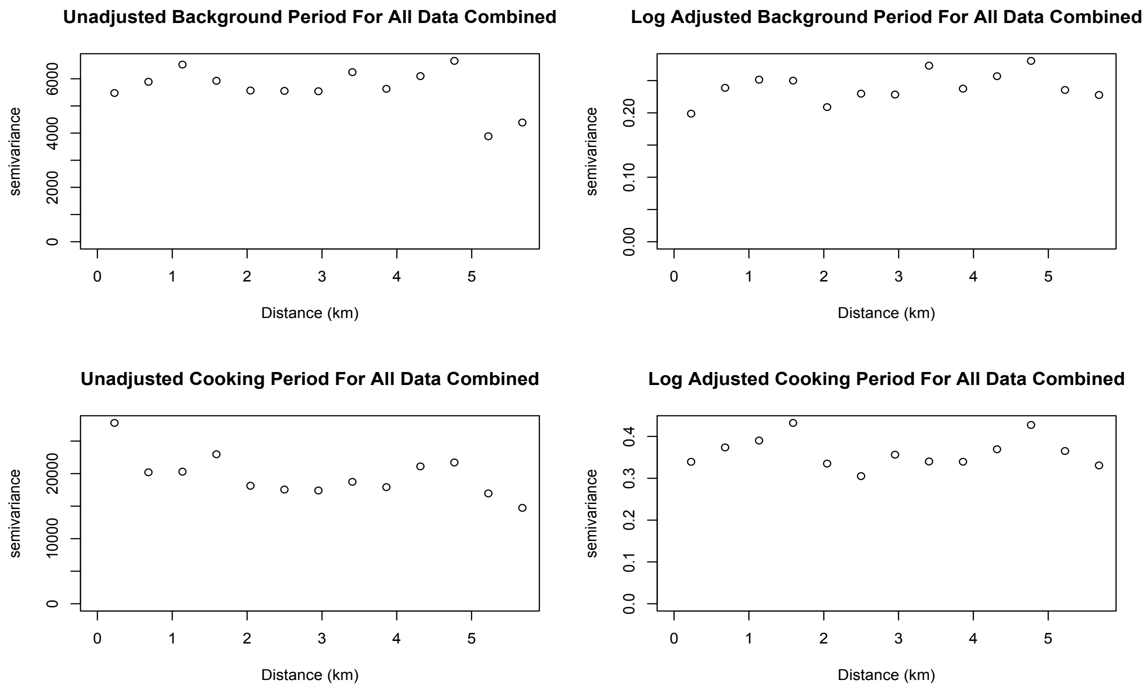

Figure 9: Pooled $PM_{2.5}$ concentration data classical variogram estimators for background (top row) and cooking (bottom row). Left column is unadjusted $PM_{2.5}$ concentration data and right column is natural log adjusted $PM_{2.5}$ concentration data.

However, further evaluation is necessary where samples located in high-density housing areas are parsed out from those in more rural locales. Beyond this, next steps for this analysis include evaluation of spatial correlation for BC and ratio of BC/$PM_{2.5}$. Additional evaluation will focus upon various functions for variogram fitting across what has been analyzed as well as that proposed.

Spatial Prediction Model Development

Upon further variogram assessment, a spatial regression model will be developed in order to predict $PM_{2.5}$ and BC concentration at unsampled locations across the VDC sites. This specific approach will utilize both ambient measured BC and exfiltration estimates (presented in Chapters 3 and 4) from the ~3,000 homes located in the cookstove VDC's that are enrolled in the parent trial. The model approach that will be used is known in the geostatistical literature as universal kriging[8–10], which is a regression model-based approach for optimizing spatial prediction. It can also be thought of as a linear prediction model with a mean structure that is nonstationary[9]. This spatial regression model has the general form:

$$Y(\mathbf{s}) = \beta_0 + \beta_1 X_1(\mathbf{s}) + \beta_2 X_2(\mathbf{s}) + \ldots + \beta_p X_p(\mathbf{s}) + \varepsilon(\mathbf{s}), \text{ where } \varepsilon(\mathbf{s}) \sim N(\mathbf{0}, \boldsymbol{\Sigma}) \qquad (1)$$

where Y is the outcome variable at the specified location s, $X_1(\mathbf{s})$, …, $X_p(\mathbf{s})$ are the covariates of interest indexed by location **s**, β's are their associated effects, and $\varepsilon(\mathbf{s})$ is the spatially correlated random error term (assumed Gaussian)[11]. The $\boldsymbol{\Sigma}$ component within the error term is the variance-covariance matrix for the residuals within the universal kriging model, which characterizes spatial dependence[11]. Inference for parameters in Equation (1), including both mean component β's and parameters used to describe spatial variation in $\boldsymbol{\Sigma}$ are based on well-established geostatistical techniques[7,9–11]. Inference for Equation (1) is based on generalized least squares yielding best, linear, and unbiased predictors (BLUPs), with the optimality criteria of "best" defined to minimize mean-squared prediction error[9]. Possible data transformation to achieve normality for the regression assumption will be based on the Box-Cox family of power transforms, which has been successfully applied in the spatial setting[12].

The outcome $Y(\mathbf{s})$ in Equation (1) will be ambient measured BC, while the primary covariate $X_1(\mathbf{s})$ are homes enrolled in the parent cookstove trial treated as point sources. Specifically, homes will provide point estimates by converting indoor nephelometric PM data to $PM_{2.5}$ equivalents (utilizing quality control methods presented in Chapter 2). These data will be further combined with PM exfiltration and BC component estimates presented in Chapters 3 and 4. Locations of the sampled ambient BC and households are not spatially coincident. The household BC covariate $X_1(\mathbf{s})$ will therefore be defined as the average (during daily cooking time) household BC measurement for households closest to each ambient sample location. Estimates are available for how often the improved cookstoves are being utilized, thus we can account for the impact of stove use compliance. How many "close" households to use will be determined based on prediction performance and subsequent spatial cross validation techniques[7]. Additional covariates that will be assessed for inclusion are wind speed, wind direction (as a categorical variable, thus allowing us to assume isotropy), temperature, relative humidity, population density, distance to potential point sources, and potential interaction between variables. Model analysis will follow standard statistical practices that will include model relevance (via AIC), examination of unusual outliers (via Cook's distance score), correlation (via Pearson's correlation coefficient), and assessment of covariate significance (for a p value <0.05). Furthermore, utilizing the centroid measurements of each VDC, temporal variation throughout the sampling period will be assessed via the construction of a temporal variogram, similar to what was used to assess spatial correlation. If deemed necessary, a temporal based covariate will be included within the statistical model to appropriately adjust for temporal variation within the sampling period of each VDC. The technique of cross validation will be utilized in order to assess model accuracy. Examples of this technique include utilizing a leave-one-out approach or withholding subsets of sampled BC outdoor data from the analysis and then predicting upon them given the remaining values[9]. Prediction maps will be created using ArcGIS 10.2.0 (ESRI Inc., Redlands CA) as well as in the R Statistical Computing Environment (Version 3.0.2; 2013-09-25).

Summary and Proceeding Work

This study involves three main steps. First, ambient $PM_{2.5}$ data were collected at numerous sites across the four VDC's participating in the parent cookstove trial. Ongoing current work will characterize the spatial distribution of $PM_{2.5}$ and BC over these VDC areas during morning cooking and background periods. Future work includes the development of a spatial model that will allow for the assessment of local scale PM and BC concentrations based on indoor to outdoor cookstove emissions. Furthermore, prediction of BC at unsampled locations across the four cookstove VDC's will also be integrated into this model development. Projected publications stemming from this work include 1) Spatial Characterization of Black Carbon during Cooking and Non-Cooking Periods in Village Settings and 2) The Development of a Spatial Prediction Model for Village Level Ambient BC and $PM_{2.5}$. This research sets the foundation to characterize the spatial distribution of black carbon across a much larger area using satellite-based optical sensors.

6 Future Work Assessing Ambient Air Pollution Due to Use of Cookstoves in the Indo-Gangetic Plain: Scale of Influence and Policy Implications

Introduction

Since black carbon (BC) within the Indo-Gangetic Plain (IGP) is considered to be a huge source and major contributor to hydrological cycle change and glacial retreat, it is critical to address the need for improving inventories of BC emissions. Existing inventories within the IGP suffer from limited representation of rural sources, reliance on idealized or point source estimates, and the difficulty of distinguishing between bulk BC sources (cookstoves, kilns, etc.). Current projections also do a poor job of accounting for the amount of BC that actually makes it into the ambient air to affect local air quality and subsequently transported to climate sensitive regions. The future work suggested here focuses on the need for developing improved emissions inventories as well as understanding associated health and economic impacts related to emission transport. This need can be addressed by focusing on three main objectives. They are:

1) Integrate a wider, geographically representative, field-based measurement strategy with satellite-derived data to estimate the contribution of cookstove-generated black carbon concentration across the IGP.
2) Estimate transport of black carbon from the IGP to glaciated regions of the Himalayas using methods that are descriptive (remote sensing) and predictive (physically-based climate models).
3) Project the regional impact on health and economic indicators based on direct evidence from cookstove related interventions.

Detailed Approach for Future Work

Objective 1: Integrate a wider, geographically representative, field-based measurement strategy with satellite-derived data to estimate the contribution of cookstove-generated black carbon concentration across the IGP.

Remote sensing applications have enormous potential for air pollution assessment. Given constraints that limit air quality measurement, remote sensing applications provide an alternative to assess pollutant concentrations, particularly in areas of limited accessibility. This objective seeks to improve remote sensing applications by utilizing the geostatistical model (to be developed, outlined in Chapter 5) as a "ground truth", in order to create an inference model utilizing satellite data. Furthermore, this objective will result in the generation of a spatially distributed inventory of BC emissions across the IGP, with a focus on difficult-to-characterize diffuse rural emissions.

The most direct satellite measurement for generating an estimate of $PM_{2.5}$ is aerosol optical depth (AOD), which is a measure of the light extinction by aerosol scattering and absorption in the atmospheric column[1]. AOD can be used as an input variable in statistical models to predict $PM_{2.5}$ since it reflects the integrated amount of particles in the vertical column[1–3]. Moderate Resolution Imaging Spectroradiometer (MODIS), a satellite-based optical sensor, could be one of the providers of data for this purpose. MODIS is the preferred instrument since it provides daily global coverage in 36 spectral bands, ranging from 0.4μm to 14.4μm, at varying spatial resolutions[4–8]. Currently, the highest resolution available for single MODIS images at the desired bands is 1km by 1km. MODIS provides products for various geophysical properties, including but not limited to aerosol properties. There are two satellites that collect MODIS data, Terra and Aqua, each providing daily snapshots at approximately 10:30am and 1:30pm (GMT +5:45), respectively. MODIS aerosol product data have been validated via a series of ground based sun photometers called the Aerosol Robotic Network (AERONET)[7].

Even though the use of MODIS provides for the most direct approach to measure BC or $PM_{2.5}$, other complimentary satellite sensors, measurements, and products can also be examined. Examples of other satellite instruments or measurements to include could be land cover type, vegetation index, surface albedo, near-surface humidity, and broadband visible and near-infrared radiance at sensor. In addition, the use of other indirect remote sensing approaches that are capable of estimating $PM_{2.5}$ as a function of AOD could be considered. Being open to the use of several different satellites and their associated products will contribute to an increased likelihood of successfully achieving this objective.

Since all satellite data sources provide some type of measurement value for each pixel (image), it will be necessary to alter the spatial prediction model from Chapter 5 to generate an aggregated value that will line up with and match the resolution of the same boundaries as the data provided by the satellite imagery. This can be approached by aggregating the values in the prediction model via the methodology of block kriging. This method of kriging is applicable to predicting an average value associated with a certain region(s) of interest utilizing data from specific locations within that area[9,10]. Results from Equation (1) in Chapter 5 can be used to optimally predict the VDC spatially averaged cookstove generated BC. Block kriging[9,10] empirically estimates the following quantity:

$$Z(B) = \frac{1}{|B|} \int_B Z(s)\,ds \qquad (1)$$

Where *B* represents a VDC region. Spatially averaged VDC BC can then be used to support efforts to link ambient BC to remote sensed products that have been outlined.

Data Analysis Plan for Objective 1

A multivariate linear regression (MLR) model will be developed that will utilize covariates that include satellite imagery products (e.g., measuring aerosol optical depth, surface albedo, land cover type, etc.) averaged over the data collection sample time frame discussed in Chapter 5. The response variable will be the predicted BC concentration at ground level generated from the spatial prediction model. The spatial prediction model will act as the "ground truth" for these aerosol constituents. Satellite imagery will be imported into ArcGIS 10.0.2 (ESRI Inc., Redlands CA) and averaged from an equivalent time period overlapping the field sampling campaign. Inclusion of other covariates such as population density, meteorological data, as well as interaction coefficients, will be assessed for this model in order to improve the model fit. Model fit will be assessed using standard statistical processes including correlation, model relevance (via AIC), and analysis of unusual outliers (via Cook's distance score). Once a model has been developed, relevant covariates will be used in order to develop estimates of BC and $PM_{2.5}$ across the rest of the IGP region. It is recognized that VDC level data collected from work conducted in Chapter 5 is not representative of ground truth across many parts of the IGP region, especially regions of heavy urbanization. Additional sensitivity analysis will be considered for this modeling approach. Further consideration will be given to the utilization of existing data sets in other parts of the IGP for creation of area-level estimates along with the collection of additional data in other parts of the IGP. All statistical analysis will be conducted in the R Statistical Computing Environment (Version 3.0.2; 2013-09-25)

To summarize this approach, by utilizing predicted BC concentrations generated from remaining work discussed in Chapter 5, block kriging will be performed in order to generate regional estimates that will act as the response variable. Multiple satellite data resources will be used as covariates, along with other variables such as meteorological data, in an inference regression model to assess the ability to ascertain BC ground-level outdoor data. Finally, upon development of this regression model, covariates deemed significant predictors will be used to develop an emission inventory of ambient ground-level BC across the IGP region.

Some limitations of this aim include some satellites (such as MODIS) inability to see through clouds. This is one of the reasons why the monsoon season was excluded during sampling discussed in Chapter 5. Another limitation may be the ability to parse out brown carbon through satellite imagery analysis, as brown carbon absorbs in the near UV range, which is below the 400nm lower limit. One approach could be to estimate the amount of brown carbon based upon estimating the ratio found between brown and black carbon using the optical analysis technique[11] from the field sampling campaign. However, other approaches will also be explored to address this issue as research progresses.

Evaluating Satellite Imagery Regression Model Performance Beyond Existing Study Site

In order to properly assess whether the regression model developed in this objective is accurately predicting BC or $PM_{2.5}$ concentration, additional field data will be collected from two VDC's outside of the current parent cookstove intervention trial. Since there are no indoor PM measurements in the non-intervened VDCs, a single day of indoor sampling will be conducted per household using the same methods as in the parent intervention study[12]. Sampling equipment, personnel, and other resources deemed necessary, will be utilized from Johns Hopkins in order to conduct this additional data collection pending reception of appropriate funding. Ultimately, 60% of the homes within these VDC's will be sampled, which is consistent with the percentage of homes involved in the current cookstove trial. Furthermore, outdoor air sampling will also be conducted across these VDC's using the same methods outlined in Chapter 5. Other covariates will also be recorded that are thought to affect concentration of outdoor BC, which may include distance to major roads/point sources and meteorological patterns. Similar statistical analysis will be performed, utilizing approaches from Chapter 5 and Objective 1.

In addition to assessing model performance, this aspect of Objective 1 will allow for contrasting spatial distribution of BC in non-intervened VDCs with those in the current cookstove trial where 60% of the homes have an intervention stove. Two approaches will be utilized to estimate the impact of stove intervention of ambient BC. The first approach will be a comparison of the spatially modeled BC in the intervened and non-intervened VDCs. Differences across a VDC and within villages can be used to estimate the spatially averaged impact of the intervention. Alternately, modeling the intervention impact by using the pre-intervention indoor PM concentration data to estimate exfiltration using techniques discussed in Chapter 3 can also be performed.

Objective 1 Summary

Objective 1 will yield a regression model capable of using satellite imagery, along with other covariates such as land cover or meteorological information, to predict ambient ground-level BC or $PM_{2.5}$. The development of this model will allow for the utilization of satellite imagery across the entire IGP region to create an emission inventory for these agents, with a particular focus on hard to characterize rural emissions in this region.

Objective 2: Estimate transport of black carbon from the IGP to glaciated regions of the Himalayas using methods that are descriptive (remote sensing) and predictive (physically-based climate models).

The spatially adjusted estimates of outdoor PM and BC generated under Objective 1 are highly relevant to problems of air quality and climate. From an air quality perspective, cookstove generated PM that remains near the surface represent a potential health threat at village scale. For climate, airborne PM and BC can lead to local warming or cooling, depending on their chemical characteristics and on interactions with cloud formation, and those aerosols deposited in snow covered regions can act to accelerate the melting process. This deposition related climate influence is of particular concern in glaciated regions, like the Himalayas, where large volumes of aerosols transported from neighboring lowland regions may be accelerating glacier retreat, causing changes in the hydrological cycle and positive feedbacks on alpine warming.

Connecting near-surface estimates of PM and BC concentrations in the source region to regional concentrations and subsequent export to neighboring mountains is not a problem to be taken lightly. Boundary layer stability, localized convection, topographically driven flows, and chemical and radiative processes all influence aerosol concentrations and transport, and failure to resolve these phenomena in an atmospheric model can bias simulation of aerosol processes. This objective proposes to overcome these challenges by implementing the newly developed NASA Unified Weather

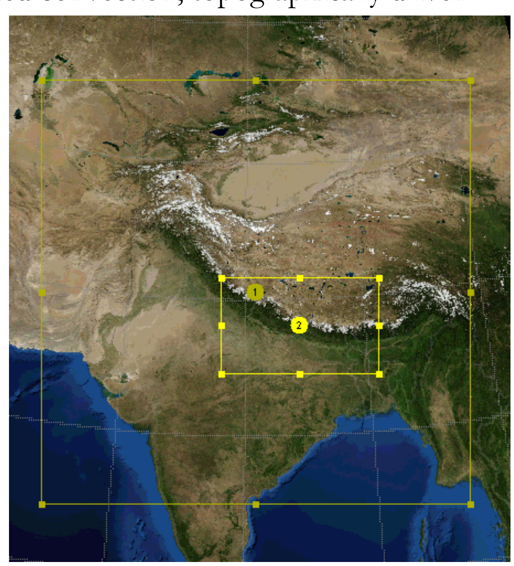

Figure 1: Proposed NU-WRF modeling

Research and Forecasting (NU-WRF) model[13] for extended simulations over a domain that includes the IGP and Himalayan mountains, as well as neighboring regions relevant to the synoptic scale circulations. The NU-WRF modeling system combines WRF[14], NCAR's state of the art regional climate model, with the Goddard Chemistry Aerosol Radiation and Transport (GOCART)[15] model, the NASA Land Information System[16], the Goddard Satellite Data Simulator Unit (G-SDSU)[17] and other NASA assimilation and modeling systems. NU-WRF has been applied to studies of aerosol chemistry[18] and land-atmosphere interactions[19], and is under continued development at NASA Goddard Space Flight Center.

In this application, NU-WRF will be implemented with two domains: an outer domain at 12km resolution that uses 50km NASA Modern Era Retrospective Analysis for Research and Applications (MERRA)[20] fields for lateral boundary conditions and a 4km resolution inner domain that will include GOCART chemistry (Figure 1). Both domains will use the Goddard long wave and shortwave radiation schemes, the YSU planetary boundary layer parameterization[21], and Noah Land Surface Model implemented within LIS[16]. Additional nesting to 1.3km will be considered for select areas or periods of interest. Two week NU-WRF simulations will be performed in each season and for two contrasting synoptic atmospheric conditions, for a total of 16 weeks of simulation time with active chemistry. This simulation plan is designed to provide explicit resolution of convective processes in the inner domain, to include moderately high resolution (12km) of surrounding topography and coastlines, and to capture a range of representative weather conditions. In adopting this approach, the goal is to establish a modeling system that can provide credible simulation of PM processes in the IGP/Himalaya region under diverse atmospheric conditions and to compare the inventory/simulation method to other published methods. Time allowing, simulations can be extended to generate full seasonal or annual estimates of PM concentrations and transport.

NU-WRF simulations will be evaluated using a suite of conventional and satellite observations. Conventional data will include WMO-reporting meteorological stations as well as additional stations in the IGP. Satellite data to be used as points of comparison against the simulation may include products generated by MODIS[22], CloudSat[23], and CALIPSO[24]. In order to further evaluate satellite data, G-SDSU will be employed to provide inverse modeled estimates of satellite retrievals, ensuring a physically consistent comparison between satellite measurements and NU-WRF simulated fields. It should be noted that the intention is to treat WRF simulations and satellite-derived data as independent methodologies to constrain estimates of BC and $PM_{2.5}$ loading.

While some previous studies have addressed the question of aerosol transport to the Himalayas[25–28], no previous work was found that has combined field derived indoor-outdoor model based transport estimates with a high resolution regional climate model that includes atmospheric chemistry, or that has used satellite data simulation as a tool for evaluating modeled aerosol concentrations in data sparse regions. Each aspect of this approach is critical for appropriate simulation of PM processes in this topographically and climatically complex part of the world.

With regards to overall modeling uncertainty, it is recognized that the research flow depends on a statistical regression model at each stage, results of which each carry uncertainty. This uncertainty can be propagated through the research using tools of Monte Carlo simulation and conditional simulation. In the spatial setting, conditional simulation techniques[9] are often used to propagate uncertainty when spatial prediction results are used on input covariates to a second stage regression, which matches the approach in Objective

1. Spatial and non-spatial versions of these simulation techniques will be explored as an option for propagating uncertainty through the outlined research objectives.

Objective 2 Summary

Objective 2 will aim to utilize the satellite emission inventory of BC and $PM_{2.5}$ generated from Objective 1 to run regional climate simulations in order to study the transport of these agents from the IGP, considered to be the source region, to the Himalayas which are considered a climate sensitive zone due to the amount of glaciers and snow pack present in the region.

Objective 3: Project the regional impact on health and economic indicators based on direct evidence from cookstove related interventions.

There are numerous policy implications that can be better understood based upon the analyses conducted from the previous objectives. Of particular interest is the associated health and economic impact that would be derived based upon implementing various mitigation options that would alter the levels of BC and $PM_{2.5}$ in the IGP region. Implementing mitigation options targeted towards reduction of BC sources would have an automatic co-benefit of improving climate and health on a variety of scales[29]. Conversely, understanding interventions negative interactions that may take place upon climate and health, such as implementing chimneys on stoves to increase ventilation to the outdoors thus leading to more BC export but a reduction in indoor PM, are equally important to quantify in order to properly understand the trade-offs involved with such measures. With increasing investment occurring towards mitigation of BC, understanding the impact associated with such interventions is becoming increasingly critical in order to maximize and properly allocate all resources. Analyses from Objective 1 and 2 will provide for robust BC and $PM_{2.5}$ estimates across the IGP with transport to the Himalayas, thus setting the stage to assess these agents impact to climate and associated economic and health effects from glacier loss and hydrological cycle alteration. Furthermore, understanding the impacts from glacier melt is important, especially within the context of assessing the value of clean cookstoves and how they contribute to the overarching goal of protecting the Himalayan glaciers. However, although altering $PM_{2.5}$ and BC levels have a climate impact and studies have been done to better understand the short and long-term effects of doing so[30,31], it is vital to frame the importance of reduction of these aerosols to local health and economic impacts within the IGP so that policy makers may better understand the implications of such measures in less abstract terms.

In order to develop proper policy recommendations, a more comprehensive understanding must be developed with regards to understanding the health and economic impacts associated with $PM_{2.5}$ levels in the IGP region. A tool to conduct this kind of assessment is the use of the Environmental Benefits Mapping and Analysis Program (BenMAP; Abt Associates Inc., Bethesda, MD)[32]. BenMAP is a software, used in international settings, that assesses the impact of changes to air quality to population level health and economic outcomes[32,33]. Typically, epidemiological data is used to develop concentration-response functions that are capable of quantifying the associations between pollutant exposures and the incremental changes in adverse health outcomes based upon the exposure difference[33,34]. Additional inputs to the BenMAP software necessary to perform health and economic assessment are population census and growth projection data, air quality modeling and monitoring data, and valuation functions for economic impact assessment related to changes in morbidity and mortality[34,35].

Current work related to health impact assessment from cookstove generated emissions to outdoor air in the IGP is limited to estimations from stove and fuel usage and subsequent projections to outdoor air concentrations[36]. This approach is novel because of the utilization of an inventory generated from the basis of satellite imagery and regional climate modeling trained on actual ground based measurements (Objective 1 and 2) in order to assess associated health and economic impacts in this region of the world. The goal is to use the emission inventory generated from Objective 1 and 2 in order to assess immediate impacts to the health and economic burden based upon the evaluation of various interventions in stove type being introduced and the incremental changes in the outcomes sought. Utilization of this method to assess immediate benefits to air pollution reduction using inventory data have previously been conducted with other pollutants[37]. In addition to using the emission inventory, further evaluation will occur of various concentration-response functions for health-associated impacts, valuation functions for economic impacts, and population census data from the countries of interest within the IGP region. Furthermore, developing health related risk functions will be investigated based upon the findings from the parent cookstove trial currently underway via its assessment of health burden tied to traditional stoves against intervention stoves.

Working in partnership with the partner institution NGO, Nepal Nutrition intervention Project Sarlahi, and utilizing the contacts with government, other NGO's based in the IGP and academic institutions, these findings will be communicated in order to increase awareness of the need for further investment into reducing PM levels and the need for continued work in this area.

Objective 3 Summary

Objective 3 will utilize the emission inventory and regional transport model developed in Objective 1 and 2 to develop health and economic impact assessments in the IGP region. These assessments will be developed via the use of BenMAP software and will subsequently be communicated to other relevant institutions and organizations through the form of publications, conferences, and presentations.

Expected Results

If successful, this project will provide detailed regional estimates of cookstove related household BC emissions. This will be a unique dataset that can be used for a wide variety of air pollution health or climate change studies. While housing styles and cooking practices are not uniform across the world, the scenarios modeled in this study will have regional relevance across the IGP. The IGP includes northern and eastern India, the most populous parts of Pakistan, parts of southern Nepal, and almost all of Bangladesh. If successful, this study will provide a model that can be applied to other areas of the world.

Results of this study will be relevant to policy decisions about cookstove interventions that result in improved indoor air quality by increasing outdoor air pollution. Reductions in risk associated with lowering indoor air pollution may be offset by increases in ambient air pollution. An assessment of changes in BC associated with the implementation of an improved cookstove with a chimney designed to reduce indoor air pollution will also be provided. The use of satellite imagery trained to a “ground truth” based upon household and spatial modeling (discussed in Chapter 5) should reduce uncertainties associated with estimating cookstove related BC emissions and as a result improve climate change modeling. Furthermore, by estimating the impact of an ongoing intervention on local and regional ambient BC, this study will also be in the position to conduct health and economic impact assessments for the IGP region.

Summary

The purpose of this project is to build upon existing work that will provide robust estimates and model transport of BC emissions from biomass cooking on a local and regional scale in the IGP, and estimate changes associated with health and economic outcomes related to the changing of emissions associated with the introduction of future interventions. If successful, this project will reduce the uncertainty with respect to cookstove biomass combustion on local and regional BC emissions by using spatial models that will provide a "ground truth" for satellite remote sensing. Finally, estimates will be developed with regards to the impact upon health and economic outcomes based upon examining incremental changes associated with interventions designed to improve air quality across the IGP region. This information is needed to fully asses the impact of cookstove interventions on both health and climate change and how to best develop policies that will allocate resources to address this problem in the most effective manner. Figure 2 outlines the proposed work.

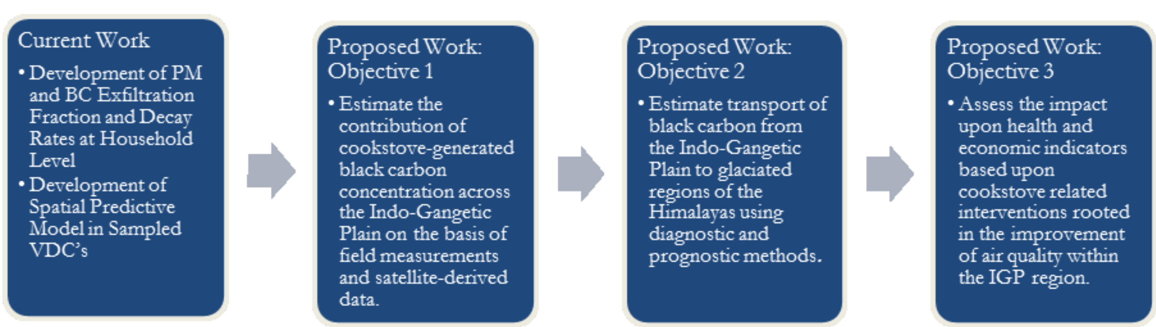

Figure 2: Summary of Future Work

7 Conclusion

Summary of Findings

This dissertation furthers the body of knowledge in the field of exposure assessment and climate change emissions as a result of cooking with biomass fuels in village homes. Specifically, research was conducted into cooking with biomass fuels and the role traditional and alternative cooking methods play in emitting black carbon emissions to the environment.

Chapter 2 explored a range of humidity and gravimetric equivalency adjustment approaches as it relates to use of a nephelometric device, the pDR-1000, to measure particulate matter emissions created by the use of cooking with biomass fuels. Providing an approach to determine humidity corrected gravimetric equivalent $PM_{2.5}$ concentrations will allow for systematic comparisons of exposure-response relationships in health studies using the pDR-1000. Traditionally, quality control adjustments to the pDR-1000 involve a two-step approach adjusting for relative humidity (RH) above 60%, followed by applying a linear relationship to ascertain the $PM_{2.5}$ gravimetric equivalent. This research found that for adjustments related to relative humidity, an overestimation bias exists at the 75% RH value and that an underestimation bias exists at low RH (<30%). Therefore, we proposed utilizing humidity adjustment equations that encompassed the entire RH range. In regards to gravimetric equivalency conversion, our study found that new proposed linear gravimetric conversion equations with log transformed variables and either a spline or quadratic term demonstrated a better fit. PM concentration measured in our study during biomass burning ranged from ~600 $\mu g/m^3$ to ~66,000 $\mu g/m^3$, which was much broader relative to other published studies. This wide range of concentration is believed to be the reason why the new proposed linear gravimetric methods had a better fit. Furthermore, an integrated conversion equation was proposed, allowing for humidity adjustment and gravimetric conversion in one step. This integrated method is preferred because it only involves one response variable (gravimetric $PM_{2.5}$ concentration), avoids overfitting, encompasses the entire RH range, and is relatively quick and straightforward. This study had many strengths, including measurement of PM caused by biomass burning in real-world homes in rural Nepal as well as accounting for PM over a very broad concentration range not seen in previous studies.

Chapter 3 focused on developing PM exfiltration estimates for traditional, open-design cookstoves. Little is known about air exchanges and pollution exfiltration from homes utilizing traditional stoves in low and middle-income countries. For health or climate change studies reliant upon knowing cookstoves impact to outdoor air quality, the source of concern is the house and stove together. Current stove-based emission factors do not provide for a direct estimate of the amount of pollution exfiltrating from the house. The house, to some extent, acts as a barrier to pollutants leaving or entering the house. A fraction of PM produced during cooking events will settle and deposit on surfaces indoors, including the roof or cracks within the walls of the house. Remaining PM will escape to the exterior environment either via direct (chimney) or indirect (window/doors and cracks) ventilation. The use of traditional, open-design cookstoves resulted in an average PM exfiltration fraction due to indirect ventilation of 26% (ranging from 6% to 58%). This value represents a significant departure from previously cited estimates that are based on theoretical calculations. Furthermore, this research found that window/door status was a significant predictor of PM exfiltration, while fuel type was not. Two additional components were examined as a part of this study. One component was an analysis on whether air exchange rates measured held true to the assumption of perfect mixing. Typical ventilation studies often assume that instantaneous (perfect) mixing occurs throughout the room when a pollutant is released. In order to test if the assumption of perfect mixing could be made, a small study examined the impact artificial mixing had upon air exchange rates within a mock house at the field site in Nepal. Our findings indicated no statistically significant difference between air exchange rates measured under artificial mixing vs. no mixing, allowing us to assume that perfect mixing was taking place in village homes within Nepal. We also determined the fraction of $PM_{2.5}$ that was comprised of black carbon during simulated cooking periods. The average ratio of black carbon to $PM_{2.5}$ measured was 37%, which was reflective of what has been found in similar studies. To our knowledge, the approach utilized to determine PM exfiltration in this low resource, field-based setting has never been done before. Many strengths were associated with this study including presenting field-based estimates for air exchange and PM exfiltration in village homes in rural Nepal, as well as assessing variability of exfiltration fraction across multiple fuel types and window/door status in a real-world setting.

Chapter 4 built upon research conducted in Chapter 3 by focusing on providing PM exfiltration estimates for alternative stoves. These stoves often employ a chimney to redirect pollutants to the exterior environment. This direct form of ventilation only accounts for some of the PM exiting the home. Additional PM still exfiltrates via indirect ventilation and both routes of exfiltration, direct and indirect, must be accounted for when assessing how much PM exfiltrates when using alternative stoves that utilize a chimney. Alternative stoves from this study are being used in the parent, cookstove trial in Nepal. They include the Envirofit Stove Original Model (G3300/G3355) with chimney, Manufacturer Altered Envirofit Stove with chimney, NNIPS Altered Envirofit Stove with chimney, and a locally constructed Improved Mud Brick Stove with chimney. The use of alternative stoves in a village-like home resulted in a higher overall average exfiltration percentage due to direct and indirect ventilation. Also, a large contrast in overall exfiltration percentage was found between the traditional stove and alternative stoves. This further underscores the need for a better understanding of what the climate benefits may be from implementing such options on a large scale. The primary strength of the work presented in this chapter was that field-based measurements assessing exfiltration across window/door status and fuel type were taken in a village-like home in rural Nepal.

Chapter 5 presented ongoing work separated into three main stages. Current work involves the creation of exposure maps that will characterize spatial distribution of $PM_{2.5}$ and BC over during cooking and background periods across the four cookstove VDC areas in the parent trial. Ambient $PM_{2.5}$ data has been collected across the VDCs with preliminary results showing minimal spatial dependence. However, further analysis is needed to assess spatial dependence between high-density housing areas and more rural areas within the VDC's. Future work involves the development of a spatial model that will allow for the assessment of indoor to outdoor cookstove emissions. Prediction of BC at unsampled locations across the four cookstove VDC's will also be integrated into this model development.

Limitations

The research presented in this dissertation had several limitations. The quality control adjustment equations presented in Chapter 2 are applicable for a very broad PM concentration range (~600 $\mu g/m^3$ to ~66,000 $\mu g/m^3$). However, further research is required to assess how the relationships for humidity and gravimetric adjustment may change at concentrations below 600 $\mu g/m^3$. Furthermore, we presented several approaches for combined quality control adjustment. Our choice for which specific equation to use was based on our data set. A limitation to this paper is that readers should assess their own data in order to choose the combined quality control method that works best for them utilizing the approach presented in the paper. Chapters 3 and 4 had several limitations with regards to the simulated cooking test protocol. Data such as burn rate, air-fuel ratio, flame turbulence, and combustion temperature were not measured. Changes that might be due to combustion efficiencies were not taken into account for the alternative stoves. Mixing factor analysis was limited by a small sample size and the assessment was conducted in a mock house at the field site and should be expanded to real homes along with an increased sample size. With regards to evaluation of indoor black carbon from integrated $PM_{2.5}$ measurements, oversaturation of a majority of filters occurred, thus highlighting a key limitation to the methodology used to measure black carbon. In addition, all data collected for black carbon analysis was conducted utilizing a simulated cooking event (water boil test) and further assessment is needed over the course of actual cooking events.

Environmental and Public Health Implications

Inhabitants of the Indo-Gangetic Plain region are reliant upon a stable hydrological cycle and annual glacier and snow pack melt as a source of fresh water. In addition to greenhouse gas emissions, black carbon is playing a dominant role in potentially destabilizing the climate in this region and threatening the livelihoods of nearly 1 billion people. However, large uncertainty in black carbon emission inventories within the Indo-Gangetic Plain region exists and further research is needed in order to decrease variability of existing climate change models reliant upon these inventories.

This dissertation provides a comprehensive assessment of the black carbon contribution generated by traditional, open-design cookstoves as well as alternative stoves at the household level in an area within the Indo-Gangetic Plain. Understanding the contribution that traditional and alternative cookstoves play in the production of black carbon is critical to developing a better understanding of how cookstove emissions contribute to regional ambient air quality and associated climate change impacts.

8 References

Chapter 1 References

1. Wallack JS, Ramanthan V. Other Climate Changers-Why Black Carbon and Ozone Also Matter, The. *Foreign Aff*. 2009;88:105.
2. *Integrated Assessment of Black Carbon and Tropospheric Ozone*. UNEP and WMO; 2011. Available at: http://www.unep.org/dewa/portals/67/pdf/BlackCarbon_report.pdf.
3. USAID/ECO-Asia CDCP. Black Carbon Emissions in Asia: Sources, Impacts, and Abatement Opportunities. 2010. Available at: http://www.cleanenergyasia.net/library/black-carbon-emissions-asia-sources-impacts-and-abatement-opportunities.
4. Rehman IH, Ahmed T, Praveen PS, Kar A, Ramanathan V. Black carbon emissions from biomass and fossil fuels in rural India. *Atmos Chem Phys Discuss*. 2011;11:10845–10874.
5. Ramanathan, V. *Climate Impacts of Black Carbon*. 2175 Rayburn House Office Building Washington D.C.; 2010.
6. Jacobson MZ. Short-term effects of controlling fossil-fuel soot, biofuel soot and gases, and methane on climate, Arctic ice, and air pollution health. *J Geophys Res*. 2010;115.
7. Schmidt CW. Black Carbon: The Dark Horse of Climate Change Drivers. *Environ Health Perspect*. 2011;119(4):A172.
8. Ramanathan V, et al. Atmospheric Brown Clouds Regional Assessment Report with Focus on Asia. 2008. Available at: http://tinyurl.com/68r7mpd.
9. Adler T. Better Burning, Better Breathing: Improving Health with Cleaner Cook Stoves. *Environ Health Perspect*. 2010;118(3):A124-A129.
10. Anenberg SC, Schwartz J, Shindell D, et al. Global Air Quality and Health Co-benefits of Mitigating Near-Term Climate Change through Methane and Black Carbon

Emission Controls. *Environ Health Perspect*. 2012;120(6):831-839. doi:10.1289/ehp.1104301.

11. WHO | Indoor air pollution and health. 2011. Available at: http://www.who.int/mediacentre/factsheets/fs292/en/. Accessed October 14, 2011.

12. Granderson J, Sandhu JS, Vasquez D, Ramirez E, Smith KR. Fuel use and design analysis of improved wood burning cookstoves in the Guatemalan Highlands. *Biomass Bioenergy*. 2009;33(2):306-315. doi:10.1016/j.biombioe.2008.06.003.

13. Bruce N, Perez-Padilla R, Albalak R. Indoor air pollution in developing countries: a major environmental and public health challenge. *Bull World Health Organ*. 2000;78(9):1078–1092.

14. Balakrishnan K, Sankar S, Parikh J, et al. Daily average exposures to respirable particulate matter from combustion of biomass fuels in rural households of southern India. *Environ Health Perspect*. 2002;110(11):1069.

15. Baumgartner J, Schauer JJ, Ezzati M, et al. Patterns and predictors of personal exposure to indoor air pollution from biomass combustion among women and children in rural China: Biomass smoke exposure in rural China. *Indoor Air*. 2011;21(6):479-488. doi:10.1111/j.1600-0668.2011.00730.x.

16. Bruce N, McCracken J, Albalak R, et al. Impact of improved stoves, house construction and child location on levels of indoor air pollution exposure in young Guatemalan children. *J Expo Anal Environ Epidemiol*. 2004;14:S26-S33. doi:10.1038/sj.jea.7500355.

17. Rehfuess E, Bruce N, Smith K. Solid Fuel Use: Health Effect. In: Nriagu JO (ed.) Encyclopedia of Environmental Health, v 5, pp. 150161 Burlington: Elsevier, 2011. *Environ Health*. 2011;5:150161.

18. Shrestha G, Traina SJ, Swanston CW. Black Carbon's Properties and Role in the Environment: A Comprehensive Review. *Sustainability*. 2010;2(1):294-320. doi:10.3390/su2010294.

19. Smith K, Samet J, Romieu I, Bruce N. Indoor air pollution in developing countries and acute lower respiratory infections in children. *Thorax*. 2000;55:518-532.

20. Martin II WJ, Glass RI, Araj H, et al. Household Air Pollution in Low-and Middle-Income Countries: Health Risks and Research Priorities. *PLoS Med*. 2013;10(6):e1001455.

21. WHO | Clean household energy can save people's lives. 2014. Available at: http://www.who.int/features/2014/clean-household-energy/en/. Accessed May 20, 2014.

22. WHO | 7 million premature deaths annually linked to air pollution. 2014. Available at: http://www.who.int/mediacentre/news/releases/2014/air-pollution/en/. Accessed May 24, 2014.

23. Global Alliance for Clean Cookstoves. 2012. Available at: http://www.cleancookstoves.org/the-alliance/. Accessed September 23, 2013.

24. Bond TC, Streets DG, Yarber KF, Nelson SM, Woo JH, Klimont Z. A technology-based global inventory of black and organic carbon emissions from combustion. *J Geophys Res*. 2004;109(D14):D14203.

25. Ramanathan V, Carmichael G. Global and regional climate changes due to black carbon. *Nat Geosci*. 2008;1(4):221–227.

26. Xu B, Cao J, Hansen J, et al. Black soot and the survival of Tibetan glaciers. *Proc Natl Acad Sci*. 2009;106(52):22114.

27. Ramanathan V. Aerosols, Climate, and the Hydrological Cycle. *Science*. 2001;294:2119-2124. doi:10.1126/science.1064034.

28. Carmichael GR, Adhikary B, Kulkarni S, et al. Asian Aerosols: Current and Year 2030 Distributions and Implications to Human Health and Regional Climate Change. *Environ Sci Technol*. 2009;43(15):5811-5817. doi:10.1021/es8036803.

29. Sasser E, et al. *US EPA Report to Congress on Black Carbon: Department of the Interior, Environment, and Related Agencies Appropriations Act, 2010*. US EPA; 2012. Available at: http://www.epa.gov/blackcarbon/2012report/fullreport.pdf.

Chapter 2 References

1. National Institute of Environmental Health Sciences. Cookstoves and Indoor Air: Global Environmental Health. Available at: http://www.niehs.nih.gov/research/programs/geh/cookstoves/. Accessed November 20, 2013.
2. Clark ML, Peel JL, Balakrishnan K, et al. Health and Household Air Pollution from Solid Fuel Use: The Need for Improved Exposure Assessment. *Environ Health Perspect*. 2013. doi:10.1289/ehp.1206429.
3. Martin II WJ, Glass RI, Araj H, et al. Household Air Pollution in Low-and Middle-Income Countries: Health Risks and Research Priorities. *PLoS Med*. 2013, 10, 10.1371/journal.pmed.1001455.
4. Thermo Electron Corporation. MODEL pDR-1000AN/1200 personal DataRAM Instruction Manual. 2003. Available at: http://www.envirosupply.net/manuals/ThermoElectron_PersonalDataRAM_pDR-1000AN-1200.pdf. Accessed July 20, 2013.
5. Wallace LA, Wheeler AJ, Kearney J, et al. Validation of continuous particle monitors for personal, indoor, and outdoor exposures. *J Expo Sci Environ Epidemiol*. 2010;21(1):49-64. doi:10.1038/jes.2010.15.
6. Richards L. Optical properties of the San Joaquin Valley aerosol collected during the 1995 integrated monitoring study. *Atmos Environ*. 1999;33(29):4787-4795. doi:10.1016/S1352-2310(99)00267-8.
7. Wu C-F, Delfino RJ, Floro JN, et al. Evaluation and quality control of personal nephelometers in indoor, outdoor and personal environments. *J Expo Anal Environ Epidemiol*. 2004;15(1):99-110. doi:10.1038/sj.jea.7500351.

8. McMurry PH, Zhang X, Lee C-T. Issues in aerosol measurement for optics assessments. *J Geophys Res*. 1996;101(D14):19189. doi:10.1029/95JD02342.

9. Lowenthal DH, Rogers CF, Saxena P, Watson JG, Chow JC. Sensitivity of estimated light extinction coefficients to model assumptions and measurement errors. *Atmos Environ*. 1995;29(7):751-766. doi:10.1016/1352-2310(94)00340-Q.

10. Sioutas C, Kim S, Chang M, Terrell LL, Gong H. Field evaluation of a modified DataRAM MIE scattering monitor for real-time PM2.5 mass concentration measurements. *Atmos Environ*. 2000;34(28):4829-4838. doi:10.1016/S1352-2310(00)00244-2.

11. Chakrabarti B, Fine PM, Delfino R, Sioutas C. Performance evaluation of the active-flow personal DataRAM PM2.5 mass monitor (Thermo Anderson pDR-1200) designed for continuous personal exposure measurements. *Atmos Environ*. 2004;38(20):3329-3340. doi:10.1016/j.atmosenv.2004.03.007.

12. Laulainen NS. *Summary of conclusions and recommendations from a visibility science workshop*; United States Department of Energy: Washington D.C., USA, 1993. Available at: http://www.osti.gov/servlets/purl/10149541-uEhPL2/. Accessed June 13, 2013.

13. Day DE, Malm WC. Aerosol light scattering measurements as a function of relative humidity: a comparison between measurements made at three different sites. *Atmos Environ*. 2001;35(30):5169-5176. doi:10.1016/S1352-2310(01)00320-X.

14. Wallace L, Williams R, Rea A, Croghan C. Continuous weeklong measurements of personal exposures and indoor concentrations of fine particles for 37 health-impaired North Carolina residents for up to four seasons. *Atmos Environ*. 2006;40(3):399-414. doi:10.1016/j.atmosenv.2005.08.042.

15. Both AF, Balakrishnan A, Joseph B, Marshall JD. Spatiotemporal Aspects of Real-Time PM $_{2.5}$: Low- and Middle-Income Neighborhoods in Bangalore, India. *Environ Sci Technol*. 2011;45(13):5629-5636. doi:10.1021/es104331w.

16. Fischer SL, Koshland CP. Field performance of a nephelometer in rural kitchens: effects of high humidity excursions and correlations to gravimetric analyses. *J Expo Sci Environ Epidemiol*. 2006;17(2):141–150.

17. Howard-Reed C, Rea AW, Zufall MJ, et al. Use of a continuous nephelometer to measure personal exposure to particles during the U.S. Environmental Protection Agency Baltimore and Fresno Panel studies. *J Air Waste Manag Assoc 1995*. 2000;50(7):1125-1132.

18. Liu LJS, Slaughter JC, Larson TV. Comparison of light scattering devices and impactors for particulate measurements in indoor, outdoor, and personal environments. *Environ Sci Technol*. 2002;36(13):2977-2986.

19. Wallace LA, Mitchell H, O'Connor GT, et al. Particle Concentrations in Inner-City Homes of Children with Asthma: The Effect of Smoking, Cooking, and Outdoor Pollution. *Environ Health Perspect*. 2003;111(9):1265-1272. doi:10.1289/ehp.6135.

20. Cookstove Replacement for Prevention of ALRI and Low Birthweight in Nepal - Full Text View - ClinicalTrials.gov. Available at: http://www.clinicaltrials.gov/ct2/show/NCT00786877?term=nepal+cookstove&rank=1. Accessed March 27, 2014.

21. LeClerq S. Personal communication: Cookstove construction description. March 11th 2010.

22. Bailis R, Ogle D, MacCarty N, Still D. The Partnership for Clean Indoor Air. The Water Boiling Test (WBT), Version 3.0. Availiable online: http://www.pciaonline.org/files/WBT_Version_3.0_0.pdf (accessed on 11/27/2013).
23. Rosner B. *Fundamentals of biostatistics*. 7th ed; Brooks/Cole Cengage Learning: Boston, MA, USA, 2011.
24. David James and Kurt Hornik (2012). *chron: Chronological Objects which Can Handle Dates and Times*; http://CRAN.R-project.org/package=chron, R package version 2.3-43.
25. Wickham, H. *gplot2: Elegant graphics for data analysis*. Springer: New York, USA, 2009.

Chapter 3 References

1. Xu B, Cao J, Hansen J, et al. Black soot and the survival of Tibetan glaciers. Proc Natl Acad Sci. 2009;106(52):22114.
2. Ramanathan V. Aerosols, Climate, and the Hydrological Cycle. Science. 2001;294:2119-2124. doi:10.1126/science.1064034.
3. Ramanathan V, et al. Atmospheric Brown Clouds Regional Assessment Report with Focus on Asia. 2008. Available at: http://tinyurl.com/68r7mpd.
4. Schmidt CW. Black Carbon: The Dark Horse of Climate Change Drivers. Environ Health Perspect. 2011;119(4):A172.
5. Ramanathan V, Carmichael G. Global and regional climate changes due to black carbon. Nat Geosci. 2008;1(4):221–227.
6. Wallack JS, Ramanthan V. Other Climate Changers-Why Black Carbon and Ozone Also Matter, The. Foreign Aff. 2009;88:105.
7. WHO | Indoor air pollution and health. Available at: http://www.who.int/mediacentre/factsheets/fs292/en/. Accessed October 14, 2011.
8. Bond TC, Streets DG, Yarber KF, Nelson SM, Woo JH, Klimont Z. A technology-based global inventory of black and organic carbon emissions from combustion. J Geophys Res. 2004;109(D14):D14203.
9. Adler T. Better Burning, Better Breathing: Improving Health with Cleaner Cook Stoves. Environ Health Perspect. 2010;118(3):A124-A129.
10. USAID/ECO-Asia CDCP. Black Carbon Emissions in Asia: Sources, Impacts, and Abatement Opportunities. 2010. Available at: http://www.cleanenergyasia.net/library/black-carbon-emissions-asia-sources-impacts-and-abatement-opportunities.

11. Anenberg SC, Schwartz J, Shindell D, et al. Global Air Quality and Health Co-benefits of Mitigating Near-Term Climate Change through Methane and Black Carbon Emission Controls. Environ Health Perspect. 2012;120(6):831-839. doi:10.1289/ehp.1104301.

12. Sasser E, et al. US EPA Report to Congress on Black Carbon: Department of the Interior, Environment, and Related Agencies Appropriations Act, 2010. US EPA; 2012. Available at: http://www.epa.gov/blackcarbon/2012report/fullreport.pdf.

13. Rehman IH, Ahmed T, Praveen PS, Kar A, Ramanathan V. Black carbon emissions from biomass and fossil fuels in rural India. Atmos Chem Phys Discuss. 2011;11:10845–10874.

14. Salje H, Gurley ES, Homaira N, et al. Impact of neighborhood biomass cooking patterns on episodic high indoor particulate matter concentrations in clean fuel homes in Dhaka, Bangladesh. Indoor Air. 2014;24(2):213-220. doi:10.1111/ina.12065.

15. Balakrishnan K, Sankar S, Parikh J, et al. Daily average exposures to respirable particulate matter from combustion of biomass fuels in rural households of southern India. Environ Health Perspect. 2002;110(11):1069.

16. Bruce N, Perez-Padilla R, Albalak R. Indoor air pollution in developing countries: a major environmental and public health challenge. Bull World Health Organ. 2000;78(9):1078–1092.

17. Reid H, Smith K. Indoor Smoke Exposures from Traditional and Improved Cookstoves: Comparisons among Rural Nepali Women. Mt Res Dev. 1986:293-303.

18. Begum BA, Paul SK, Dildar Hossain M, Biswas SK, Hopke PK. Indoor air pollution from particulate matter emissions in different households in rural areas of Bangladesh. Build Environ. 2009;44(5):898-903. doi:10.1016/j.buildenv.2008.06.005.

19. Smith KR. Air Pollution and Rural Biomass Fuels in Developing Countries: a Pilot Village Study in India and Implications for Research and Policy.

20. Venkataraman C. Residential Biofuels in South Asia: Carbonaceous Aerosol Emissions and Climate Impacts. Science. 2005;307(5714):1454-1456. doi:10.1126/science.1104359.

21. National Risk Management Research Laboratory RTP, NC. Greenhouse Gases From Small-Scale Combustion Devices In Developing Countries: Phase IIA Household Stoves in India. 2000.

22. MacCarty N, Ogle D, Still D, Bond T, Roden C. A laboratory comparison of the global warming impact of five major types of biomass cooking stoves. Energy Sustain Dev. 2008;12(2):56–65.

23. Smith KR. Biofuels, Air pollution, and Health: A Global Review. New York: Plenum Press; 1987.

24. Williams PRD, Unice K. Field Study of Air Exchange Rates in Northern Highlands of Peru. Environ Forensics. 2013;14(3):215-229. doi:10.1080/15275922.2013.814182.

25. McCracken JP, Smith KR. Emissions and efficiency of improved wood burning cookstoves in Highland Guatemala. Environ Int. 1998;24(7):739–747.

26. Cookstove Replacement for Prevention of ALRI and Low Birthweight in Nepal - Full Text View - ClinicalTrials.gov. Available at: http://www.clinicaltrials.gov/ct2/show/NCT00786877?term=nepal+cookstove&rank=1%20(accessed%20Mar%2027,%202014. Accessed April 3, 2014.

27. LeClerq S. Personal Communication: Cookstove construction description. 2010.

28. Soneja S. Preliminary Data Analysis on Housing and Fuel Characteristics for Sarlahi District, Nepal. 2011.

29. Sherman MH. Tracer-gas techniques for measuring ventilation in a single zone. Build Environ. 1990;25(4):365–374.

30. ACGIH. Industrial Ventilation: A manual of Recommended Practice. 2010th ed. Cincinnati, OH: ACGIH; 2010.

31. Moore R. Tracer Gas Testing Applications for Industrial Hygiene Evaluations. EHS Today. 2004. Available at: http://ehstoday.com/industrial_hygiene/instrumentation/ehs_imp_36992/. Accessed October 27, 2011.

32. Samfield M. Project Summary: Air Infiltration Measurements Using Tracer Gases: A Literature Review. Research Triangle Park, NC: United States Environmental Protection Agency; 1995. Available at: http://nepis.epa.gov/Exe/ZyPDF.cgi/30003X2I.PDF?Dockey=30003X2I.PDF. Accessed April 3, 2014.

33. Bailis R, D. Ogle, MacCarty N, et al. The Partnership for Clean Indoor Air. The Water Boiling Test (WBT), Version 3.0. 2007:http://www.pciaonline.org/files/WBT_Version_3.0_0.pdf.

34. Yan B, Kennedy D, Miller RL, et al. Validating a nondestructive optical method for apportioning colored particulate matter into black carbon and additional components. Atmos Environ. 2011;45(39):7478-7486. doi:10.1016/j.atmosenv.2011.01.044.

35. Shrestha G, Traina SJ, Swanston CW. Black Carbon's Properties and Role in the Environment: A Comprehensive Review. Sustainability. 2010;2(1):294-320. doi:10.3390/su2010294.

36. Feigley CE, Bennett JS, Lee E, Khan J. Improving the Use of Mixing Factors for Dilution Ventilation Design. Appl Occup Environ Hyg. 2002;17(5):333-343. doi:10.1080/10473220252864932.

37. Drivas PJ, Simmonds PG, Shair FH. Experimental characterization of ventilation systems in buildings. Environ Sci Technol. 1972;6(7):609–614.

38. Maroni M, Seifert B, Lindvall T. Indoor Air Quality: A Comprehensive Reference Book. Elsevier; 1995.

39. DiNardi S. The Occupational Environment: Its Evaluation, Control, and Management, Second Edition. 2nd edition. Fairfax, Va: Aiha; 2003.

40. David James and Kurt Hornik (2012). chron: Chronological Objects which Can Handle Dates and Times. R package version 2.3-43.

41. John Fox and Sanford Weisberg (2011). An {R} Companion to Applied Regression, Second Edition. Thousand Oaks CA: Sage. URL: http://socserv.socsci.mcmaster.ca/jfox/Books/Companion.

42. Felipe de Mendiburu (2013). agricolae: Statistical Procedures for Agricultural Research. R package version 1.1-4. http://CRAN.R-project.org/package=agricolae.

43. Sarkar, Deepayan (2008) Lattice: Multivariate Data Visualization with R. Springer, New York. ISBN 978-0-387-75968-5.

44. Hadley Wickham (2011). The Split-Apply-Combine Strategy for Data Analysis. Journal of Statistical Software, 40(1), 1-29. URL http://www.jstatsoft.org/v40/i01/.

45. H. Wickham. ggplot2: elegant graphics for data analysis. Springer New York, 2009.

46. Gemechis Dilba Djira, Mario Hasler, Daniel Gerhard and Frank Schaarschmidt (2012). mratios: Inferences for ratios of coefficients in the general linear model. R package Version 1.3.17. http://CRAN.R-project.org/package=mratios.

47. Douglas Bates, Martin Maechler and Ben Bolker (2013). lme4: Linear mixed-effects models using S4 classes. R package version 0.999999-2. http://CRAN.R-project.org/package=lme4.

48. Wilson R, Spengler JD. Particles in our air: concentrations and health effects. [Cambridge, Mass.]: Harvard School of Public Health ; distributed by Harvard University Press; 1996.

49. Venkataraman C, Rao GUM. Emission Factors of Carbon Monoxide and Size-Resolved Aerosols from Biofuel Combustion. Environ Sci Technol. 2001;35(10):2100-2107. doi:10.1021/es001603d.

50. Rau JA. Composition and Size Distribution of Residential Wood Smoke Particles. Aerosol Sci Technol. 1989;10(1):181-192. doi:10.1080/02786828908959233.

51. Yan B. Personal Communication: Validity of Optical Method. 2014.

52. Just B, Rogak S, Kandlikar M. Characterization of Ultrafine Particulate Matter from Traditional and Improved Biomass Cookstoves. Environ Sci Technol. 2013:130319140434009. doi:10.1021/es304351p.

53. Van Vliet EDS, Asante K, Jack DW, et al. Personal exposures to fine particulate matter and black carbon in households cooking with biomass fuels in rural Ghana. Environ Res. 2013;127:40-48. doi:10.1016/j.envres.2013.08.009.

Chapter 4 References

1. Goldemberg J, Johansson TB, Anderson, et al. *World energy assessment: overview : 2004 update*. New York, NY: United Nations Development Programme, Bureau for Development Policy; 2004.
2. Granderson J, Sandhu JS, Vasquez D, Ramirez E, Smith KR. Fuel use and design analysis of improved wood burning cookstoves in the Guatemalan Highlands. *Biomass Bioenergy*. 2009;33(2):306-315. doi:10.1016/j.biombioe.2008.06.003.
3. Bruce N, Perez-Padilla R, Albalak R. Indoor air pollution in developing countries: a major environmental and public health challenge. *Bull World Health Organ*. 2000;78(9):1078–1092.
4. Balakrishnan K, Sankar S, Parikh J, et al. Daily average exposures to respirable particulate matter from combustion of biomass fuels in rural households of southern India. *Environ Health Perspect*. 2002;110(11):1069.
5. Baumgartner J, Schauer JJ, Ezzati M, et al. Patterns and predictors of personal exposure to indoor air pollution from biomass combustion among women and children in rural China: Biomass smoke exposure in rural China. *Indoor Air*. 2011;21(6):479-488. doi:10.1111/j.1600-0668.2011.00730.x.
6. Bruce N, McCracken J, Albalak R, et al. Impact of improved stoves, house construction and child location on levels of indoor air pollution exposure in young Guatemalan children. *J Expo Anal Environ Epidemiol*. 2004;14:S26-S33. doi:10.1038/sj.jea.7500355.
7. Smith K, Samet J, Romieu I, Bruce N. Indoor air pollution in developing countries and acute lower respiratory infections in children. *Thorax*. 2000;55:518-532.

8. Cookstove Replacement for Prevention of ALRI and Low Birthweight in Nepal - Full Text View - ClinicalTrials.gov. Available at: http://www.clinicaltrials.gov/ct2/show/NCT00786877?term=nepal+cookstove&rank=1%20(accessed%20Mar%2027,%202014. Accessed April 3, 2014.

9. Rehfuess E, Bruce N, Smith K. Solid Fuel Use: Health Effect. In: Nriagu JO (ed.) Encyclopedia of Environmental Health, v 5, pp. 150161 Burlington: Elsevier, 2011. *Environ Health*. 2011;5:150161.

10. Grieshop AP, Marshall JD, Kandlikar M. Health and climate benefits of cookstove replacement options. *Energy Policy*. 2011;39(12):7530-7542. doi:10.1016/j.enpol.2011.03.024.

11. Brauer M, Bartlett K, Regalado-Pineda J, Perez-Padilla R. Assessment of particulate concentrations from domestic biomass combustion in rural Mexico. *Environ Sci Technol*. 1995;30(1):104–109.

12. Martin II WJ, Glass RI, Araj H, et al. Household Air Pollution in Low-and Middle-Income Countries: Health Risks and Research Priorities. *PLoS Med*. 2013;10(6):e1001455.

13. WHO | 7 million premature deaths annually linked to air pollution. 2014. Available at: http://www.who.int/mediacentre/news/releases/2014/air-pollution/en/. Accessed May 24, 2014.

14. WHO | Indoor air pollution and health. 2011. Available at: http://www.who.int/mediacentre/factsheets/fs292/en/. Accessed October 14, 2011.

15. Global Alliance for Clean Cookstoves. 2012. Available at: http://www.cleancookstoves.org/the-alliance/. Accessed September 23, 2013.

16. Clark ML, Peel JL, Balakrishnan K, et al. Health and Household Air Pollution from Solid Fuel Use: The Need for Improved Exposure Assessment. *Environ Health Perspect*. 2013. doi:10.1289/ehp.1206429.

17. Wallack JS, Ramanthan V. Other Climate Changers-Why Black Carbon and Ozone Also Matter, The. *Foreign Aff*. 2009;88:105.

18. Rehman IH, Ahmed T, Praveen PS, Kar A, Ramanathan V. Black carbon emissions from biomass and fossil fuels in rural India. *Atmos Chem Phys Discuss*. 2011;11:10845–10874.

19. USAID/ECO-Asia CDCP. Black Carbon Emissions in Asia: Sources, Impacts, and Abatement Opportunities. 2010. Available at: http://www.cleanenergyasia.net/library/black-carbon-emissions-asia-sources-impacts-and-abatement-opportunities.

20. Bond TC, Sun H. Can Reducing Black Carbon Emissions Counteract Global Warming? *Environ Sci Technol*. 2005;39(16):5921-5926. doi:10.1021/es0480421.

21. Carmichael GR, Adhikary B, Kulkarni S, et al. Asian Aerosols: Current and Year 2030 Distributions and Implications to Human Health and Regional Climate Change. *Environ Sci Technol*. 2009;43(15):5811-5817. doi:10.1021/es8036803.

22. Shindell D, Lamarque J-F, Unger N, et al. Climate forcing and air quality change due to regional emissions reductions by economic sector. *Atmospheric Chem Phys*. 2008;8(23):7101–7113.

23. Jacobson MZ. Short-term effects of controlling fossil-fuel soot, biofuel soot and gases, and methane on climate, Arctic ice, and air pollution health. *J Geophys Res*. 2010;115.

24. Bond TC, Doherty SJ, Fahey DW, et al. Bounding the role of black carbon in the climate system: A scientific assessment: BLACK CARBON IN THE CLIMATE SYSTEM. *J Geophys Res Atmospheres*. 2013;118(11):5380-5552. doi:10.1002/jgrd.50171.

25. Ramanathan V, Carmichael G. Global and regional climate changes due to black carbon. *Nat Geosci*. 2008;1(4):221–227.

26. Venkataraman C. Residential Biofuels in South Asia: Carbonaceous Aerosol Emissions and Climate Impacts. *Science*. 2005;307(5714):1454-1456. doi:10.1126/science.1104359.

27. National Risk Management Research Laboratory RTP, NC. Greenhouse Gases From Small-Scale Combustion Devices In Developing Countries: Phase IIA Household Stoves in India. 2000.

28. MacCarty N, Ogle D, Still D, Bond T, Roden C. A laboratory comparison of the global warming impact of five major types of biomass cooking stoves. *Energy Sustain Dev*. 2008;12(2):56–65.

29. Roden CA, Bond TC, Conway S, Osorto Pinel AB, MacCarty N, Still D. Laboratory and field investigations of particulate and carbon monoxide emissions from traditional and improved cookstoves. *Atmos Environ*. 2009;43(6):1170-1181. doi:10.1016/j.atmosenv.2008.05.041.

30. Boy E, Bruce N, Smith KR, Hernandez R. Fuel efficiency of an improved wood-burning stove in rural Guatemala: implications for health, environment and development. *Energy Sustain Dev*. 2000;4(2):23–31.

31. Soneja S. Determination of Exfiltration Estimates for PM and BC in Traditional stoves in rural Nepal. To Be Submitted.

32. LeClerq S. Personal Communication: Cookstove construction description. 2010.

33. Adkins E, Tyler E, Wang J, Siriri D, Modi V. Field testing and survey evaluation of household biomass cookstoves in rural sub-Saharan Africa. *Energy Sustain Dev.* 2010;14(3):172-185. doi:10.1016/j.esd.2010.07.003.

34. Ryden N. Personal Communication: Regarding Envirofit G3300 Design Change. 2014.

35. Bailis R, D. Ogle, MacCarty N, et al. The Partnership for Clean Indoor Air. The Water Boiling Test (WBT), Version 3.0. 2007:http://www.pciaonline.org/files/WBT_Version_3.0_0.pdf.

36. David James and Kurt Hornik (2012). *chron: Chronological Objects which Can Handle Dates and Times.* R package version 2.3-43.

37. John Fox and Sanford Weisberg (2011). *An* {R} *Companion to Applied Regression, Second Edition.* Thousand Oaks CA: Sage. URL: http://socserv.socsci.mcmaster.ca/jfox/Books/Companion.

38. Felipe de Mendiburu (2013). *agricolae: Statistical Procedures for Agricultural Research.* R package version 1.1-4. http://CRAN.R-project.org/package=agricolae.

39. Sarkar, Deepayan (2008) *Lattice: Multivariate Data Visualization with R.* Springer, New York. ISBN 978-0-387-75968-5.

40. Hadley Wickham (2011). *The Split-Apply-Combine Strategy for Data Analysis.* Journal of Statistical Software, 40(1), 1-29. URL http://www.jstatsoft.org/v40/i01/.

41. Koziński JA, Saade R. Effect of biomass burning on the formation of soot particles and heavy hydrocarbons. An experimental study. *Fuel.* 1998;77(4):225-237. doi:10.1016/S0016-2361(97)00201-9.

42. Hinds WC. *Aerosol Technology: Properties, Behavior, and Measurement of Airborne Particles*. 2 edition. New York: Wiley-Interscience; 1999.

43. Wilson R, Spengler JD. *Particles in our air: concentrations and health effects*. [Cambridge, Mass.]: Harvard School of Public Health ; distributed by Harvard University Press; 1996.

44. Kar A, Rehman IH, Burney J, et al. Real-Time Assessment of Black Carbon Pollution in Indian Households Due to Traditional and Improved Biomass Cookstoves. *Environ Sci Technol*. 2012:120227093219008. doi:10.1021/es203388g.

45. Salje H, Gurley ES, Homaira N, et al. Impact of neighborhood biomass cooking patterns on episodic high indoor particulate matter concentrations in clean fuel homes in Dhaka, Bangladesh. *Indoor Air*. 2014;24(2):213-220. doi:10.1111/ina.12065.

Chapter 5: References

1. Rehman IH, Ahmed T, Praveen PS, Kar A, Ramanathan V. Black carbon emissions from biomass and fossil fuels in rural India. *Atmos Chem Phys Discuss*. 2011;11:10845–10874.
2. Venkataraman C. Residential Biofuels in South Asia: Carbonaceous Aerosol Emissions and Climate Impacts. *Science*. 2005;307(5714):1454-1456. doi:10.1126/science.1104359.
3. Bond TC, Doherty SJ, Fahey DW, et al. Bounding the role of black carbon in the climate system: A scientific assessment: BLACK CARBON IN THE CLIMATE SYSTEM. *J Geophys Res Atmospheres*. 2013;118(11):5380-5552. doi:10.1002/jgrd.50171.
4. Xu B, Cao J, Hansen J, et al. Black soot and the survival of Tibetan glaciers. *Proc Natl Acad Sci*. 2009;106(52):22114.
5. Cookstove Replacement for Prevention of ALRI and Low Birthweight in Nepal - Full Text View - ClinicalTrials.gov. Available at: http://www.clinicaltrials.gov/ct2/show/NCT00786877?term=nepal+cookstove&rank=1%20(accessed%20Mar%2027,%202014. Accessed April 3, 2014.
6. Yan B, Kennedy D, Miller RL, et al. Validating a nondestructive optical method for apportioning colored particulate matter into black carbon and additional components. *Atmos Environ*. 2011;45(39):7478-7486. doi:10.1016/j.atmosenv.2011.01.044.
7. Cressie NAC. *Statistics for spatial data*. J. Wiley; 1993.
8. Diggle P, Ribeiro Jr. P. *Model-based Geostatistics*. 1st ed. Springer; 2007.
9. Waller LA, Gotway CA. *Applied spatial statistics for public health data*. Wiley-IEEE; 2004.
10. Schabenberger O, Gotway CA. *Statistical methods for spatial data analysis*. CRC Press; 2005.
11. Curriero F. Lecture Notes: Spatial Analysis and GIS II 140.663. 2010.

12. Christensen OF, Diggle PJ, Jr PJR. Analyzing Positive-Valued Spatial Data: the Transformed Gaussian Model. In: Monestiez P, Allard D, Froidevaux R, eds. *geoENV III — Geostatistics for Environmental Applications*. Quantitative Geology and Geostatistics. Springer Netherlands; 2001:287-298. Available at: http://link.springer.com/chapter/10.1007/978-94-010-0810-5_25. Accessed May 10, 2014.

Chapter 6: References

1. Lee H, Liu Y. A novel calibration approach of MODIS AOD data to predict PM2.5 concentrations. *Atmospheric Chem Phys*. 2011:7991-8002.
2. Hu Z, Rao KR. Particulate air pollution and chronic ischemic heart disease in the eastern United States: a county level ecological study using satellite aerosol data. *Environ Health*. 2009;8(1):26.
3. Outdoor Air Pollution and Health – A Review of the Contributions of Geotechnologies to Exposure Assessment - Springer. Available at: http://link.springer.com/chapter/10.1007%2F978-94-007-0329-2_3#page-1. Accessed November 26, 2013.
4. NSIDC: MODIS Data - Frequently Asked Questions. *Natl Snow Ice Data Cent*. 2009. Available at: http://nsidc.org/data/modis/faq.html#11. Accessed December 3, 2011.
5. NASA Goddard Space Flight Center: MCST Website - Home page. *NASA Goddard Space Flight Cent*. 2011. Available at: http://mcst.gsfc.nasa.gov/. Accessed January 7, 2012.
6. NASA Goddard Space Flight Center: MODAPS Services - FAQ. 2007. Available at: http://modaps.nascom.nasa.gov/services/faq/. Accessed January 7, 2012.
7. Ichoku C, Kaufman Y, Remer L, Levy R. Global aerosol remote sensing from MODIS. *Adv Space Res*. 2004;34(4):820–827.
8. Volland A. NASA - World's Largest Aerosol Sensing Network Has Leafy Origins. 2009. Available at: http://www.nasa.gov/topics/earth/features/aeronet.html. Accessed January 25, 2012.
9. Waller LA, Gotway CA. *Applied spatial statistics for public health data*. Wiley-IEEE; 2004.
10. Schabenberger O, Gotway CA. *Statistical methods for spatial data analysis*. CRC Press; 2005.

11. Yan B, Kennedy D, Miller RL, et al. Validating a nondestructive optical method for apportioning colored particulate matter into black carbon and additional components. *Atmos Environ*. 2011;45(39):7478-7486. doi:10.1016/j.atmosenv.2011.01.044.

12. Cookstove Replacement for Prevention of ALRI and Low Birthweight in Nepal - Full Text View - ClinicalTrials.gov. Available at: http://www.clinicaltrials.gov/ct2/show/NCT00786877?term=nepal+cookstove&rank=1%20(accessed%20Mar%2027,%202014. Accessed April 3, 2014.

13. Integrated Modeling of Aerosol, Cloud, Precipitation and Land Processes at Satellite-Resolved Scales. *NASA Model Guru Community NU-WRF*. 2012. Available at: https://modelingguru.nasa.gov/community/atmospheric/nuwrf. Accessed June 14, 2012.

14. Skamarock, W. C., and J. B. Klemp (2008), A time-split nonhydrostatic atmospheric model for weather research and forecasting applications, Journal of Computational Physics, 227(7), 3465-3485.

15. Chin, M., P. Ginoux, S. Kinne, O. Torres, B. N. Holben, B. N. Duncan, R. V. Martin, J. A. Logan, A. Higurashi, and T. Nakajima (2002), Tropospheric Aerosol Optical Thickness from the GOCART Model and Comparisons with Satellite and Sun Photometer Measurements, Journal of the Atmospheric Sciences, 59(3), 461-483.

16. Kumar, S. V., et al. (2006), Land information system: An interoperable framework for high resolution land surface modeling, Environmental Modeling & Software, 21(10), 1402-1415.

17. Matsui, T., X. Zeng, W.-K. Tao, H. Masunaga, W. S. Olson, and S. Lang (2009), Evaluation of Long-Term Cloud-Resolving Model Simulations Using Satellite Radiance

Observations and Multifrequency Satellite Simulators, Journal of Atmospheric and Oceanic Technology, 26(7), 1261-1274.

18. Tao, Z., J. Santanello, S. Zhou, Q. Tan, E. Kemp, M. Chin, and C. D. Peters-Lidard (2012), Effect of Land Cover on Atmospheric Processes and Air Quality, (manuscript in preparation).

19. Zaitchik, B. F., J. Santanello, S. V. Kumar, and C. D. Peters-Lidard (2012), Representation of soil moisture feedbacks during drought in NASA Unified WRF (NU-WRF), Journal of Hydrometeorology, In Review.

20. Rienecker, M.M., M.J. Suarez, R. Gelaro, R. Todling, J. Bacmeister, E. Liu, M.G. Bosilovich, S.D. Schubert, L. Takacs, G.-K. Kim, S. Bloom, J. Chen, D. Collins, A. Conaty, A. da Silva, et al., 2011. MERRA - NASA's Modern-Era Retrospective Analysis for Research and Applications. J. Climate, 24, 3624-3648, doi: 10.1175/JCLI-D-11-00015.1.

21. Hong, S.-Y., Y. Noh, and J. Dudhia (2006), A new vertical diffusion package with an explicit treatment of entrainment processes, Monthly Weather Review, 134(9), 2318-2341.

22. Chu, D. A., Y. J. Kaufman, C. Ichoku, L. A. Remer, D. Tanré, and B. N. Holben (2002), Validation of MODIS aerosol optical depth retrieval over land, Geophys. Res. Lett., 29(12), 8007.

23. Perez M. CloudSat Mission Overview | NASA. *NASA CloudSat*. 2013. Available at: http://www.nasa.gov/mission_pages/cloudsat/mission/index.html#.UpO5WI2E4f8. Accessed November 25, 2013.

24. Trepte C. CALIPSO - Cloud-Aerosol Lidar and Infrared Pathfinder Satellite Observations. *NASA CALIPSO*. 2013. Available at: http://www-calipso.larc.nasa.gov/. Accessed November 25, 2013.

25. Kopacz, M., D. L. Mauzerall, J. Wang, E. M. Leibensperger, D. K. Henze, and K. Singh (2011), Origin and radiative forcing of black carbon transported to the Himalayas and Tibetan Plateau, Atmos. Chem. Phys., 11(6), 2837-2852.

26. Menon, S., D. Koch, G. Beig, S. Sahu, J. Fasullo, and D. Orlikowski (2009), Black carbon aerosols and the third polar ice cap, Atmos. Chem. Phys. Discuss., 9(6), 26593-26625.

27. Ramanathan V, Carmichael G. Global and regional climate changes due to black carbon. *Nat Geosci*. 2008;1(4):221–227.

28. Ming, J., H. Cachier, C. Xiao, D. Qin, S. Kang, S. Hou, and J. Xu (2008), Black carbon record based on a shallow Himalayan ice core and its climatic implications, Atmos. Chem. Phys., 8(5), 1343-1352.

29. Anenberg SC, Schwartz J, Shindell D, et al. Global Air Quality and Health Co-benefits of Mitigating Near-Term Climate Change through Methane and Black Carbon Emission Controls. *Environ Health Perspect*. 2012;120(6):831-839. doi:10.1289/ehp.1104301.

30. Immerzeel WW, van Beek LPH, Bierkens MFP. Climate Change Will Affect the Asian Water Towers. *Science*. 2010;328(5984):1382-1385. doi:10.1126/science.1183188.

31. Sorg A, Bolch T, Stoffel M, Solomina O, Beniston M. Climate change impacts on glaciers and runoff in Tien Shan (Central Asia). *Nat Clim Change*. 2012;2(10):725-731. doi:10.1038/nclimate1592.

32. BenMAP | US EPA. *EPA U S Environ Prot Agency*. 2013. Available at: http://www.epa.gov/air/benmap/. Accessed November 23, 2013.

33. Risley D. BenMAP: Environmental Benefits Mapping and Analysis Program.

34. Tanrikulu S, Tran C, Beaver S. *Health Impact analysis of Fine Particulate Matter in the San Francisco Bay Area*. San Francisco, CA: Bay Area Air Quality Management District; 2011.

35. Davidson K, Hallberg A, McCubbin D, Hubbell B. Analysis of PM2. 5 Using the Environmental Benefits Mapping and Analysis Program (BenMAP). *J Toxicol Environ Health A*. 2007;70(3-4):332–346.

36. Grieshop AP, Marshall JD, Kandlikar M. Health and climate benefits of cookstove replacement options. *Energy Policy*. 2011;39(12):7530-7542. doi:10.1016/j.enpol.2011.03.024.

37. Berman JD, Fann N, Hollingsworth JW, et al. Health Benefits from Large-Scale Ozone Reduction in the United States. *Environ Health Perspect*. 2012;120(10):1404-1410. doi:10.1289/ehp.1104851.

9 Appendix

Appendix A

The following abstract represents work that I contributed towards outside of my immediate research during the course of pursuing my doctorate.

Title: Performance of Alternative Cookstoves in a Home-Like Setting in Rural Nepal. (In preparation)

Authors: Ojo, Kristen, Scrafford, Carolyn, **Sutyajeet I. Soneja**, Khatry, Subarna K., LeClerq, Steven C., Checkley, William, Katz, Joanne, Tielsch, James M.

Abstract

Alternative cookstoves are designed to improve efficiency of burning biomass fuels. The Nepal Cookstove Trial (NCT) studies the effect of alternative cookstoves on family health. Our study measured indoor particulate matter (PM) concentration, boiling time, and fuel use of cookstoves during a water boil test in a house-like setting in rural Nepal. Study I was designed to select a stove for NCT; Study II evaluated stoves being used in NCT. In Study I, mean PM using wood fuel was 7033 $\mu g/m^3$, 2630 $\mu g/m^3$, and 4144 $\mu g/m^3$ for the traditional, alternative mud brick stove (AMBS) and Envirofit G-Series, respectively. Alternative stoves reduced PM concentration but increased boiling time compared to the traditional stove (p-values<0.001). Unlike AMBS, Envirofit G-series did not significantly increase fuel consumption. In Phase II, the manufacturer altered Envirofit stove (MAES) and the NNIPS altered Envirofit stove (NAES), produced lower mean PM, 1778 $\mu g/m^3$ and 1405 $\mu g/m^3$, respectively, relative to AMBS 3466 $\mu g/m^3$ for wood tests with open door/window. The liquid propane gas stove (open door/window) gave mean PM of 318 $\mu g/m^3$. AMBS did not

require more fuel than the Envirofit stoves. Results from Study I and II showed a significant reduction in PM for all alternative stoves in a controlled setting. Boiling times for most stoves differed significantly from their comparison stove, but the difference in fuel use was not significant for most stoves for Studies I and II.

10 Curriculum Vitae

Sutyajeet I. Soneja

615 North Wolfe Street, Room E6630 (919) 749-4505
Baltimore, MD 21205 sisoneja@gmail.com

Born April 17th, 1982
Mayo Clinic
Rochester, Minnesota

Education and Certifications

Johns Hopkins University Bloomberg School of Public Health in Baltimore, MD
Ph.D. Candidate, Environmental Health Sciences, July 2014
Dissertation title: "Assessing Particulate Matter and Black Carbon Emissions from Homes Using Traditional and Alternative Cookstoves in Rural Nepal"
Conducting field-based research in rural Nepal, this study is developing a new approach to quantifying the amount of black carbon emissions emitted at the household level from the use of traditional and alternative cookstoves. Furthermore, this research will assess the association between indoor and outdoor black carbon concentration related to cookstove emissions, ultimately forming the basis for the development of an emission profile for black carbon across the Indo-Gangetic Plain.

Johns Hopkins University Bloomberg School of Public Health in Baltimore, MD
Certificate in Risk Sciences and Public Policy, May 2010

North Carolina Board of Registration for Engineers and Surveyors
Certified Engineering Intern, April 2004

North Carolina State University in Raleigh, NC
B.S. Biological Engineering, May 2004
B.S. Biomedical Engineering, May 2004
Cum Laude Graduate

Research and Professional Experience

Johns Hopkins University Bloomberg School of Public Health in Baltimore, MD
Teaching Assistant, Introduction to Environmental and Occupational Health Law Course, Spring 2011

Hill's Pet Nutrition in Topeka, KS (a subsidiary of Colgate - Palmolive, Inc.)
Associate Scientist, Bioengineer (March 2005 to May 2009)
Provided professional expertise and leadership in development and implementation of novel, non-invasive methods/devices to improve animal research/testing, welfare, and overall data quality

- Project Leader for implementation of automated feed station technology used in 80% of new feline facility
  - Performed extensive statistical analysis using Excel to validate data accuracy of new feeding system
  - Developed audit procedure to ensure ongoing data integrity

    - Created SOP's, flow charts (using Visio), and diagrams for use and long term maintenance of feeding system
    - Presented to top executives (e.g., CEO of Colgate –Palmolive, Inc.) on how new feeding system operated, impacted overall business, and how it set the stage for similar development in canine research
- Supported architects, electrical contractors, and construction personnel in design of new feline research facility

Chairman of Employee Focus Subcommittee on Hill's Diversity Council (February 2007 to May 2009)

- Supervised creation of monthly events celebrating different cultures and functional areas within Hill's
- Assisted with development of new employee mentorship program
- Presented quarterly updates on progress to Senior Executive sponsors

Quintiles Transnational, Inc. in Hawthorne, NY

Editorial/Research Internship **(***May 2003 to August 2003)*

- Conducted in-depth market research on pioneering products and pharmaceutical drugs
- Assisted in the formation of Continuing Medical Education and company related presentations

Honors and Awards

- 1st Place Best Student Poster at International Society for Exposure Science/Environmental Epidemiology/and Indoor Air Quality and Climate Conference in Basel, Switzerland, August 2013
- Honorable mention for Poster Presentation at Environmental Health Sciences Annual Research Retreat, January 2013
- The David Leslie Swift Scholarship in Environmental Health Engineering, April 2012
- APHA Environmental Section 8th Annual Student Scholarship Award, August 2011
- Environmental, Energy, Sustainability, and Health institute (E^2SHI) Seed Grant, May 2011
- National Institute of Environmental Health Sciences Training Grant Fellowship, August 2009
- Awarded Best Senior Design Project by Faculty and Peers within Department of Biological Engineering, May 2004

Presentations

Oral presentation: Department of Environmental Health Sciences Research Seminar. "Assessing Black Carbon Emissions from Traditional Cookstoves in South Asia" Sutyajeet Soneja, James Tielsch, Frank Curriero, Benjamin Zaitchik, Steve, Chillrud, Subarna Khatry, Patrick Breysse. Johns Hopkins Bloomberg School of Public Health. Baltimore, MD. March 11th, 2014.

Oral presentation: The Environmental, Energy, Sustainability, and Health institute (E^2SHI) Special Seminar. "Assessing Climate Change Emissions from Traditional Cookstoves in South Asia" Sutyajeet Soneja, James Tielsch, Frank Curriero, Benjamin Zaitchik, Steve, Chillrud, Subarna Khatry, Patrick Breysse. Johns Hopkins University. Baltimore, MD. September 12th, 2013.

Oral presentation: Division of Environmental Health Engineering Special Seminar. "A Field Experience in Nepal: A Photographic Journey through Research, Daily Life, and all the In-Betweens" Sutyajeet Soneja. Johns Hopkins Bloomberg School of Public Health. Baltimore, MD. October 2nd, 2013.

Poster presentation: International Society for Environmental Epidemiology. "Characterizing the Spatial Distribution of Ambient Black Carbon During Cooking and Noncooking Periods in Rural, Southern Nepal" Sutyajeet Soneja, James Tielsch, Frank Curriero, Benjamin Zaitchik, Subarna Khatry, Patrick Breysse. Seattle, Washington. August 22nd, 2014. (Abstract Accepted)

Poster presentation: International Society for Exposure Science/International Society for Environmental Epidemiology/International Society for Indoor Air Quality and Climate. "Assessment of Household Emissions due to Cookstoves in Southern Nepal" Sutyajeet Soneja, James Tielsch, Frank Curriero, Benjamin Zaitchik, Subarna Khatry, Patrick Breysse. Basel, Switzerland. August 22nd, 2013.

Poster presentation: Environmental Health Sciences Annual Research Retreat. "Quantifying black carbon emissions from traditional cookstoves in southern Nepal and northern India" Sutyajeet Soneja, Patrick Breysse, James Tielsch, Franck Curriero, Ben Zaitchik. Johns Hopkins University. Baltimore, MD. January 18th, 2013.

Poster presentation: The Environmental, Energy, Sustainability, and Health institute (E^2SHI) Symposium. "Quantifying black carbon emissions from traditional cookstoves in southern Nepal and northern India" Sutyajeet Soneja, Patrick Breysse, James Tielsch, Franck Curriero, Benjamin Zaitchik. Johns Hopkins University. Baltimore, MD. April 26th, 2012.

Poster presentation: Undergraduate Research Symposium. "Design of a Device to Enhance Sea Turtle Hatching Success" Yousif Alkadhi, Jacqueline Cotter, Ryan O'Quinn, Sutyajeet Soneja, Kiran Venkatesh. North Carolina State University. Raleigh, NC. May 2004.

Manuscripts in Preparation

Ojo, Kristen, Scrafford, Carolyn, **Sutyajeet I. Soneja**, Khatry, Subarna K., LeClerq, Steven C., Checkley, William, Katz, Joanne, Tielsch, James M. Performance of Alternative Cookstoves in Nepal. (In preparation)

Sutyajeet I. Soneja, Chen C, Tielsch JM, Katz J, Zeger SL, Checkley W, Curriero FC, Breysse PN. Humidity and Gravimetric Equivalency Adjustments for Nephelometer-Based Particulate Matter Measurements of Emissions from Solid Biomass Fuel Use in Cookstoves. *International Journal of Environmental Research and Public Health*. Published 2014, June 19th.

Sutyajeet I. Soneja, Tielsch JM, Curriero FC, Zaitchik B, Chillrud S, Khatry S, Breysse PN. Determining Particulate Matter and Black Carbon Exfiltration Estimates for Traditional Cookstove Use in Rural Nepalese Village Households. (In preparation)

Sutyajeet I. Soneja, Tielsch JM, Curriero FC, Zaitchik B, Khatry S, Breysse PN. Characterizing Particulate Matter Exfiltration Estimates for Intervention Cookstoves in a Village-Like Household in Rural Nepal. (In preparation)

Sutyajeet I. Soneja, Curriero FC, Tielsch JM, Zaitchik B, Chillrud S, Khatry S, Breysse PN. Spatial Assessment of the Association of Black Carbon for Indoor versus Outdoor Air Emitted from Traditional Cookstoves. (In preparation)

Professional Memberships

- International Society for Exposure Science
- International Society for Environmental Epidemiology
- American Public Health Association
- American Geophysical Union

Collaborations

- PhD Advisor Patrick Breysse, Professor, Department of Environmental Health Sciences, Johns Hopkins University
- Benjamin Zaitchik, Assistant Professor, Department of Earth and Planetary Sciences, Johns Hopkins University
- Frank Curriero, Associate Professor, Department of Environmental Health Sciences, Johns Hopkins University
- James Tielsch, Professor and Chair, Department of Global Health, George Washington University
- Steven Chillrud, Senior Research Scientist, Lamont-Doherty Earth Observatory, Columbia University
- Nepal Nutrition Intervention Project Sarlahi
- Alison Geyh, Associate Professor, Department of Environmental Health Sciences, Johns Hopkins University

Additional Coursework

- Spatial Statistics and GIS
- Applications of Satellite Remote Sensing in Air Pollution Exposure Science
- Energy Policy Choices and Public Health
- The Global Environment and Public Health
- Air Resources Modeling and Management
- Introduction to Environmental and Occupational Health Law

Additional Skills and Activities

- Programming capability in R statistical software, ArcGIS, and geospatial statistical analysis
- *Languages:* English (Native); Hindi (Conversational)

- President of Environmental Health Sciences Student Organization, Johns Hopkins University, 2012-2013; Vice-President from 2011-2012
- Member of Hill's Pet Nutrition United Way Steering Committee, 2008-2009
- Head Coach of Hill's Company Softball Team, 2005-2009
- Hobbies include traveling (e.g., throughout North America, Europe, and Asia), photography, and playing sports